Biogeochemistry of selected supraglacial ecosystems in coastal Antarctica

Thesis submitted for the award of Degree of

DOCTOR OF PHILOSOPHY

In

MARINE SCIENCE

School of Earth, Ocean and Atmospheric Sciences

GOA UNIVERSITY

By

GAUTAMI DEV SAMUI

(National Centre for Polar & Ocean Research)

August 2019

Statement of the Candidate

As required under the University Ordinance OA-19.8 (v), I hereby state that the present thesis titled "Biogeochemitry of selected supraglacial ecosystems in coastal Antarctica" is my original contribution and the same has not been submitted on any previous occasion. Literature related to the problem investigated has been cited. Due acknowledgements have been made wherever facilities and suggestions have been availed.

Gautami Dev Samui

Date

THESIS CERTIFICATE

As required under the University Ordinance OA-19.8 (viii), it is certified that the thesis titled "Biogeochemistry of selected supraglacial ecosystems in coastal Antarctica", submitted by Gautami Dev Samui for the award of the Degree of Philosophy in Marine Science, is based on the original studies carried out by her under my supervision. The thesis or any part of the thesis has not been previously submitted for any other degree or diploma in any University or Institution.

Dr. Thamban Meloth
Research Supervisor
Scientist F
National Centre for Polar and Ocean Research
Headland Sada, Vasco-da-Gama,
Goa-403804, India

Table of contents

Acknowledgements

List of tables

List of figures

Abbreviations

1. Introduction **1-13**

1.1 Antarctica and its role in global system 1
1.2 Organic carbon in Antarctic ice sheet and its global significance 3
1.3 Glacial environments 4
1.4 Supraglacial environments and its role in biogeochemical cycling 6
1.4.1 Surface snow 6
1.4.2 Blue ice 8
1.4.3 Cryoconite holes 9
1.4.4 Role of photochemistry and microbial activity in DOM cycling 11
1.5 Objectives of the study 12

2. Material and methods **14-37**

2.1.Study Area 14

2.2. Sampling 15
2.2.1 Surface snow 15
2.2.2 Blue ice 18
2.2.3 Cryoconite holes 18
2.3. Field experiments 20
2.3.1 Primary production 21
2.3.2 Bacterial production 24
2.3.3 Radioassay 27
2.3.4 In-situ experiment (experimental system) 27
2.3.5 In-situ experiment (natural system) 28
2.4. Analytical methods 31
2.4.1 Total organic carbon 31
2.4.2 Dissolved organic carbon 33

2.4.3 Ionic chemistry 33
2.4.3.1 Carboxylate ions 33
2.4.3.2 Inorganic ions 35
2.4.4 Mineralogy of cryoconite sediment samples 35
2.4.5 Bacterial cell abundance and microbial morphology 36
2.4.6 Dust particles 37

3. Glaciochemistry of surface snow and blue ice in coastal Antarctica 38-60

3.1. Introduction 38
3.2. Results 41
3.2.1 Surface snow 41
3.2.1.1 Princess Elizabeth Land (PEL) 41
3.2.1.2 Amery Ice Shelf (AIS) 45
3.2.2 Blue ice 47
3.3. Discussion 48
3.3.1 Ionic balance 48
3.3.2 Carboxylate ions 54
3.3.2.1 Atmospheric deposition of carboxylic acids on surface snow 54
3.3.2.2 Snowpack production of carboxylate ions 57
3.3.2.3 Post depositional changes of carboxylate ions within snowpack 59
3.3.2.4 Blue ice 60

4. Chemical characteristics of cryoconite holes in coastal Antarctica 61-74

4.1. Introduction 61
4.2. Results 62
4.2.1 Larsemann Hills (LHS) 62
4.2.2 central Dronning Maud Land (cDML) 64
4.2.3 Amery Ice Shelf (AIS) 65
4.3. Discussion 67
4.3.1 Hydrological connectivity within cryoconite holes 67
4.3.2 Ionic concentration trend and possible sources 70
4.3.3 Influence of microbial activity 73

5. Biogeochemical cycling in surface snow and cryoconite holes 75-105

5.1. Introduction 75
5.2. Results 78

5.2.1 Carbon fluxes 78
5.2.2 Nutrient cycling 81
5.2.2.1 Experimental system 81
5.2.2.2 Natural system 82
5.3. Discussion 83
5.3.1 Carbon fluxes 83
5.3.2 Nutrient cycling- Experimental system 84
5.3.2.1 Microbially driven changes 84
5.3.2.2 Light driven changes 88
5.3.2.3 Combined effect of light and microbes 91
5.3.2.4 Overview of carbon and nutrient cycling in the experimental system 95
5.3.3 Nutrient cycling - Natural System 98
5.3.4 Overview of nutrient cycling in the environment 103

6. Summary and conclusions 106-113
7. References
8. List of publications

Dedication

To my Parents and my Brother

Acknowledgements

This thesis has been four years in the coming and it would not be an exaggeration to state that without my supervisor Dr. Thamban Meloth's guidance and support through the years, this work would have never been possible. I am extremely grateful that he put his trust in me and gave me the opportunity to work in the Polar Cryosphere and Ice Core Studies Division of National Centre for Polar and Ocean Research (NCPOR), Goa, India. He has been more than just a supervisor, motivating me and inspiring confidence through times when I lacked both. I express my sincere gratitude to Dr. Runa Antony for being the mentor for my work. I am indebted to her for her valuable time and an invaluable friendship that has been instrumental is shaping my research and my attitude respectively.

I thank the University of Goa and Department of Marine Sciences, where I am registered to complete this Doctoral thesis. I thank my VC Nominees, Dr. G. N. Naik (University of Goa) and Dr. Maria Judith Gonsalves (National Institute of Oceanography, Goa) for their help and support in completing this work. I am grateful to the former Director of NCPOR, Dr. S. Rajan as well as the present Director of NCPOR, Dr. Ravichandran, for their support. I thank Council of Scientific and Industrial Research (CSIR) for the fellowship. I sincerely thank Ministry of Earth Sciences for the financial support throughout the tenure of this work.

I thank Dr. N. Ramaiah (NIO, Goa) and Dr. R. Kirubagaran (National Institute of Ocean Technology, Chennai) for providing their respective department's facility of Liquid Scintillation Counter. I sincerely thank Dr. Lata Gawade (NIO, Goa) and Mr. Magesh Peter (NIOT, Chennai) for carrying out the scintillation analysis in 2016 and 2017, respectively. I am grateful to Mr. Girish Prabhu, (NIO, Goa) for the X-Ray Diffraction analysis. Dr. V. Purnachandra Rao (NIO, Goa) is thanked for his help in interpretation of the XRD results. I express

my gratitude to Dr. Shanta Nair (NIO, Goa) and Dr. Loka Bharati (NIO, Goa) for their help in designing a significant part of field and lab experiments. Dr. Rahul Mohan extended the facility of Scanning Electron Microscope and Epifluroscene microscope for which, I am sincerely grateful. And the analysis would not have been possible without Sahina Gazi and Valency to conduct and aid in SEM studies, for this I am grateful. I am obliged to Mr. Ashish Painginkar and Mr. B. L. Redkar for carrying out ion chromatography analysis and isotope analysis in NCPOR. Norwegian Polar Institute is acknowledged for the Quantarctica QGIS package.

None of this would have been possible without successful Antarctic expeditions which were managed by the NCPOR (Logistics). I thank Mr. Javed Beg and the station leaders as well as the voyage leaders, Dr. Shailendra Saini, Mr. Subrata Moulik, Dr. Mahesh Badanal for ensuring all logistic support extended during the 34th and 36th Indian Scientific Expedition to Antarctica (ISEA) for completing the field component of this research. Their pains and efforts in making our passage to Antarctica and return safe cannot be thanked enough.

I thank Anish Warrier, Shridhar Jawak, Brijesh Desai, Shabnam Choudhary, John Bennet, Shramik Patil, Kaushik, Mayuri Pandey, Romal Jose, Kiral Gadodra, Rajiv Singh, Surender Singh and Nitin Naik for their indispensable help towards making the expeditions successful. Part of the sampling was carried out by Dr. K. Mahalinganathan and Dr. Runa Antony in 28th and 33rd ISEA respectively, for this I am much obliged. I thank Dr. K. Mahalinganathan and Dr. Ravi Naik for their valuable inputs during the course of this research work. The illustration summarizing my work was prepared with the help of my dear friend Midhun. I thank him for that immensely.

I dedicate my thesis to my parents and my brother, Rahul; they have endured many things during the course of these four years and lent unwavering support. I cannot thank enough my friends - Aritri, Femi, Girija, Lathika,

Raghuram, Mayuri, Shabnam, Shashi, Ashish, Vaishnavi, Ajit, Lavkush, Bhanu, Rahul, Vinay, Nuruzzama, Tariq, Ankita, Riya, Vikram, Ankit, Shramik, Manoj, Jenson, Devsamridhi, Sajesh and Sarath for the friendship, patience and support throughout. Each hard days stress has been eased by their camaraderie and the times spent together.

List of tables

3.1 Major ion (Na^+, Ca^{2+}, Mg^{2+}, K^+, NH_4^+, Cl^-, SO_4^{2-}, NO_3^-, $CH_3SO_3^-$) and H^+ concentrations in surface snow samples at Princess Elizabeth Land. 41

3.2 Concentrations of Ac^-, Fo^- and total organic carbon (TOC) in surface snow samples at Princess Elizabeth Land and Amery Ice Shelf. 44

3.3 Major ion (Na^+, Ca^{2+}, Mg^{2+}, K^+, NH_4^+, Cl^-, SO_4^{2-}, NO_3^-) and H^+ concentrations in surface snow samples at Amery Ice Shelf. 45

3.4 Major ion (Na^+, K^+, Mg^{2+}, Ca^{2+}, Cl^-, SO_4^{2-} and NO_3^-), carboxylate ion (Ac^- and Fo^-) and TOC concentration in the blue ice samples from Larsemann Hills and Amery Ice Shelf. 48

3.5 Enrichment factor of Na^+, K^+, Mg^{2+}, Ca^{2+}, Cl^-, SO_4^{2-} and NO_3^- in blue ice samples from Larsemann Hills and Amery Ice Shelf. 49

3.6 Cl^-/Na^+ ratio in the surface snow samples at Princess Elizabeth Land and Amery Ice Shelf. 52

3.7 Ion (Na^+, K^+, Mg^{2+}, Ca^{2+}, Cl^-, SO_4^{2-}, NO_3^-, Ac^- and Fo^-) and TOC concentration in blue ice, annual snow deposits and surface snow from different regions in Antarctica. 54

3.8 Concentrations of Fo^- and Ac^- observed in snow and ice from glaciers worldwide. 55

4.1 Major ion (Na^+, K^+, Mg^{2+}, Ca^{2+}, Cl^-, SO_4^{2-}, NO_3^- and F^-) and dissolved inorganic carbon (DIC) concentrations in the cryoconite holes from Larsemann Hills, central Dronning Maud Land and Amery Ice Shelf. 64

4.2 Carboxylate ions (Ac^-, Fo^-, Lc^- and Oxy^{2-}) and total organic carbon (TOC) concentrations in the cryoconite holes. 66

4.3 Enrichment factor (EF) of Na^+, K^+, Mg^{2+}, Ca^{2+}, SO_4^{2-}, NO_3^-, TOC and Cl^- in the cryoconite holes. 67

4.4 Ionic concentration of various ions in cryoconite holes from different regions of Antarctica. 70

5.1 Rates of primary and bacterial production in surface snow and cryoconite holes together with their chemical composition. Concentration of ions, DOC and TOC are represented in $\mu g\ L^{-1}$ and DIC concentration is represented in $\mu eq\ L^{-1}$. 80

5.2 Comparison of primary production in surface snow and cryoconite holes obtained in this study with that of previous studies. 85

5.3 Rates of bacterial production in surface snow and cryoconite holes obtained in this study with that of previous studies. 85

5.4 Concentration of major inorganic ions (Na^+, K^+, Mg^{2+}, Ca^{2+}, Cl^-, SO_4^{2-} and NO_3^-) on 0 day and 30th day in surface snow, and on 0 day and 25th day in cryoconite hole water. 94

5.5 Inorganic ion concentrations in sunlight-exposed and shaded cryoconite holes on 0 and 25 day. 102

List of figures

1.1 Map of Antarctica, showing major geographic regions. Inset shows Antarctic continent in the Southern Hemisphere in a polar projection. 2

1.2 Photos showing different supraglacial environments in Antarctica – a) surface snow, b) cryoconite holes, and c) blue ice. 5

1.3 Photos showing (a and b) cryoconite hole region in East Antarctica, (c) an open cryoconite hole, and (d) cryoconite hole with an ice lid. 9

2.1 Map showing selected study areas within the East Antarctica. a) central Dronning Maud Land, b) Amery Ice Shelf and c) Princess Elizabeth land. 14

2.2 Surface snow sampling transects in a) Amery Ice Shelf and b) Princess Elizabeth Land in East Antarctica. 17

2.3 Sampling locations of blue ice at a) Amery Ice Shelf and b) Larsemann Hills in East Antarctica. 18

2.4 Map with the insets showing sampling locations of Cryoconite holes in a) central Dronning Maud Land, b) Amery Ice Shelf and c) Larsemann Hills. 19

2.5 Site locations of the *in-situ* experiments performed on surface snow and cryoconite holes. 20

2.6 In-situ field experiments and lab measurements being carried out at Larsemann Hills during 36th Indian Scientific Expedition to Antarctica, 2016-17. 23

2.7 Flowchart showing the incubation setup in the experimental system. 29

2.8 Flowchart showing the experimental setup in the natural system. 30

3.1 Spatial trend of major ions and carboxylate ions in Princess Elizabeth Land. 42

3.2 Spatial trend of major ions and carboxylate ions in Amery Ice Shelf. 46

3.3 Microscopy images of diatom frustules (a, b), bacteria (cocci) (c, d) and rod shaped bacteria (e, f) found in the surface snow samples from Amery Ice Shelf. 47

5.1 Schematic of the incubation setup in the experimental system. 77

5.2 Schematic of the incubation setup in the natural system 79

5.3 Mean primary and bacterial production in cryoconite hole water (6 samples), cryoconite hole sediment (6 samples), and surface snow (2 samples). 83

5.4 Changes in Ac^{-}, Fo^{-}, Oxy^{2-} and DOC in microbe-only treatment over a period of 30 days in surface snow and 25 days in cryoconite holes in experimental system. Negative values represent utilization/degradation and positive values represent production/accumulation. 86

5.5 Changes in Ac^{-}, Fo^{-}, Oxy^{2-} and DOC in light-only treatment over a period of 30 days in surface snow and 25 days in cryoconite holes in experimental system. Negative values represent utilization/degradation and positive values represent production/accumulation. 89
5.6 Changes in Ac^{-}, Fo^{-}, Oxy^{2-} and DOC in light+microbe treatment over a period of 30 days in surface snow and 25 days in cryoconite holes in experimental system. Negative values represent utilization/degradation and positive values represent production/accumulation. 92
5.7 Microscopy images of the cryoconite water samples showing cyanobacteria (a and b) and algae (c). 93
5.8 Changes in DOC concentration in sunlight exposed and shaded cryoconite hole. 98
5.9 Changes in Ac^{-}, Fo^{-} and Oxy^{2-} in sunlight exposed and shaded cryoconite hole. 101
5.10 Illustration showing DOM cycling in glaciers and ice sheets 105

Abbreviations

Acetate	Ac^-
Acetic acid	HAc
Amery Ice Shelf	AIS
Antarctic Circumpolar Currents	ACC
Below Detection Limit	bDL
Calcium acetate	$Ca(Ac)_2$
Calcium formate	$Ca(Fo)_2$
Central Dronning Maud Land	cDML
Dissolved Inorganic Carbon	DIC
Dissolved Organic Carbon	DOC
Dissolved Organic Matter	DOM
Enrichment Factor	EF
Expanded Polypropylene	EPP
Formate	Fo^-
Formic acid	HFo
Hydroxyl radical	$^{\cdot}OH$
Lactate	Lc^-
Larsemann Hills	LHS
Non sea salt Calcium	$nssCa^{2+}$
Non sea salt Sulphate	$nssSO_4^{2-}$
Organic Carbon	OC
Oxalate	Oxy^{2-}
Princess Elizabeth Land	PEL
Sea salt sodium	$ssNa^+$
Sea salt sulphate	$ssSO_4^{2-}$
Scanning Electron Microscopy	SEM
Total Organic Carbon	TOC

Chapter 1

Introduction

1.1 Antarctica and its role in global system

Antarctica is a land of extremes and is the southernmost continent on Earth and lies almost concentrically around the South Pole **(Fig. 1.1)**. The continent is divided into East and West Antarctica by a 3220 km long range of mountains called Trans-Antarctic Mountains. East Antarctica majorly consists of high ice covered plateau, while West Antarctica is consisted of groups of island which are covered and bonded together by ice. Antarctica contains approximately 27×10^6 km^3 of ice (Fretwell et al., 2013; Lythe et al., 2001), which is about 90% of world's ice and 70% of world's fresh water. If this ice melted, the sea water level would increase by 58 m (Fretwell et al., 2013). The ice sheets in the continent are fed by deposition of snow and frosts which remains frozen due to continuous low temperature conditions throughout the year. As a result of accumulation, snowpack gets compressed and eventually gets transformed into solid ice which contains unique records of past climate and atmosphere. Ninety eight percent of the continent's surface is covered by thick ice sheets with an average thickness of approximately 2 km (Fretwell et al., 2013).

Although isolated, Antarctica is connected to the rest of the world through oceanic and atmospheric circulations. The continent is encircled by Southern Ocean dividing the polar region from the tropical oceans. The Southern Ocean controls the natural release of CO_2 from the oceans and helps to absorb anthropogenic CO_2. The Antarctic Circumpolar Currents (ACC), which is the major oceanographic feature of the Southern Ocean, plays a

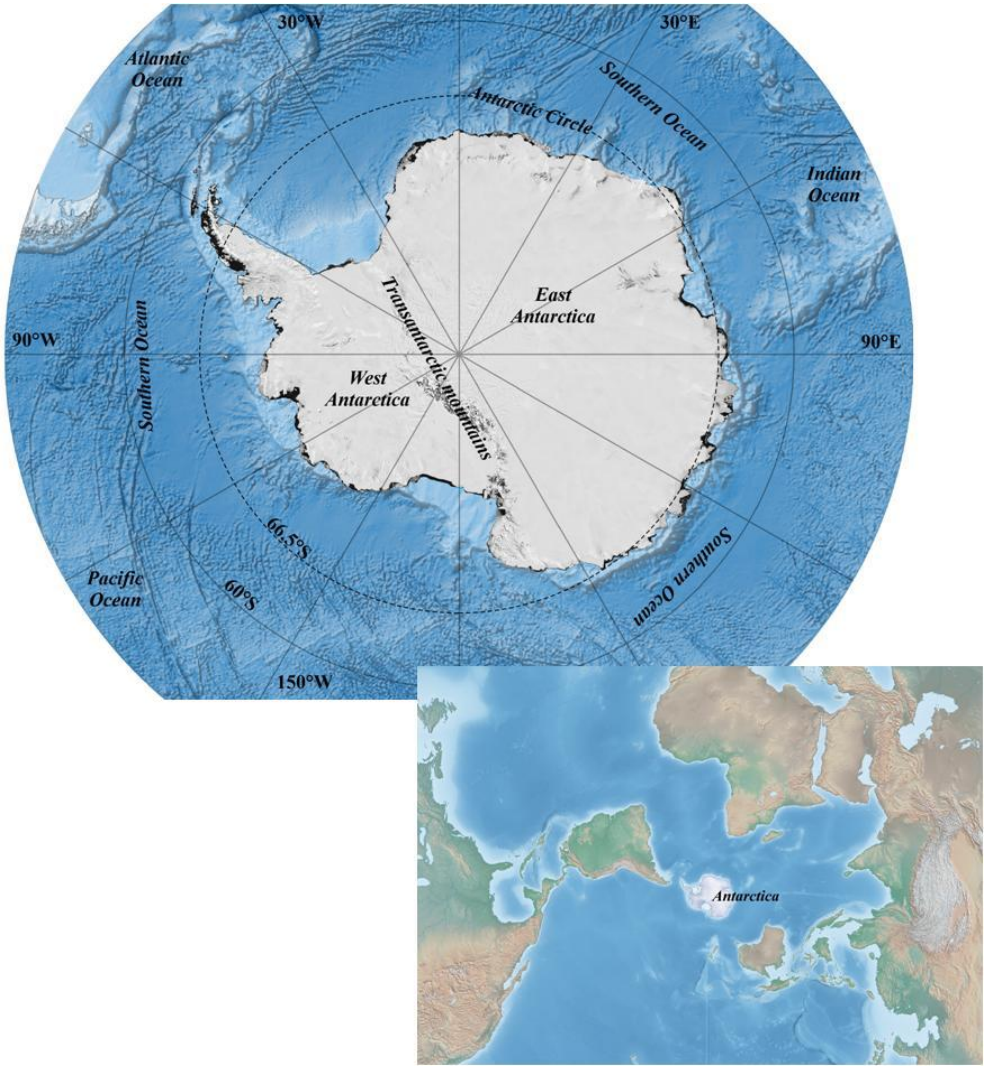

Fig. 1.1. Map of Antarctica, showing major geographic regions. Inset shows Antarctic continent in the Southern Hemisphere in a polar projection.

significant role in global ocean's circulation by linking three main ocean basins (Atlantic, Pacific and Indian ocean) into one global system by transporting heat and salt from one ocean to another. The Southern Ocean currents also play a significant role in the global nutrient cycling between oceans and the atmosphere. Global climate system is driven by solar radiation, most of which is received by low latitudes subsequently creating a large equator to pole temperature difference. Atmospheric and oceanic

circulations respond to this temperature gradient by transporting heat polewards (Trenberth and Caron, 2001) and therefore, the continent acts as the global heat sink. During the winter, due to lack of solar radiation, a strong temperature gradient develops which isolates a pool of cold air over the Antarctic region. This pool of cold air together with surrounding strong winds (developed around this thermal gradient) forms the polar vortex. This vortex plays a significant important role in the global atmospheric circulation and the ozone hole formation over the Antarctic region (Schoeberl and Hartmann, 1991).

Due to high elevation, lack of cloud and water vapour in atmosphere, isolation from warm maritime air masses, the Antarctic continent experiences very low temperature with -94 °C as the minimum recorded air temperature (Scambos et al., 2018; Turner et al., 2009a). Fluctuating light levels are observed in the continent with continuous light in the summer and continuous darkness during winter. High intensities of solar radiations and high albedo are general characteristics of the Antarctic meteorological conditions (Dana et al., 1998; Hoinkes, 1960). The climate in the continent is extremely dry and is also characterized by strong katabatic winds (Turner et al., 2009b). Antarctica and Southern Ocean are critically important parts of the Earth system. Since ice is highly reflecting, it helps Antarctica remain cold through the ice albedo effect. Further, the large extent of sea ice around Antarctica leads to the production of cold and dense water that plunges to the depths, driving the global thermohaline circulations. The Southern Ocean takes up nearly 40% of the global annual uptake of CO_2 from the atmosphere, thus playing a vital role in the global carbon cycle. Antarctica, therefore, plays an important role in global climate system and is a key component of the Earth system in order to understand present and past atmospheric weather and climate processes, oceanic and atmospheric circulation patterns as well as complex interactions between wide range of ecosystems.

1.2. Organic carbon in Antarctic ice sheet and its global significance

Antarctica contains approximately 5.4×10^{15} g C, which is about 91% of the global glacial estimate of organic carbon (OC) content (Hood et al., 2015). Although,

the glacial OC store is very small compared to OC content in permafrost soils (1600 × 10^{15} g C), glacial discharge of OC and its rapid transfer to the aquatic systems downstream exceeds the potential OC removal from soils. This makes the Antarctic glaciers a globally significant hydrological reservoir of OC (Hood et al., 2015). This glacial pool of OC also contributes to regional climate warming and glacier melting (McConnell et al., 2007) as it absorbs incoming solar radiation (Doherty et al., 2010) and decreases the surface albedo (Hansen and Nazarenko, 2004). Considering the increased climate warming and subsequent glacial melting, glacial runoff from Antarctic ice sheets can liberate about 20% (0.24 × 10^{12} g C per year) of global glacial estimate of OC through runoff (Hood et al., 2015). Such significant inputs of glacial dissolved organic matter (DOM) and nutrients are believed to impact downstream ecological functioning (Hood et al., 2009; Singer et al., 2012). For example, glacial DOM entering the aquatic systems is likely to stimulate the heterotrophic activity and subsequently contribute to CO_2 emissions to the atmosphere (Singer et al., 2012). However, the scale of the impact would largely depend on the composition of the materials released. Therefore, an improved knowledge of the amount and nature of organic matter and nutrients associated with the Antarctic environments are of importance for a robust understanding of its impacts on local, regional, and global scales.

1.3 Glacial environments

Glaciers and ice sheets can be characterized into three different environments: supraglacial, subglacial and englacial environments (Hodson et al., 2008). Supraglacial environment comprises the surface/top layer of ice which can freely interact with the overlying atmosphere and receives solar radiation as well as deposition of dust, aerosols and microbial inocula (Stibal et al., 2017). Various supraglacial environments include surface snow/ice, debris and stable aqueous environments such as supraglacial lakes and cryoconite holes **(Fig. 1.2)**.

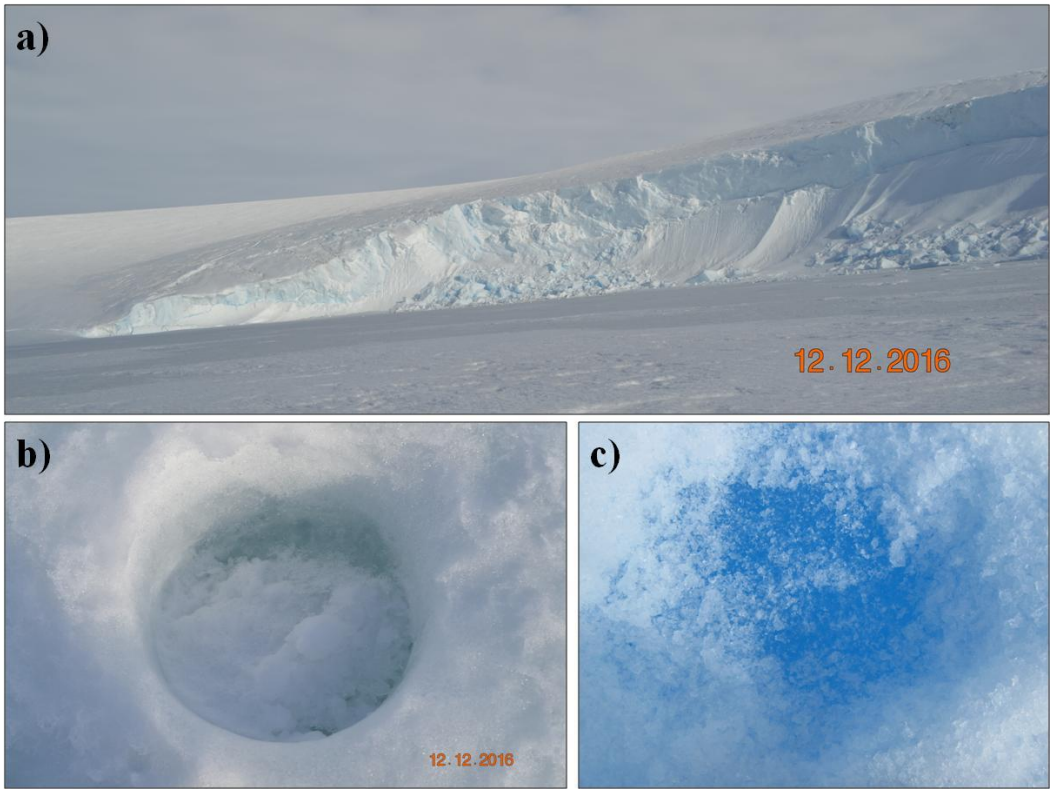

Fig. 1.2. Photos showing different supraglacial environments in Antarctica – a) surface snow, b) cryoconite holes, and c) blue ice.

On the other hand, subglacial environments are those glacial subsystems which lie beneath an ice mass and remain in close contact with overlying ice, including the cavities and channels beneath the ice that are not influenced by subaerial processes (Menzies and Shilts, 2002). Some of these channels can be followed for hundreds of kilometres (Remy and Legresy, 2004). Subglacial environments are permenantly dark and hence, heterotrophy and chemolithotrophy are the primary viable metabolisms occurring in these environments (Miller and Whyte, 2011). Lake Vostok in Antarctcia, the largest lake on Earth, is a classic example of subglacial system. Englacial environments are those systems which can convey water, nutrients, atmospheric gases and biota into the glaciers (Hodson et al., 2008). They include deep, entombed environments, but also the vertical walls of crevasses and moulins. Structures in the ice

produced by tension, such as crevasses, allow water to penetrate into the ice sheet, significantly affecting the glacial processes. These different glacial environments differ vastly in terms of their water content, nutrient abundance, redox potential, ionic strength, rock-water contact, pressure, solar radiation and pH conditions (Hodson et al., 2008). In the past decade, carbon cycling on glaciers and ice sheets has received a lot of attention as they host microbial communities that interact with their physical and chemical environments resulting in distinct processes and feedbacks that impact glacier nutrient cycling, albedo, melt rates and regional atmospheric carbon concentrations. This doctoral research focus on the biogeochemical cycling within selected supraglacial ecosystems.

1.4 Supraglacial environments and its role in biogeochemical cycling

Supraglacial systems include surface snow/ice and dynamic flowing components like surface runoff, both sheet flow and channelized. Photosynthesis is an important and unique feature of the supragacial environments (than englacial and subglacial environments) and has a significant feedback on the biological and the physical features of the system. Supraglacial ecosystems are rapidly changing as a result of climate change causing a retreat of the margins of ice sheet and glaciers and expansion of the biologically active ablation areas. They can also significantly impact the neighbouring ecosystems (including subglacial and englacial) through meltwater percolation and export of OC, microbial communities and nutrients. Present study focus on three major supraglacial environments - surface snow, blue ice and cryoconite holes **(Fig. 1.2)**.

1.4.1 Surface snow

Among various supraglacial features, surface snow has the maximum aerial extent over the Antarctic continent. Snow cover is a critical component of the climate system as it interacts with the overlying atmosphere over a range of time and space (Davies, 1994). Chemical composition of the snowfall depends on the moisture sources as well as the trajectory of the air mass through which snow is falling, altitude of the location where snowfall occurs and also on the meteorological conditions during

snowfall (Davies et al., 1992). For example, in coastal regions of Antarctica, maritime air masses are the major source of primary atmospheric aerosol particles such as Na^+, Cl^-, SO_4^{2-} and Mg^{2+} (Traversi et al., 2004). Snowpack undergoes numerous metamorphic changes due to melt/freeze cycles, meltwater percolation, water vapor movement, and crystal (grain) growth. Apart from affecting the physical and structural properties of the snowpack, such processes also affect distribution of chemical species (Cragin and McGilvary, 1995). Changes in snow chemistry largely reflect the changes in atmospheric chemistry and dynamics resulting from variations in biogeochemical cycling (Dibb and Jaffrezo, 1997). In turn, various processes occurring within the snow can impact the surrounding atmosphere, surface reflectivity and heat budget. Sunlit snow is photochemically active and the photochemical production of a variety of chemicals in snow/ice and their subsequent release may significantly impact the chemistry of the overlying atmosphere (Grannas et al., 2007). In the remote high latitudes, such emissions from the snow can dominate boundary layer chemistry and have a higher significance than low latitudes where boundary layers are anthropogenically perturbed (Grannas et al., 2007).

Reduction in snowcover as a result of increased global warming can reduce the net emission of trace gases from snow into the atmosphere, while increasing processes that occur on the underlying surfaces (Grannas et al., 2007). In addition, changes in precipitation rates will affect the atmospheric scavenging processes. Volatile reactive species emitted from snow and subsequent photochemical reactions can also contribute to depletion of ozone at the polar boundary layer (Simpson et al., 2007). Presence of organic matter and deposited dust in snow surface can affect the surface reflectivity. This can further reduce the photolysis rates within the snowpack and also affect the fate of snowpack products. In addition, Antarctic surface snow harbours variety of microbial communities which is as abundant as 10^5 cells mL^{-1} (Carpenter et al., 2000; Michaud et al., 2014) and contains organic carbon with concentration ranging from 13 to 900 µg L^{-1} (Antony et al., 2011; Grannas et al., 2004; Legrand et al., 2013; Lyons et al., 2007). These values are much lower compared to other environments such as fresh water lakes showing TOC concentration as high as 9.5 mg L^{-1} of TOC (Lyons et al.,

2000) and 10 - 100 times higher bacterial abundance than snow (Säwström et al., 2002; Takacs and Priscu, 1998). Compared to this, oceanic water contains higher TOC concentration of about 55 µM (Kahler er al., 1997) and bacterial cell density of about 10^6 cells mL^{-1} (Graneli et al., 2004). However, carbon fluxes through microbial activity within snowpack show that they are important in carbon cycling through production or utilization of DOM (Skidmore et al., 2000; Yallop et al., 2012). Furthermore, recent data have shown 362 km^3 of meltwater production per year through surface and sub-surface melting of snow in Antarctica, which is about 31% of its total area (Liston and Winther, 2005). This estimate suggests that snowpack can potentially affect the downstream ecosystem by feeding it with DOM, microbial matter and nutrients.

1.4.2. Blue ice

Blue ice areas are among the most peculiar phenomena of the Antarctic ice sheet (Bintanja, 1999). Most of the Antarctic region consists of large snow-accumulation areas. However, coastal regions and areas close to exposed land masses in Antarctica are marked with areas having negative mass balance and are characterized by blue ice regions (Autenboer, 1962; Bintanja et al., 1993, 1997; Liston et al., 1999; Orheim and Lucchita, 1988). It is formed when the snow cover is continuously removed and polished by strong winds and/or by sublimation. Blue ice area exists in the peripheral regions of Antarctica which experiences strongest katabatic winds (Bintanja, 1999; Hodson et al., 2013). Blue ice area covers approximately 2% of the Antarctic continent (Bintanja et al., 1999; Liston and Winther, 2005; Winther et al., 2001). Amery Ice Shelf located in East Antarctica encloses the largest blue ice area on Earth (Liston and Winther, 2005). Blue ice is characterized by lower albedo of 0.57 compared to refrozen snow having an albedo of 0.7 (Bintaja et al., 1997; Lenaerts et al., 2017). Strong winds removing the snow cover and low albedo of the blue ice surface causes deep penetration of solar radiation which further results in sub-surface melting (Kingslake et al., 2017; Liston et al., 1999). The surface and sub-surface melting of blue ice contribute about 15% of total surface and sub-surface melting in the Antarctic continent (Hodson et al., 2013; Liston and Winther, 2005). The persistent melt layer

within the blue ice increases the runoff which otherwise would have restricted to yearly events when air temperatures crosses freezing point (Boggild et al., 1995). Translucence of blue ice is particularly important for photosynthesis. Study showing deep penetration of photosynthetic active radiation through blue ice to a depth of about 84 cm (Hodson et al., 2013). Although, biogeochemical studies in blue ice are rare, study by Hodson et al. (2013) shows microbial activity in the cryoconite holes engraved in the blue ice surface.

1.4.3. Cryoconite holes

Cryoconite holes are vertical cylindrical holes found on glacier surfaces and are filled with water overlying a thin layer of sediment at the bottom **(Fig. 1.3)**.

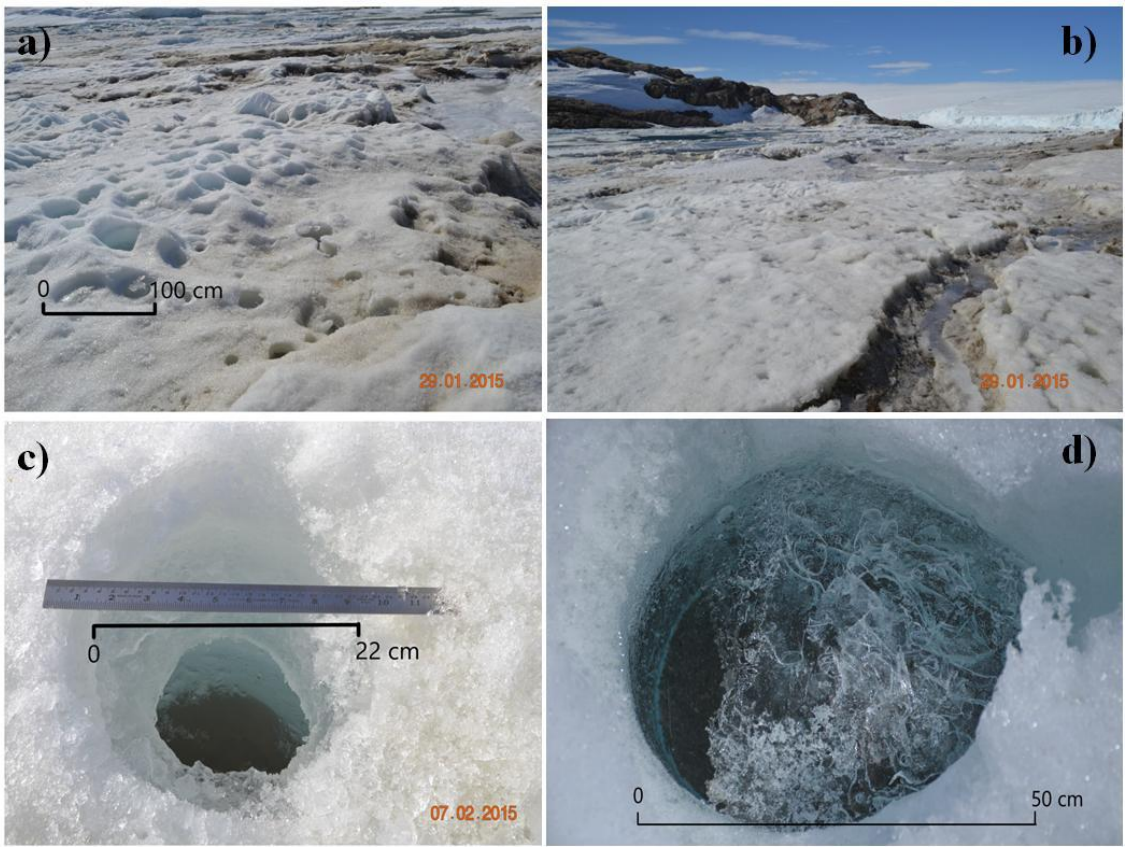

Fig. 1.3. Photos showing (a and b) cryoconite hole region in East Antarctica, (c) an open cryoconite hole, and (d) cryoconite hole with an ice lid.

Cryoconite holes can potentially contribute to about 13% of glacial melt (Fountain et al., 2004). They are formed when windblown dust and organic matter of low albedo accumulate on the snow surface resulting in the melting of ice beneath it (McIntyre, 1984; Podgrony and Grenfell, 1996). The depth and diameter of the cryoconite holes vary from a few centimetres to nearly one meter (Fountain et al., 2004; McIntyre, 1984; Tranter et al., 2004). Development of the depth of the holes enhances in clear weather which are dominated by solar radiation (McIntyre, 1984). Apart from the physical parameters, resident microbes within the cryoconite holes also enhance melting by metabolic energy (Fountain et al., 2004; Gerdel and Drouet, 1960; McIntyre, 1984; Steinbock, 1936). They are commonly found in the ablation regions of glaciers worldwide (Fountain et al., 2004; Hodson et al., 2013) and are common features in cold and polythermal glaciers of polar regions and higher altitudes (Anesio et al., 2007; Edwards et al., 2011; Fountain et al., 2004; Säwström et al., 2002; Takeuchi, 2002). They are also found in the temperate regions with low melt rates and deficient runoffs incapable of washing the sediments off the glacier surface (Anesio et al., 2010).

Chemical composition of the cryoconite hole majorly reflects the chemistry of snowmelt and the debris through which it is formed. However, due to the abundance of microorganisms inoculated by the sediments forming the cryoconite holes, they are sites for biogeochemical cycling of carbon, nitrogen and other nutrients (Anesio et al., 2009; Cook, 2016; Fountain and Tranter, 2008; Hodson et al., 2010; Stibal et al., 2008; Säwström et al., 2002; Telling et al., 2014) on otherwise relatively passive glaciers and ice sheets. Cryoconite holes harbour larger diversity of microorganisms than snowpack (Steinbock, 1936; Säwström et al., 2002; Takeuchi et al., 2000). Higher rates of microbial production are observed in cryoconite hole sediments than the overlying water (Foremann et al., 2007). Using a conservative average cryoconite hole distribution in non-Antarctic glacier regions, Anesio et al. (2009) proposed that the cryoconite holes have the potential to fix as much as 64×10^9 g carbon per year. The ultimate decay of the cryoconite holes is caused by either shrinkage of the holes via

accumulation of ice on the walls of the cryoconite holes or via breaching of water through the walls by the growing supraglacial drainage (McIntyre, 1984). Thus, cryoconite holes can provide a mechanism for the storage of chemical and microbial constituents on the glacier surface and can significantly affect the rate of their transfer to the supraglacial or subglacial drainage systems.

It is evident that the supraglacial ecosystems have a potential role in the carbon dynamics. In particular, surface snow and cryoconite holes are more active and diverse microbial habitats on the glacier surface sequestering carbon from the atmosphere and recycling organic carbon from various sources into more labile carbon substrates. To understand the role of these supraglacial environments in biogeochemical cycling and its impact on the downstream ecosystem, it is critical to understand the compositional characteristics of these ecosystems. However, majority of studies dealing with the distribution and sources of biogeochemical species in supraglacials environments were focused on inorganic ionic species in surface snow. Studies dealing with cryoconite holes are limited to few regions of Antarctica with no or scarce data available in the East Antarctic region. There is rarely any study on blue ice, which provides information on the biogeochemical characteristics. Additionally, despite the significance of OC in the global carbon dynamics, information on the distribution and sources of OC in different supraglacial ecosystems are scarce and limited to Arctic, Alpine and few regions of Antarctica. Antarctica being a huge continent, such sparse data hinders any meaningful inferences on the carbon dynamics of Antarctic cryosphere. Therefore, an understanding of the chemical characteristics and biogeochemical cycling of various supraglacial environments in Antarctica would be crucial in elucidating their contribution to global biogeochemical processes.

1.4.4. Role of photochemistry and microbial activity in DOM cycling

Organic carbon on the glaciers is highly reactive and as a result of photochemical degradation, it may get completely oxidised to CO_2 or get partially oxidized (Ward and Cory, 2016). Such processes could alter the chemical composition of the DOM before it is exported to downstream. Photochemical activity on OC also

produces reactive gas species and free radicals that may impact the oxidative capacity of the overlying atmosphere (Grannas et al., 2007). Further, supraglacial DOM is an important source of energy for resident microbial communities (Amato et al., 2007; Antony et al., 2016), the mineralization of which by heterotrophic bacteria can result in an increase in atmospheric CO_2 concentrations. Organic carbon produced by autotrophic communities is a dominant substrate for microbes in the glaciers (Antony et al., 2014; Bhatia et al., 2010). However, microbial activity may also get affected by the changes in the intensity of solar radiation (Bagshaw et al., 2016). Photomineralization of bioreactive DOM is potentially an important factor determining the net effect of irradiation on the bioreactivity of DOM (Obernosterer and Benner, 2004). The source of the DOM component may also determine the photoreactivity as well as bioreactivity of the DOM (Obernosterer and Benner, 2004). Thus, quantifying the effect of coupled 'photo-biological' activity of DOM is crucial in the understanding of the DOM cycling. Such studies are particularly of importance during the summer season due to higher temperatures, melting and sunlight. Therefore, in this doctoral study, detailed measurements and experiments were carried out to understand the role of selected supraglacial ecosystems on biogeochemical cycling and gain insights on how DOM and nutrients are transformed through photochemical and microbial activity in Antarctic supraglacial environments.

1.5 Objectives of the study

Major objectives of the doctoral study are:

1. To understand the compositional characteristics in spatially distinct and different supraglacial environments like cryoconite holes, blue ice and snowpack in Antarctica.

2. To study the carbon cycling associated with cryoconite holes and their significance in coastal Antarctica.

The present study focuses on three geographically different regions within East Antarctica, namely Princess Elizabeth Land, Amery Ice Shelf and central Dronning

Maud Land. To meet the objectives of the study, chemical characteristics of surface snow, blue ice and cryoconite holes from selected areas in East Antarctica were studied. Subsequently, *in-situ* field experiments were conducted to: 1) quantify the rates of primary production and bacterial production within snow and cryoconite holes, 2) advance the understanding of how photochemistry and biology interact to determine the fate of DOM on the glacier surface, and 3) assess the relative importance of photo-degradation versus microbial degradation in these unique ecosystems.

Chapter 2

Materials and methods

2.1 Study area

The present study focus on three geographically different regions within the East Antarctica, namely Princess Elizabeth Land (PEL), Amery Ice Shelf (AIS) and central Dronning Maud Land (cDML) (**Fig. 2.1**).

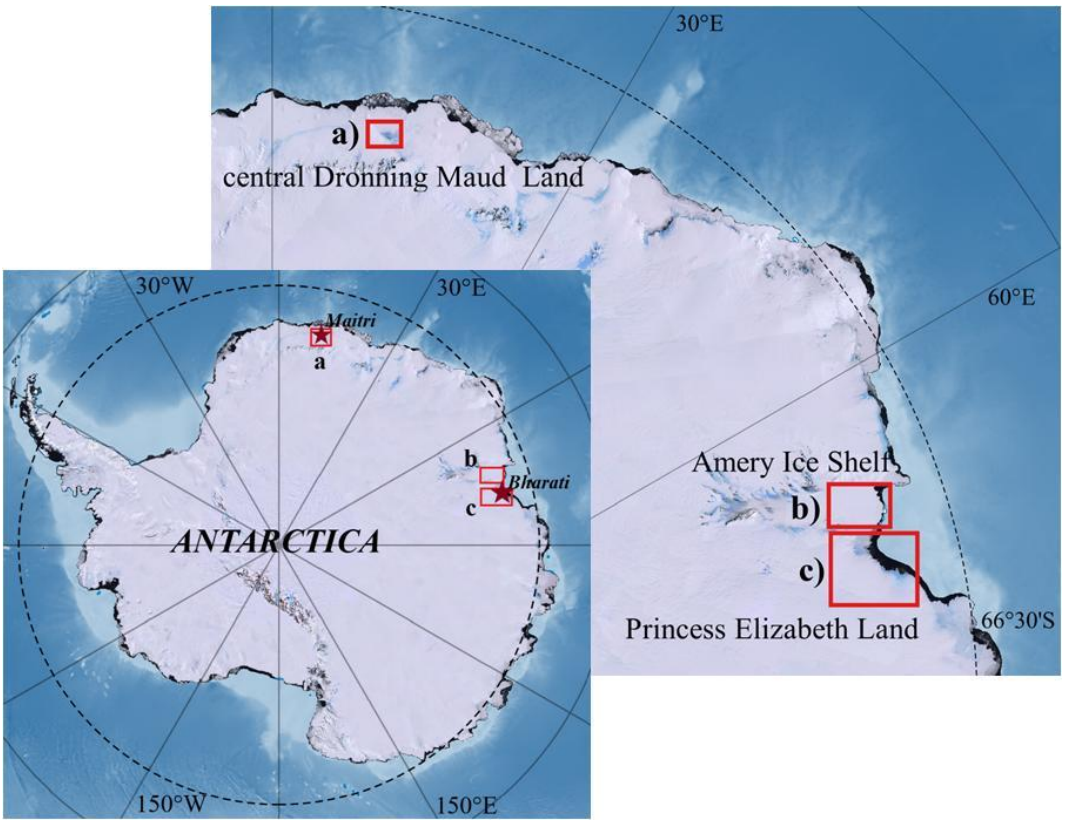

Fig. 2.1. Map showing the selected study areas within the East Antarctica. a) central Dronning Maud Land, b) Amery Ice Shelf and c) Princess Elizabeth Land.

Princess Elizabeth Land lies within 73 to 88 °E longitudes in East Antarctica (Indian Ocean Sector) and hosts the Lambert glacier which is the largest glacier basin that feeds

the largest ice shelf in East Antarctica, i.e., Amery Ice Shelf. Princess Elizabeth Land is bounded at the western end by the Amery Ice Shelf (Indian Ocean sector) which is the largest ice shelf in East Antarctica. The Amery Ice Shelf lies within 69 to 75 °E longitudes in East Antarctica and extends inland from Pridz bay and MacKenzie bay to approximately 320 km inland where, it is fed by Lambert glacier. No exposed mountain range is present near the surface snow sampling site. However, cryoconite hole and blue ice sampling sites were located 110 km away from coast near a prominent rock promontory. Surface snow, blue ice and cryoconite hole samples were collected from the PEL region. Cryoconite hole sampling site in the PEL region is located in a valley near Thala fjord at South Grovnes peninsula in the Larsemann Hills (LHS). The sampling site at LHS is located in a coastal valley surrounded by hills at the northern and southern region, an ice wall on the eastern side and the Thala fjord on the western side. The open cryoconite holes in this region seem to be hydrologically connected with supraglacial streams flowing at the study site. There are no exposed mountain chains near the surface snow and blue ice sampling site at PEL.

Central Dronning Maud Land (cDML) lies within 0 to 20 °E longitudes in East Antarctica (Atlantic Ocean Sector) and is located approximately 2000 km from the PEL region. The ice sheet in cDML region is separated by approximately 100 km from the open ocean by the Nivilsen Shelf. Central Dronning Maud Land hosts the Schirmarcher Oasis which is one of the smallest Antarctic oases. Schirmarcher Oasis is comparatively an ice free region and is a home of number of exposed hills and several lakes. Cryoconite hole samples were collected from the blue ice region immediately north of Schirmarcher Oasis that is surrounded by nunataks (exposed land mass).

2.2 Sampling

2.2.1 Surface snow

Surface snow samples were collected along a 180 km coastal-inland transect at PEL and a 130 km coastal transect at AIS, East Antarctica (**Fig. 2.2**). In PEL region, beginning at 10 km from coast, eighteen surface snow samples (~10 cm deep) were collected at 10 km interval up to 180 km inland in January, 2008 during the 28th Indian

Scientific Expedition to Antarctica (ISEA) (**Fig. 2.2**). The sampling sites were located at an elevation between 267 and 2210 m above mean sea level (m a.s.l). In the AIS region, starting at 10 km from the coast, thirteen surface snow samples were collected at 10 km interval up to 130 km along a transect perpendicular to the coastline covering an elevation from near sea level to 62 m a.s.l. Sampling at AIS was carried out in January and February, 2014 during the 33rd ISEA (**Fig. 2.2**). The surface snow samples in this study represent the early spring and summer snowfall events as observed from the snow accumulation rate obtained from 1 m snow cores collected from the same sampling stations in AIS (unpublished data) and PEL (Mahalinganathan et al., 2012).

Sampling in both the regions was carried out 50 m upwind from the helicopter landing site to avoid any contamination. At PEL, surface snow samples were collected in pre-cleaned Low Density Polyethylene (LDPE) bags using pre-cleaned polypropylene scoop. For storage, sampling bags containing samples were sealed and kept at −20 °C in Expanded Polypropylene (EPP) boxes. Organic carbon measurements in samples stored in plastic bags may get minor contamination from the material of the storage bags. At AIS, surface snow samples for organic carbon measurements were collected in air tight, pre-cleaned and combusted (450 °C, 4 h) amber glass bottles using sterile teflon scoops. Prior to use, sample collection bottles were cleaned by soaking in 0.5% HNO_3 solution followed by thorough rinsing in fresh ultrapure water and combustion at 450 °C for 4 h. Sample bottles were tightly closed while ensuring that no snow grain was stuck to the caps to prevent contamination resulting from improper closure of the bottle. The bottles were not opened until analysis to minimise atmospheric exchange. Samples for inorganic ion and microbial analysis were collected in sterile Whirl-pak bags. All samples were stored and transported at −20 °C in EPP boxes. Sub-sampling for various analyses was carried out in clean conditions in a laminar flow placed inside a −15 °C cold room.

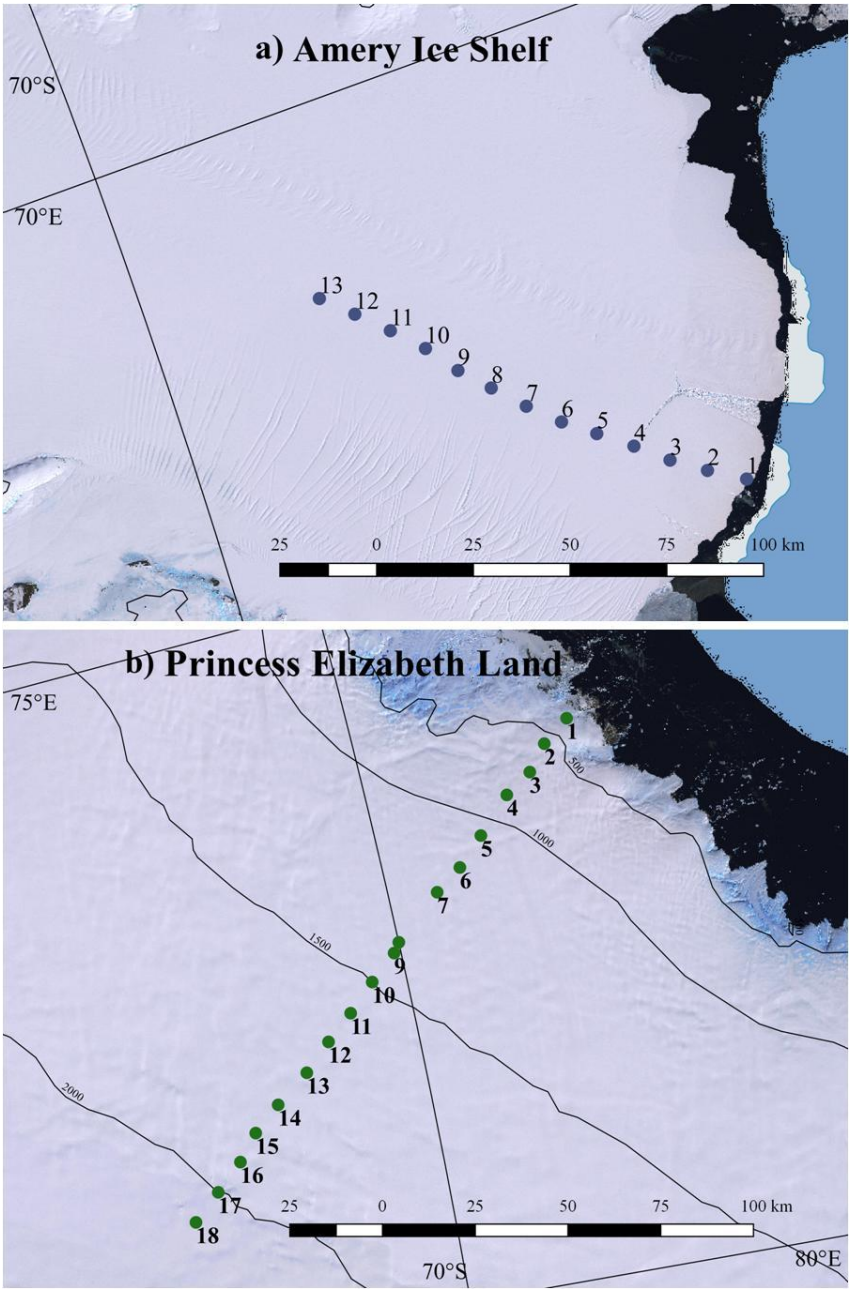

Fig. 2.2. Surface snow sampling transects in a) Amery Ice Shelf and b) Princess Elizabeth Land in East Antarctica.

2.2.2 Blue ice

Blue ice samples (cores of approximately 1 m depth) were collected from LHS and AIS using KOVACS Mark IV coring device during the 33rd ISEA, 2013-14 (**Fig. 2.3**).

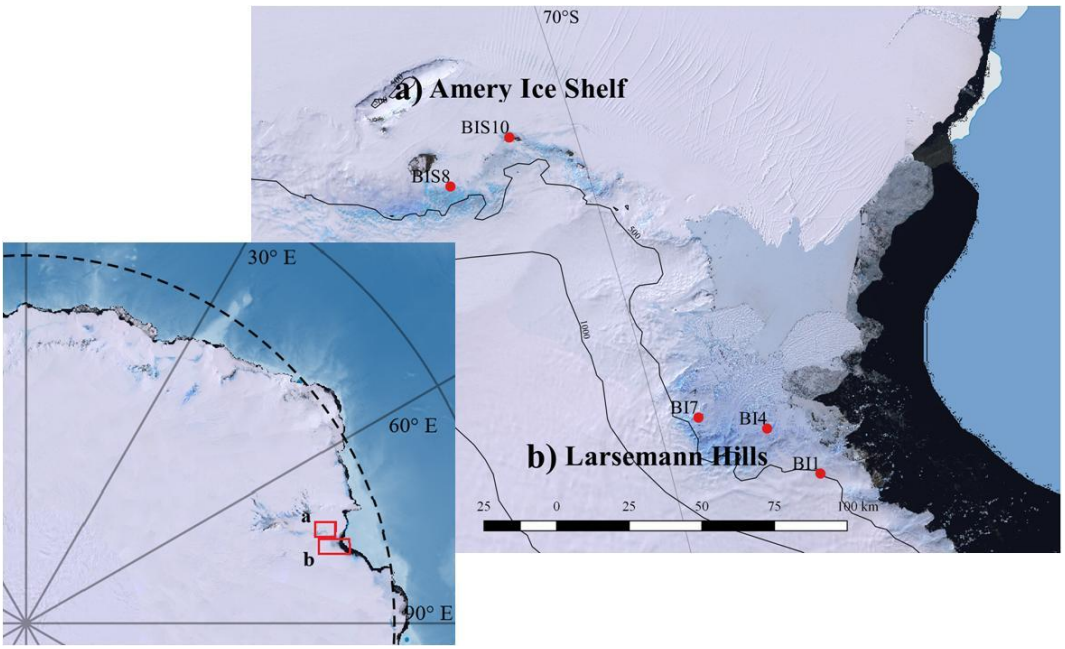

Fig. 2.3. Sampling locations of blue ice at a) Amery Ice Shelf and b) Larsemann Hills in East Antarctica.

Three samples from LHS and two samples from AIS region were collected with a sampling interval of ~ 25 km between samples at each location (**Fig. 2.3**). The samples were immediately transferred to pre-cleaned LDPE bags, sealed and stored at −20 °C until analysis. Sub-sampling was carried out using custom made vertical band saw inside −15 °C cold room. Two/three samples were strategically sub-sampled from each core and analyzed to ensure repeatability of the measurements in a core.

2.2.3 Cryoconite holes

Cryoconite hole samples were collected from LHS, AIS and cDML during the 33rd ISEA, 2013-14 (**Fig. 2.4**).

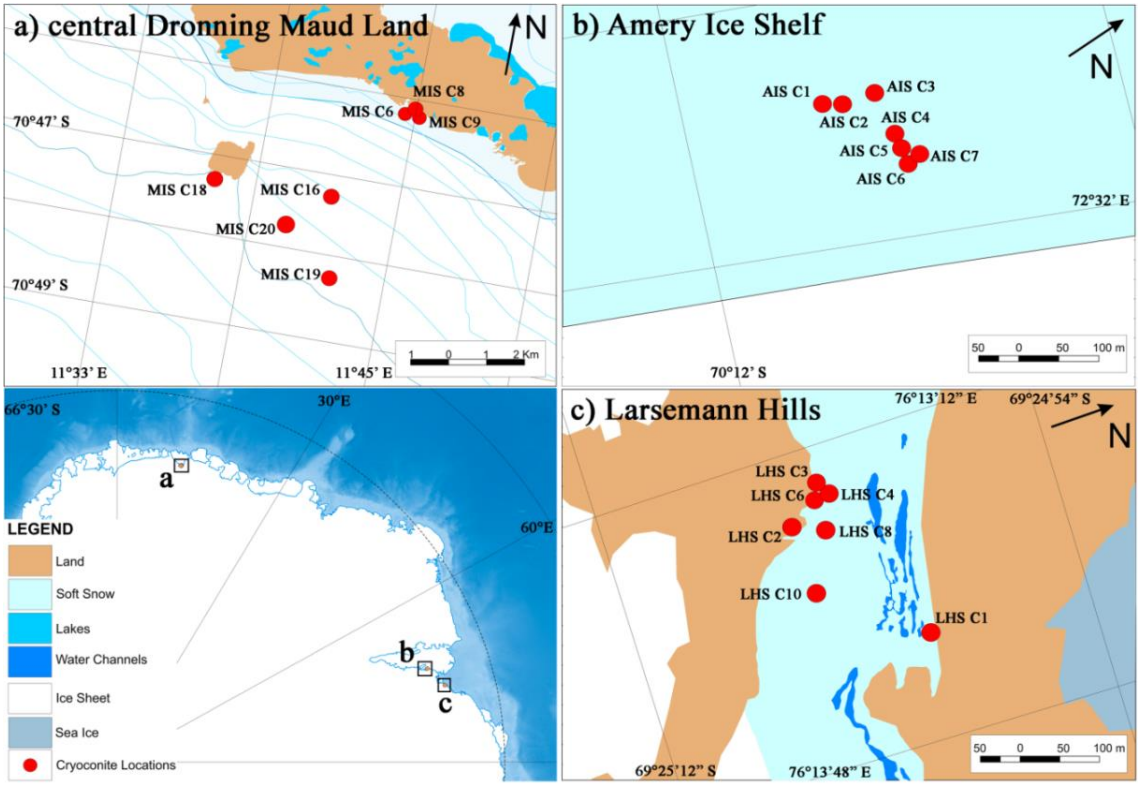

Fig. 2.4. Map with the insets showing sampling locations of Cryoconite holes in a) central Dronning Maud Land, b) Amery Ice Shelf, and c) Larsemann Hills.

In LHS, sampling was carried out in January during the summer season. Melt-water samples from the cryoconite holes for organic carbon analysis were collected in pre-cleaned and combusted amber glass containers using sterile 50 mL syringes. Melt-water samples for microbial measurements and inorganic ion analysis were collected in Whirl-pak bags in a similar manner. Cryoconite hole sediment samples were collected using a sterile poly-propylene scoop. The cryoconite holes in AIS and cDML were collected during February and early March, respectively, and were found to be in the frozen state. The frozen cryoconite holes were drilled using a KOVACS Mark IV coring device. Samples were immediately transferred to pre-cleaned LDPE bags and sealed. Seven cryoconite holes were sampled from each study region. All samples were stored and transported at −20 °C in EPP boxes.

2.3 Field experiments

In order to understand carbon and nutrient cycling in surface snow and cryoconite holes in the LHS region of East Antarctica, *in-situ* experiments were carried out during the 36th ISEA, 2016-17 (**Fig. 2.5**). *In-situ* measurements of primary and bacterial production were carried out together with photo-biochemical experiments designed to understand the photochemical and microbial processing of dissolved organic matter (DOM) and nutrient cycling. To better understand the impact of photochemical and microbial processes occurring individually or in concert, an experimental system was set up wherein, samples (snow and cryoconite hole water) were collected in pre-cleaned, combusted quartz tubes and incubated in the field for nearly 30 days under four different conditions as explained in **section 2.3.4**.

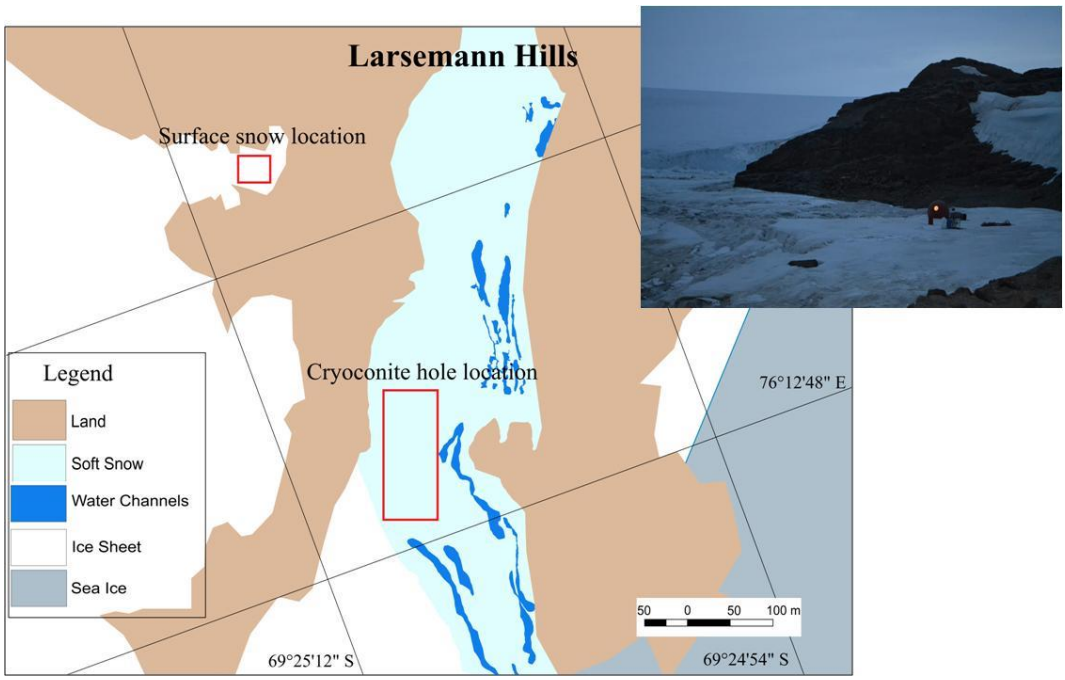

Fig. 2.5. Site locations of the *in-situ* experiments performed on surface snow and cryoconite holes.

Experiments were also carried out to understand carbon and nutrient cycling in the natural cryoconite hole system under light and dark conditions, by monitoring two cryoconite holes for 25 days - one exposed to sunlight and the other shaded to limit

photochemical activity. The experiments on surface snow were carried out during December and January, 2016, while the experiments on cryoconite holes were carried out during January and February, 2016 (**Fig. 2.6**). Samples retrieved from the *in-situ* experiments were safely stored and transported at −20 °C in EPP boxes. Details of the *in-situ* experiments are as follows:

2.3.1 Primary production

Primary production or rate of carbon fixation by autotrophs in supraglacial samples was determined by tracing the uptake of radioactive ^{14}C-$NaHCO_3$ from the dissolved inorganic form to organic carbon (Knap et al, 1996).

Reagents:

1. *Working solution*: ^{14}C-$NaHCO_3$ of radioactive concentration, 5 µCi mL^{-1}.
2. *Sterile ultrapure water*: Ultrapure water was autoclaved at 120 °C for 20 min followed by cooling and filtration through sterile 0.22 µm nuclepore filter membrane (Whatmann).
3. *Trace metal grade HCl solutions*: 2 N and 0.5 N
4. *Sterile buffered formalin (37%)*: Formalin (37%) was buffered using sodium tetraborate followed by filter sterilization using 0.22 µm nucleopore membrane.
5. *Ethanolamine*

Setup:

1. *Cleaning*: Containers and vials used during the experiment were cleaned by soaking them in 0.5 N HCl solution for 24 h followed by thorough rinsing with ultrapure water.
2. *Sample collection*: 40 mL of surface snow and cryoconite hole water samples were collected in pre-cleaned 50 mL polycarbonate tubes and 1 g of cryoconite sediment was collected in pre-cleaned 15 mL High Density Polyethylene (HDPE) centrifuge tubes. For light incubation, 12 samples were collected in separate clear tubes and for dark incubation, 12 samples were collected in separate tubes covered with aluminium foil.

3. *Time zero samples*: Time zero samples were prepared by the addition of buffered formalin (final concentration, 5%) to kill the microbial cells. Six samples each from light and dark incubation setup were used as time zero samples.
4. *Sample inoculation and incubation*: The surface snow and cryoconite hole water samples were amended with 200 µL of working solution and cryoconite sediment samples were amended with 300 µL of working solution. Surface snow samples were then incubated for 72 h, while cryoconite water and cryoconite sediment samples were incubated for 48 h.
5. *Total DPM (disintegration per minute)*: For total DPM measurement, an aliquot of 200 µL of sample inoculated with radioisotope was taken in a scintillation vial and spiked with 200 µL ethanolamine to prevent the escape of CO_2 to the atmosphere.
6. *Terminating the incubation*: To terminate the time zero incubations, samples were immediately processed to extract the organic matter using the filtration or centrifugation methods as described below. Incubations after 72 h in surface snow samples and after 48 h in cryoconite water and cryoconite sediment samples were terminated by the addition of 37% buffered formalin (final concentration, 5%) followed by extraction of the organic matter using filtration or centrifugation method..
7. *Extraction using filtration method*: Maintaining low light conditions, organic matter from incubated surface snow and cryoconite hole water samples was extracted by filtering the samples through GF/F filter membranes (25 mm) followed by washing thoroughly with cold and sterile ultrapure water. The extracted filters were then transferred to 20 mL scintillation vials followed by addition of 1 mL, 2N HCl to remove the excess dissolved inorganic carbon that remained unutilized. The filters were then dried under the fume hood. Radioactivity was measured using a Wallac DSA 1409-001 Liquid Scintillation Counter.
8. *Extraction using centrifugation method*: Organic matter from the cryoconite sediments were extracted by addition of 2 mL, 2N HCl followed by vortexing for 30 s and drying under the fume hood. Radioactivity was measured using liquid scintillation counting technique.

Fig. 2.6. In-situ field experiments and lab measurements being carried out at Larsemann Hills during 36th Indian Scientific Expedition to Antarctica, 2016-17.

Primary production rate estimations

Primary production in surface snow and cryoconite hole samples carried out with ^{14}C-$NaHCO_3$ solution was estimated using the **equation 2.1** (Knap et al., 1996) as:

$$\text{Primary productivity rate } (\mu g\ C\ L^{-1}\ d^{-1}) = \left(\left(\frac{SDPM}{V}\right) \times \left(\frac{DIC \times 0.20 \times 10^{-3}}{TDPM}\right) \times \left(\frac{1.05}{T}\right)\right.$$

equation 2.1

where, SDPM = Disintegration per minute (DPM) measured in extracted samples

V = Volume of sample incubated in L

DIC = Dissolved Inorganic Carbon concentration in the sample in $\mu g\ C\ L^{-1}$

0.20 =Volume of unfiltered sample (^{14}C-$NaHCO_3$ added) used for total DPM measurement in mL

TDPM = Total DPM measured from 0.20 mL of unfiltered sample (^{14}C-$NaHCO_3$ amended) spiked with ethanolamine

1.05 = value used for correction for lower uptake of ^{14}C carbon compared to ^{12}C

T = period of incubation in days

2.3.2 Bacterial production

Bacterial production or the rate of biomass synthesis by the heterotrophic community in the supraglacial environment was estimated by tracing the incorporation of methyl-^{3}H-Thymidine into the cold Trichloroacetic acid (TCA)-insoluble cell fractions following a small incubation (Knap et al., 1996; Fuhrman and Azam, 1982).

Reagents:

1. *Stock solution*: Methyl-^{3}H-Thymidine of 18000 mCi $mmol^{-1}$ (specific activity) and 1 mCi mL^{-1} (radioactive concentration) was stored in 96% ethanol in refrigerator.
2. *Working solution*: An aliquot of radio-labelled reagent was taken in a pre-cleaned glass vial and the ethanol was evaporated under the laminar flow. Forty eight microlitres of methyl-^{3}H-Thymidine with radioactive concentration of 1 mCi mL^{-1} was then taken in another pre-cleaned glass vial and 10 mL of sterile ultrapure water was added to obtain a working solution of 4 µM.
3. *Sterile buffered formalin (37%)*: Formalin (37%) was buffered using sodium tetraborate followed by filter sterilisation using sterile 0.22 µm nucleopore membrane.
4. *Sterile ultrapure water*: Ultrapure water was autoclaved at 120 °C for 20 min followed by cooling and filtering through sterile 0.22 µm nuclepore filter membrane (Whatmann).
5. *Trichloroacetic acid*: 100% (weight/volume) TCA solution was prepared by adding 100 g TCA (Merck, reagent grade, Emsure) to 100 mL sterile ultrapure water and 5% (weight/volume) TCA solution was prepared by adding 5 g TCA to 100 mL sterile ultrapure water. TCA solutions were stored in refrigerator and used chilled.

6. *Ethyl acetate*

Setup:

1. *Cleaning*: Containers and vials used during the experiment were cleaned by soaking them in 0.5 N HCl solution for 24 h followed by thorough rinsing in ultrapure water.
2. *Sample collection*: 40 mL of surface snow and cryoconite water samples were collected in pre-cleaned 50 mL polycarbonate tubes and 2 g of cryoconite sediment samples were collected in pre-cleaned 15 mL HDPE centrifuge tubes. For each incubation setup, 24 sample tubes were prepared which included 12 control killed samples.
3. *Control*: Control samples were prepared by killing the microbes by the addition of buffered formalin, 37% (final concentration, 5%). For each incubation setup, 12 control killed samples were prepared.
4. *Time zero samples*: Time zero samples were prepared by the addition of buffered formalin, 37% (final concentration, 5%) followed by addition of 100% TCA cold solution (final concentration, 5%). For each incubation setup, 6 samples and 6 control killed samples were used as time zero samples.
5. *Sample inoculation and incubation*: The surface snow and cryoconite water samples were inoculated with 400 µL of working solution to get final concentration of 40 nM and cryoconite sediment samples were inoculated with 500 µL of working solution. The surface snow samples were then incubated for 72 h, while cryoconite water and cryoconite sediment samples were incubated for 48 h.
6. *Terminating the incubation*: To terminate the time zero incubations, samples were immediately processed to extract the precipitated biomass using filtration or centrifugation method. Incubations after 72 h in surface snow samples and after 48 h in cryoconite water and sediment samples were terminated by addition of 37% buffered formalin (final concentration, 5%) to kill the microbial cells and 100% cold TCA solution (final concentration, 5%) to precipitate the biomass synthesized followed by extraction of the precipitated biomass.

7. *Extraction using filtration method*: Termination of the surface snow and cryoconite hole water incubations was followed by extraction of the biomass by filtering the samples through 0.22 µm cellulose nitrate filter (Whatmann) followed by washing with 5 mL, 5% cold TCA solution and cold sterile ultrapure water. The filters were then carefully transferred in 20 mL scintillation vials and 1 mL ethyl acetate was added to dissolve the filter followed by drying under the fume hood. Radioactivity was measured using a Wallac DSA 1409-001 Liquid Scintillation Counter.
8. *Extraction using centrifugation method*: Followed by terminating the incubation in cryoconite sediments, biomass was extracted by centrifugation at 2000 rpm for 10 min. The precipitate obtained was washed with 2 mL, 5% cold TCA solution to remove the soluble fraction in the samples by vortexing for 1 min followed by centrifugation. The precipitate thus obtained was finally washed thrice, each time with 5 mL cold and sterile ultrapure water in the similar way. Radioactivity in the extracted biomass was counted using liquid scintillation counting technique.

Bacterial production rate estimations

Following the extraction, cellulose nitrate filters in the scintillation vials were dissolved in 1 mL ethyl acetate followed by drying under fume hood. Radioassay was carried out after adding 10 mL scintillation cocktail followed by thorough vortexing for 30 s. Hourly rate of radio-labelled Thymidine (Thy) incorporation by sample was estimated using **equation 2.2** as (Knap et al., 1996; Fuhrman and Azam, 1982):

$$\text{Thy incorporation } (\text{mole L}^{-1}\,\text{h}^{-1}) = \text{DPM} \times 4.5 \times 10^{-13} \times \left(\frac{1}{\text{SA}}\right) \times \left(\frac{1}{\text{v}}\right) \times \left(\frac{1}{\text{T}}\right)$$

equation 2.2

where, DPM = Disintegration per minute measured in extracted samples

SA = Specific activity of the methyl-^{3}H-Thymidine inoculated in C_i mol^{-1}

4.5×10^{-13} = factor used for converting DPM into C_i

V = Volume of sample in L

T = Incubation time in hours

Thymidine incorporation was converted into bacterial production using conversion factors 2×10^{18} cells mol^{-1} and 11×10^{-15} g C $cell^{-1}$ (Takacs and Priscu, 1998; Takacs et al., 2001).

2.3.3 Radioassay

Radioassay was carried out by liquid scintillation counting technique using Wallac DSA 1409-001 Scintillation Counter equipped with Europium-152 gamma source. Prior to radioassay, 10 mL of Cocktail W, a naphthalene based scintillation cocktail (Spectrochem) was added in 20 mL HDPE scintillation vial containing the extracted samples in filter membrane followed by vortexing for 30 s. Contaminated reagents and solutions used during the sample incubation and processing can influence the radioactivity measurements carried out on samples. Thus, radioactivity was measured in TCA solution, buffered formalin, ethyl acetate, ultrapure water used washing and preparing the solutions, scintillation cocktail and the filter membranes and was found to be ranging from 10 to 33 dpm. In order to determine the background radioactivity in the supraglacial samples, radioactivity was measured in the samples without radio-labelled substrate added to it. Throughout the experiment and analysis, stringent precautions were taken to avoid any spillage and radioactivity in and around the working area was regularly measured using Geiger counter. No spillage occurred during the experiment.

2.3.4 *In-situ* experiment (Experimental system)

Surface snow and cryoconite water were collected in pre-cleaned quartz tubes using sterile scoops and syringes, respectively. The samples were incubated in field for 30 days (surface snow) and 25 days (cryoconite hole) in the following conditions:

1. *Only light*: To study the effect of only light on DOM and nutrient cycling, microbial activity was inhibited in surface snow by adding a biocide, while cryoconite hole

samples were filtered using 0.22 µm Omnipore PTFE filters (Merck Biosciences). Since, the compound used as the biocide may interfere with the ionic or organic carbon measurements, biocides were selected keeping in the mind the nature of the analysis to be carried out. Samples for ionic measurements were spiked with chloroform ($CHCl_3$) and samples for TOC and DOC measurements were spiked with sodium azide (NaN_3). Blanks comprised of the fresh ultrapure water and the biocide were incubated and analysed in the same way as the samples. Cryoconite water samples were filtered using the methodology described in **section 2.4.2** to avoid any contamination during the filtration.

2. *Microbes in absence of light*: To study the effect of microbes alone on the DOM concentration and nutrient cycling, samples containing the resident microbes were incubated in quartz tubes wrapped with aluminium foil to prevent any penetration of light.
3. *Both light and microbes*: To study the effect of both light and microbes, quartz tubes with surface snow and cryoconite water samples containing the resident microbial communities were incubated under ambient light conditions.
4. *Control*: Quartz tubes containing surface snow samples spiked with biocide and cryoconite water samples filtered through 0.22 µm Omnipore PTFE filters, and wrapped with aluminium foil served as the controls.

Samples retrieved on 0 and 30 day (surface snow) or 25 day (cryoconite hole water) were analysed for ionic composition and concentration, total organic carbon (TOC) and dissolved organic carbon (DOC) concentration. Samples were incubated in triplicates. Flow chart in **Fig 2.7** describes the experimental setup.

2.3.5 *In-situ* experiment (Natural System)

In the experimental system, it was challenging to simulate various natural environmental conditions such as DOM input, nutrient exchange between the cryoconite sediment and the overlying water, concomitant microbial activity, as well as, physical conditions such as atmospheric exchange, etc. Therefore, to better understand the DOM and nutrient cycling in these environments in natural conditions, a second

experiment was designed where two cryoconite holes subjected to different light conditions (i.e. full solar exposure and restricted light exposure) were monitored over a period of 25 days. In this experiment, two cryoconite holes of similar dimensions and close to each other were chosen.

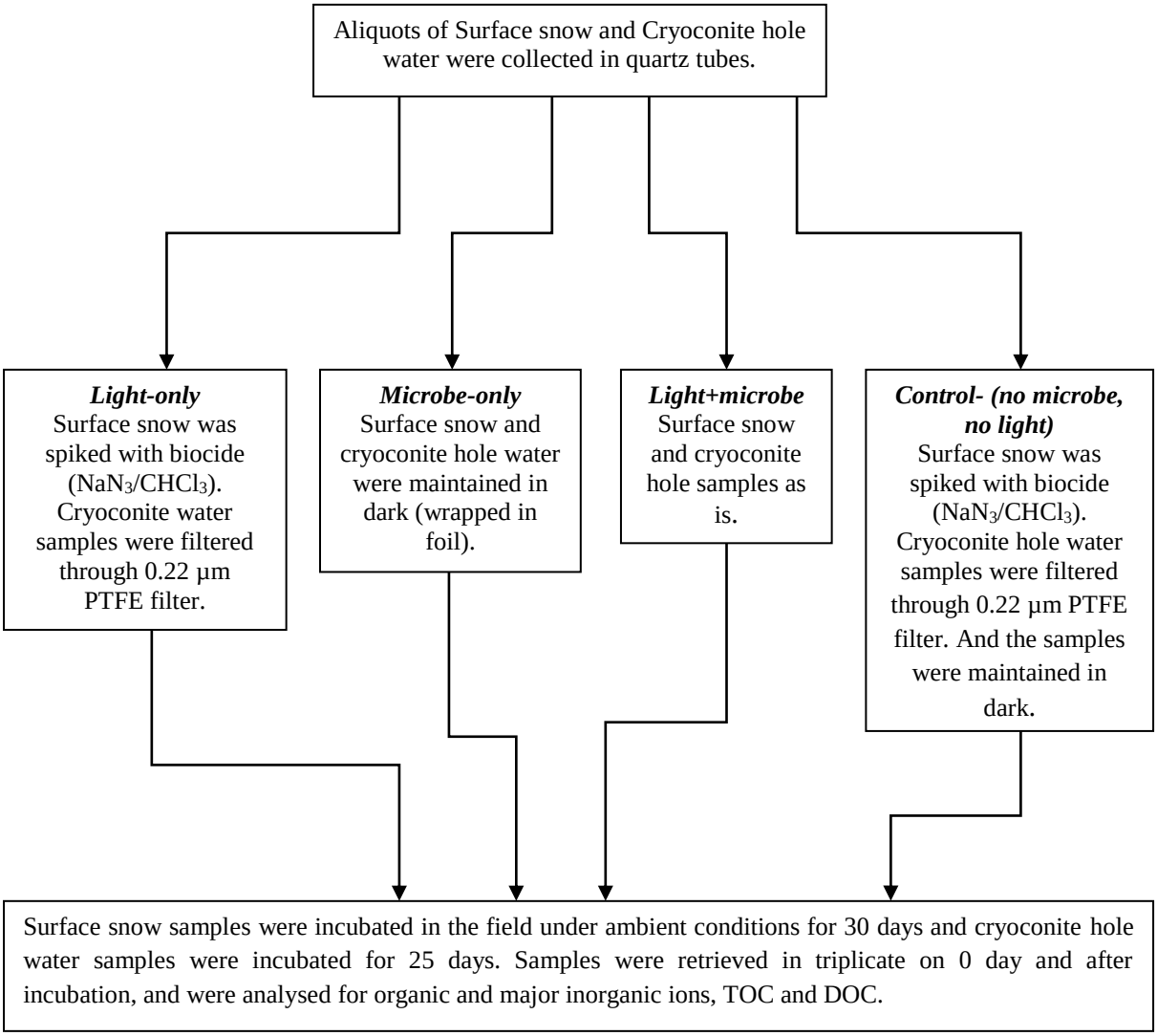

Fig. 2.7. Flowchart showing the incubation setup in the experimental system.

One cryoconite hole was monitored in its natural condition and the other cryoconite hole was shaded to inhibit the light penetration. Samples were collected in triplicates from both the cryoconite holes at the beginning (0 day) and at the end of the experiment

on 25th day. Samples for organic carbon analysis were collected in pre-cleaned and combusted glass containers. Samples for inorganic ion analysis were collected in pre-cleaned Polypropylene (PP) vials. Cryoconite hole sediment samples were collected in sterile Whirl-pak bags using sterile PP scoops. Stringent measures were taken while sampling to avoid any contamination. Flow chart in **Fig 2.8** shows the experimental setup in the natural system.

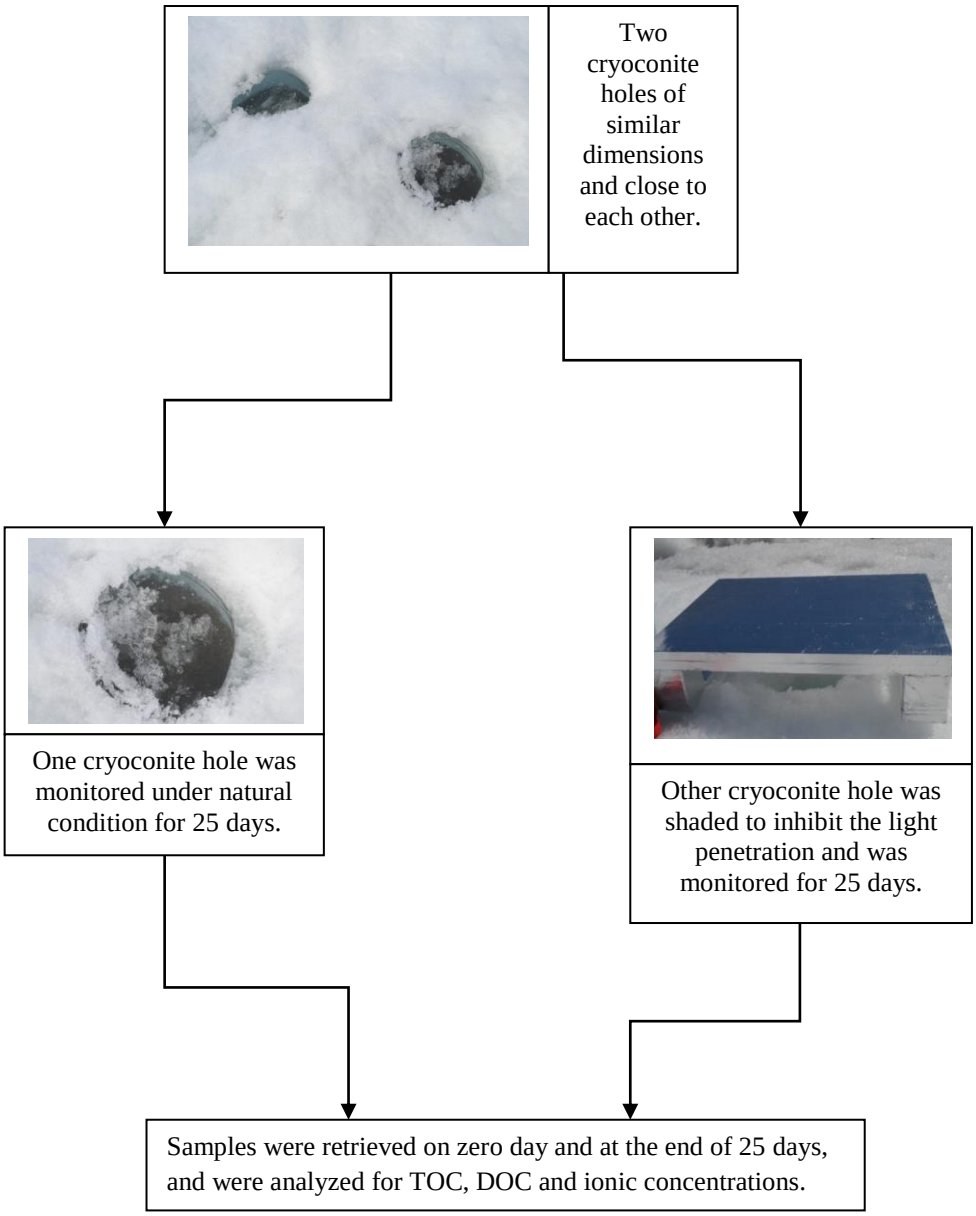

Fig. 2.8. Flowchart showing the experimental setup in the natural system.

2.4 Analytical Methods

2.4.1 Total Organic Carbon

Total organic carbon measurements in the supraglacial samples were carried out using high sensitivity TOC analyzer (Shimadzu TOC-V_{CPH}). For the TOC measurements, non-purgeable organic carbon (NPOC) method was used with the sample injection volume of 2 mL. Two millilitres of sample from the sealed vial placed in the auto-analyser was drawn into the syringe followed by addition of 2 mL of 2 N HCl (Trace metal grade) solution. High purity N_2 gas was sparged at a flowrate of 150 mL min^{-1} to eliminate the inorganic carbon from the samples. The sample free from inorganic carbon was automatically transported to the quartz combustion tube containing platinum catalyst and heated to 680 °C. This process converts the remaining carbon in the samples which is majorly the organic carbon, to CO_2. Carbon dioxide is then carried by the carrier gas through a dehumidifier and a halogen scrubber to the non-dispersive Infrared Detector (NDIR) cell for detection and quantification.

Calibration was carried out using the solution of reagent grade potassium hydrogen phthalate with concentration ranging from 10 to 500 µg L^{-1} and the carbon concentration in the ultrapure water used for the generation of the calibration curve was taken into account. To determine the detection limit, 12 blank samples comprised of fresh ultrapure water were analysed and the standard deviation (SD) was determined. Detection limit, defined as three times the ratio of SD to the slope of calibration curve with intercept zero, was determined to be 10.0 µg L^{-1}. The instrument blank determined using the automated blank checking program of the instrument was below detection limit (bDL). The carbon contamination from the 2 N HCl solution used for acidifying the samples during the analysis was determined by analysing the ultrapure water with increasing additions of acid and was found to be bDL. In order to check for possible contamination during the sample handling and melting, 3-4 blanks comprising ultrapure water were processed in a similar manner as that of samples over the course of a day of sample analysis. The blank measurements showed values ranging from bDL to 10 µg L^{-1}. Relative standard deviation of the measurements and the instrumental precision

based on replicate injections of the standard was better than 10%. Minimum of three measurements were recorded for each sample to ensure the repeatability.

Organic carbon in sediments were analysed in Total Organic Carbon analyzer (TOC-V series SSM-5000A from Shimadzu) with NDIR cell for detection and quantification. Glucose was used as the carbon standard. Prior to organic carbon measurement, each sediment sample was dried, powdered and treated with trace metal grade 2N HCl in order to remove inorganic carbon from the sample. Hundred milligram of treated sample was placed in a clean ceramic sample boat, which was transferred into a 900 °C catalytic (mixture of cobalt oxide and platinum) combustion chamber inside the SSM-5000A and oxidized to CO_2 in the presence of O_2. Carbon dioxide was then carried by O_2 for detection in the NDIR detector. The analytical precision was better than 5%.

Measurements of organic carbon present in trace level in supraglacial samples from remote regions may get influenced by organic gases present in atmosphere, storage conditions, as well as photolysis on exposure to light. Therefore, stringent precautions were taken beginning from the sample collection to organic carbon measurements. Containers and vials made of amber glass were used for sample collection, processing and standard preparation. Prior to use, the containers and vials were cleaned by soaking in 0.5% HNO_3 solution for 24 h followed by thorough rinsing in ultrapure water and combustion at 450 °C for 4 h. To avoid any overestimation of organic carbon caused by prolonged storage of melted sample, as well as, the intervention of organic gases present in the atmosphere, each sample was melted in screw tight glass containers inside a class-100 clean room just prior to the analysis using the TOC analyser. Contamination caused due to storage of samples in EPP boxes was determined by analysing the blanks comprising ultrapure water stored and analysed in the same way as the samples and was found to be bDL. In case of samples stored in LDPE bags, possible contamination from the material of the bag was estimated by analysing the samples from the outer portion touching the material of the bag, as well as, the sample from central portion of the bag that was at no time in contact with the

material. Organic carbon concentration in the samples from the outer portion was higher than sample from central portion by 108 µg L^{-1} (Antony et al., 2011). Thus, sub-sampling for OC measurements was carried out from the central portion of the LDPE bag in aseptic conditions under the laminar flow placed inside the -15 °C cold room.

2.4.2 Dissolved Organic Carbon

Dissolved Organic Carbon was measured in supraglacial samples using high sensitivity TOC analyzer (Shimadzu TOC-V_{CPH}) as described in section 2.4.1. Prior to analysis, samples were filtered through pre-cleaned 0.22 µm Omnipore PTFE filter (Merck Biosciences) to remove the particulate fraction of organic matter that is majorly comprised of microbial cells. The PTFE filters were cleaned by soaking in 10% trace metal grade HCl solution followed by thorough rinsing and soaking in fresh ultrapure water for 3 days with daily replacement of fresh water and a final rinse with fresh ultrapure water. Prior to each sample filtration, 1 L of ultrapure water was passed through the filter followed by measurement of background DOC concentration. Background DOC concentration ranged from bDL to 11.2 µg L^{-1}. Organic carbon (OC) measured in the sample before filtration represents the TOC concentration, while OC measured in sample after filtration represented the DOC concentration. Dissolved organic carbon concentration of each sample was corrected with respect to the background DOC concentration obtained from analysis of blanks.

2.4.3 Ionic chemistry

Ionic measurements in the supraglacial samples were carried out using ion chromatography placed in a class-100 clean room. Various ions measured in the samples included four major carboxylate ions, namely Acetate (Ac^-), Formate (Fo^-), Lactate (Lc^-) and Oxalate (Oxy^{2-}) and the major inorganic ions (Na^+, K^+, Mg^{2+}, Ca^{2+}, NH_4^+, $CH_3SO_3^-$, Cl^-, SO_4^{2-} and NO_3^-).

2.4.3.1 Carboxylate ions

Carboxylate ions were measured using Dionex ICS 2000, anion exchange Ion Chromatography system. Dionex ICS 2000 was equipped with an automated Eluent

Generator (EG50) and an electrical conductivity detector (CD25). IonPac AS11-HC (4 mm) column and IonPac AG11-HC (4 mm) Guard column with an ASRS-ULTRA Anion Self Regenerating Suppressor were used for the separation of carboxylate ions. Potassium hydroxide (KOH) was used as the eluent. The sample injection volume was 1 mL. The gradient program reported by Käkölä et al. (2008) for measurements of carboxylate ion was optimized in order to measure low concentrations of carboxylate ions found in supraglacial ecosystems in the Antarctic region. High purity carboxylate ion standard solutions from Inorganic Ventures (IV) with concentrations ranging from 1 to 20 µg L^{-1} were used for calibration. Detection limit was determined to be 0.1 µg L^{-1} for Ac^- and Fo^-, 1.0 µg L^{-1} for Oxy^{2-} and 2.0 µg L^{-1} for Lc^-.

Only glass containers and vials were used for preparation of standard solutions as well as for the collection and processing of supraglacial samples, in order to prevent any possible contamination from plastic material. Prior to use, the glass containers and vials were soaked in ultrapure water for 24 h followed by sonication in ultrapure water for 30 min at room temperature and combustion at 450 °C for 4 h. However, surface snow samples from PEL region (**Chapter 3**), used for carboxylate ions measurements were collected in LDPE bags due to logistic reasons. To estimate the possible contamination caused by the plastic material, concentration of carboxylate ions was determined in the snow sub-sampled from the outer portion touching the material of the bag as well as from central portion of the bag that was never in contact with the material of the bag. Carboxylate ion concentration in the outer portion of snow was determined to be 2-3 times higher than the central portion of snow. Thus, surface snow was sub-sampled from the central portion of the bag for carboxylate ion analysis. Measurements of various organic compounds present at trace levels in remote supraglacial environments may get influenced by contamination resulting from organic gases present in the atmosphere and by photolysis on exposure to light. Therefore, to prevent any analytical error, the chromatographic standards were analyzed on a daily basis throughout the period of analysis. The analytical precision estimated from the daily scrutiny of standards was better than 10% and each sample was analyzed in triplicate to ensure the repeatability of measurements. To prevent any light induced

transformation of carboxylate ions leading to error, amber glass containers and vials were used.

In order to estimate the possible contamination during the sample handling and melting, 4–6 blanks comprising ultrapure water were processed in a similar manner as that of the samples over the course of a day of sample analysis. The blank measurements showed values ranging from bDL to 6 µg L^{-1} for Ac^-, Fo^-, Lc^- and Oxy^{2-}. The respective daily blank values were subtracted from the sample values. Contamination caused during storage of samples in EPP boxes was estimated by measuring the carboxylate ion content in ultrapure water that was stored and analyzed in the similar way as the samples. The storage bottle blank values of the carboxylate ions were found to be below detection limit.

2.4.3.2 Inorganic ions

Inorganic anions ($CH_3SO_3^-$, Cl^-, SO_4^{2-} and NO_3^-) were measured using Dionex ICS 2000 as described for carboxylate ion analysis in **section 2.4.3.1**. Cations (Na^+, K^+, Mg^{2+}, Ca^{2+} and NH_4^+) were measured using Dionex DX-2500, cation exchange ion chromatography system equipped with DS 6 Conductivity Detector and CSRS-ULTRA Cation Self Regenerating Suppressor. IonPac CS17 column (4 mm) and IonPac CG17 Guard column (4 mm) were used for separation of the cations. Methanesulfonic acid (CH_3SO_3H) was used as eluent and the sample injection volume was 0.1 mL. Calibration was carried out using high-purity standards from Inorganic Ventures. Detection limits achieved were 2 µg L^{-1} ($CH_3SO_3^-$), 5 µg L^{-1} (Na^+, K^+, NH_4^+, SO_4^{2-}, NO_3^- and Cl^-) and 8 µg L^{-1} (Ca^{2+} and Mg^{2+}). Analytical precision for all the ions was found to be better than 10%.

2.4.4 Mineralogy of cryoconite sediment samples

Qualitative analysis of minerals in cryoconite sediment samples was carried out using X-ray Diffraction method. Prior to analysis, samples were powdered in an agate mortar and pestle. The diffraction studies were done from 3 to 75 °2θ using a

Rigaku UltimaIV powder diffractometer with CuK_{α} radiation with a scanning speed of 1.2 °2θ/min. Silicon was used as the internal standard.

2.4.5 Bacterial cell abundance and microbial morphology

Bacterial cell abundance was determined by epifluorescence microscopy method using Nikon Ti-U Eclipse at 1000× magnification. Frozen supraglacial samples were melted in class-100 clean room. Immediately after melting, 5 mL of melted sample was stained by adding 4',6-Diamidino-2-phenylindole (DAPY) to a final concentration of 5 μg mL^{-1} and incubated for 5 min. Sample was filtered through a brown 0.22 μm isopore polycarbonate track-etched membrane filter (Millipore) followed by counting under the microscope. Staining and filtration were carried out under clean conditions inside a laminar flow hood. The number of cells was counted in 20 random fields. Bacterial cell abundance was calculated using **equation 2.3** as:

$$\text{Bacterial cell abundance (cell mL}^{-1}) = \left(\frac{A_F}{A_g}\right) \times \frac{N}{V} \qquad \textit{equation 2.3}$$

where, A_F = area of filter occupied by sample (78.57 mm^2)

A_g = Area of grid in field of view (10^{-2} mm^2)

N = Average number of cells viewed

V = Volume of sample filtered (5 mL)

Controls comprising filtered ultrapure water were processed and observed under microscope in the similar manner as the samples. Bacterial cell abundance in controls was found to be 0 cell mL^{-1}.

Scanning electron microscopy was carried out using JEOL JSM-6360 Scanning Electron Microscope. Frozen supraglacial samples were melted in a clean room and 40-50 mL of the melted samples were concentrated onto sterile 0.22 μm nuclepore (Whatmann) filters in aseptic conditions. After air drying, dried filter papers were firmly fixed onto metal stub using conductive adhesive, and platinum coated using

JEOL JFC-1600 auto fine coater. The cellular morphology was observed under the Scanning Electron Microscope.

2.4.6 Dust particles

Dust particle concentration in the surface snow samples was measured using Multisizer 4 Coulter Counter (Beckman Coulter) placed in a class-100 clean room. Analysis of dust particles of size between 1 and 25 µm diameter was carried out using a 50 µm diameter aperture. Size calibration was carried out using polystyrene latex beads of 5 µm radius and a precision better than 5% was obtained. Particle mass concentration was determined using **equation 2.4** as:

$$\text{Particle mass } (\mu g\ L^{-1}) = 2.6 \times \text{Volume of particle} \times 10^{-3} \qquad \textit{equation 2.4}$$

where, the value 2.6 denotes average particulate density of the terrestrial dust, assuming most of the wind-blown soil dust density ranged between 2.5 and 2.7 g cm^{-3} (Sugimae, 1984).

Chapter 3

Glaciochemistry of surface snow and blue ice in coastal Antarctica

3.1 Introduction

Antarctic snow and ice serves as an archive providing information on aerosol sources, global atmospheric processes and long range transport and deposition (De Angelis et al., 2012; Erbland et al., 2013; Legrand and Mayewski, 1997; Li et al., 2015; Mahalinganathan et al., 2016; Udisti et al., 1998). It is also an important site for biogeochemical processes involving various inorganic, as well as, organic species (Couch et al., 2000; Dibb and Arsenault, 2002; Grannas et al., 2004; Swanson et al., 2002). Various studies in Antarctica have provided information on spatial and temporal variation in the chemical composition (inorganic and organic species) of snow and ice (Antony et al., 2014; Bertler et al., 2005; Mahalingathan et al., 2012, 2016). Sea spray, crustal components and secondary aerosols impact the ionic budget of Antarctic snow.

The major ionic species in snow such as Na^+, K^+, Ca^{2+}, Mg^{2+}, Cl^-, SO_4^{2-} and NO_3^- determine the ionic balance of the surface snow (Legrand, 1987). Few ionic species like Na^+, K^+, Ca^{2+} and Mg^{2+} can have a marine, as well as, crustal source (Thamban et al., 2010). Chloride ion is mainly originated from sea spray, but can also be deposited as HCl in snow (Benassai et al., 2005). Sulphate ion in snow can have inputs from volcanic eruption and anthropogenic sources, in addition to the well known contribution from sea spray (Legrand and Pasteur 1998; Udisti et al., 1999). Nitrate ion has multiple sources in Antarctic environment and predominantly results from atmospheric oxidation of nitrogen oxides, photo-dissociation of N_2 and via sedimentation from polar stratospheric clouds (Legrand and Delmas, 1986; Legrand and Mayewski, 1997, Rothlisberger et al., 2000). Carboxylic acids like acetic acid

(HAc) and formic acid (HFo) are the dominant organic species in the global troposphere (Keene and Galloway, 1988; Talbot et al., 1988) due to high polarity, water solubility and low molecular weight (Chebbi and Carlier, 1996). Carboxylic acids also add to the free acidity of the atmosphere (Galloway et al., 1982; Legrand and De Angelis, 1995). Earlier studies on carboxylic acids were majorly focused on the atmospheric budgets of these acids. Globally, carboxylate ions are derived from various natural sources such as emissions from soil and vegetation (Keene and Galloway, 1988) and anthropogenic sources like biomass burning (Paulot et al., 2011; Talbot et al., 1988), while secondary sources include photochemical processes (Atkinson, 2007). Photochemical sources include ozonolysis of isoprene (majorly emitted from vegetation) producing HFo in the atmosphere (Jacob and Wofsy, 1988; Legrand and De Angelis, 1996; Souza and Carvalho, 2001). In Antarctica, year round atmospheric monitoring of HFo and HAc suggest photo-oxidation of low-molecular weight alkenes by ozone, reactions of peroxy acetyl radical with peroxyl radicals and oxidation of formaldehyde (and acetaldehyde) by hydroxyl radical ($^{\cdot}OH$) as the major sources of these acids (Legrand et al., 2004, 2012). Studies on carboxylate ion composition within snow/ice are limited and show low concentrations (Legrand and Saigne, 1988; Legrand et al., 2013; Udisti et al., 1991) which suggest poor preservation (De Angelis and Legrand, 1995) and inefficient incorporation of the acids within snow. Sources of carboxylate ions such as acetate (Ac^-) and formate (Fo^-) within snow include long range transport of anthropogenic emissions (Udisti et al., 1998) and marine emissions (Li et al., 2015). In addition, there is some evidence that photochemical production within the snowpack can also affect the composition of carboxylate ions (Dibb and Arsenault, 2002). Apart from being involved in photochemical processes, they are also important organic substrates for micro-organisms residing in surface snow (Amato et al., 2007; Antony et al., 2016).

Understanding the sources and sinks of these ions in the Antarctic snow can significantly help in understanding their role in biogeochemical cycling in these environments. However, spatial studies are imperative for an improved understanding

of the distribution, sources and transformation processes of both inorganic and organic constituents in snow, and their influence on biogeochemical processes. In addition, due to enhanced melting of the glaciers and subsequent drainage across the ice sheets and runoff to the open ocean, Antarctic snow can potentially influence the downstream ecosystem by feeding it with glacial microbes, organic matter and nutrients. Another environment that is of significance, but highly understudied are blue ice regions that are formed when snow cover is removed by strong winds and/or sublimation (Hodson et al., 2013). Surface albedo plays an important role in surface melting in Antarctica (Lenarets et al., 2017). Low albedo blue ice facilitates melting by increasing the absorption of solar radiation and significantly contributing to the meltwater drainage systems in Antarctica (Kingslake et al., 2017; Liston et al., 1999). Due to the surface and sub-surface melting during the warming season and subsequent freezing in the winter season (Liston et al., 1999), blue ice undergoes a freeze thaw cycle. Studies suggest that blue ice areas provide a habitat for microbial life, supporting both heterotrophic and photosynthetic activities (Hodson et al., 2013). However, studies on the composition of inorganic and organic components and the impact of such habitats on biogeochemical processes are severely limited. Therefore, an understanding of the chemical composition of snow and ice would be crucial in elucidating their contribution to supraglacial biogeochemical processes.

In this chapter, spatial trend of ionic species (Na^+, Ca^{2+}, Mg^{2+}, K^+, NH_4^+, Cl^-, SO_4^{2-}, NO_3^-, $CH_3SO_3^-$, Ac^- and Fo^-) in 18 surface snow samples collected along a 180 km coastal-inland transect in Princess Elizabeth Land (PEL) and 13 samples along a 130 km coastal transect in Amery Ice Shelf (AIS) have been presented along with their possible sources and implications for snow chemistry. An attempt has also been made to understand the chemical composition of blue ice in Larsemann Hills (LHS) (3 cores) and AIS (2 cores), in East Antarctica.

3.2 Results

3.2.1 Surface Snow

3.2.1.1 Princess Elizabeth Land (PEL)

Major inorganic ion (Na^+, Ca^{2+}, Mg^{2+}, K^+, NH_4^+, Cl^-, SO_4^{2-}, NO_3^- and $CH_3SO_3^-$) concentrations in the 180 km coastal-inland transect are as given in **Table 3.1**. Majority of the ions except NO_3^- and Ca^{2+} showed a significant decreasing trend ($n = 18$; $p<0.05$) with increasing distance from the coast (**Fig. 3.1**).

Table 3.1. Major ion (Na^+, Ca^{2+}, Mg^{2+}, K^+, NH_4^+, Cl^-, SO_4^{2-}, NO_3^-, $CH_3SO_3^-$) and H^+ concentrations in surface snow samples at Princess Elizabeth Land.

Distance from coast (km)	Na^+	Ca^{2+}	Mg^{2+}	K^+	NH_4^+	Cl^-	SO_4^{2-}	NO_3^-	$CH_3SO_4^-$	H^+
	μg L^{-1}									μeq L^{-1}
10	650	284	26	38	86	1026	144	56	33	-17.3*
20	348	23	36	18	17	439	217	58	33	-2.6
30	176	22	13	20	14	356	154	77	25	4
40	163	29	12	42	7	472	125	73	3	6.4
50	173	23	15	19	14	357	99	51	10	1.8
60	110	13	9	10	4	227	71	54	7	2.2
70	125	25	11	26	5	216	77	61	5	0.4
80	92	17	8	10	4	207	67	87	13	2.9
90	123	24	12	17	14	262	90	117	8	2.7
100	65	17	6	11	13	144	51	72	18	1.5
110	53	7	2	11	5	109	33	39	4	1.2
120	64	6	5	4	9	140	63	66	5	2.4
130	47	6	2	6	4	107	47	81	4	2.5
140	73	18	5	8	4	157	55	107	6	2.5
150	66	14	5	10	11	143	50	128	6	3
160	36	21	2	4	4	81	46	82	7	1.9
170	53	22	4	6	4	118	52	132	4	3.3
180	44	12	2	7	22	103	74	131	9	2.6

*Negative values of H^+ represent alkalinity (or HCO_3^- concentration).

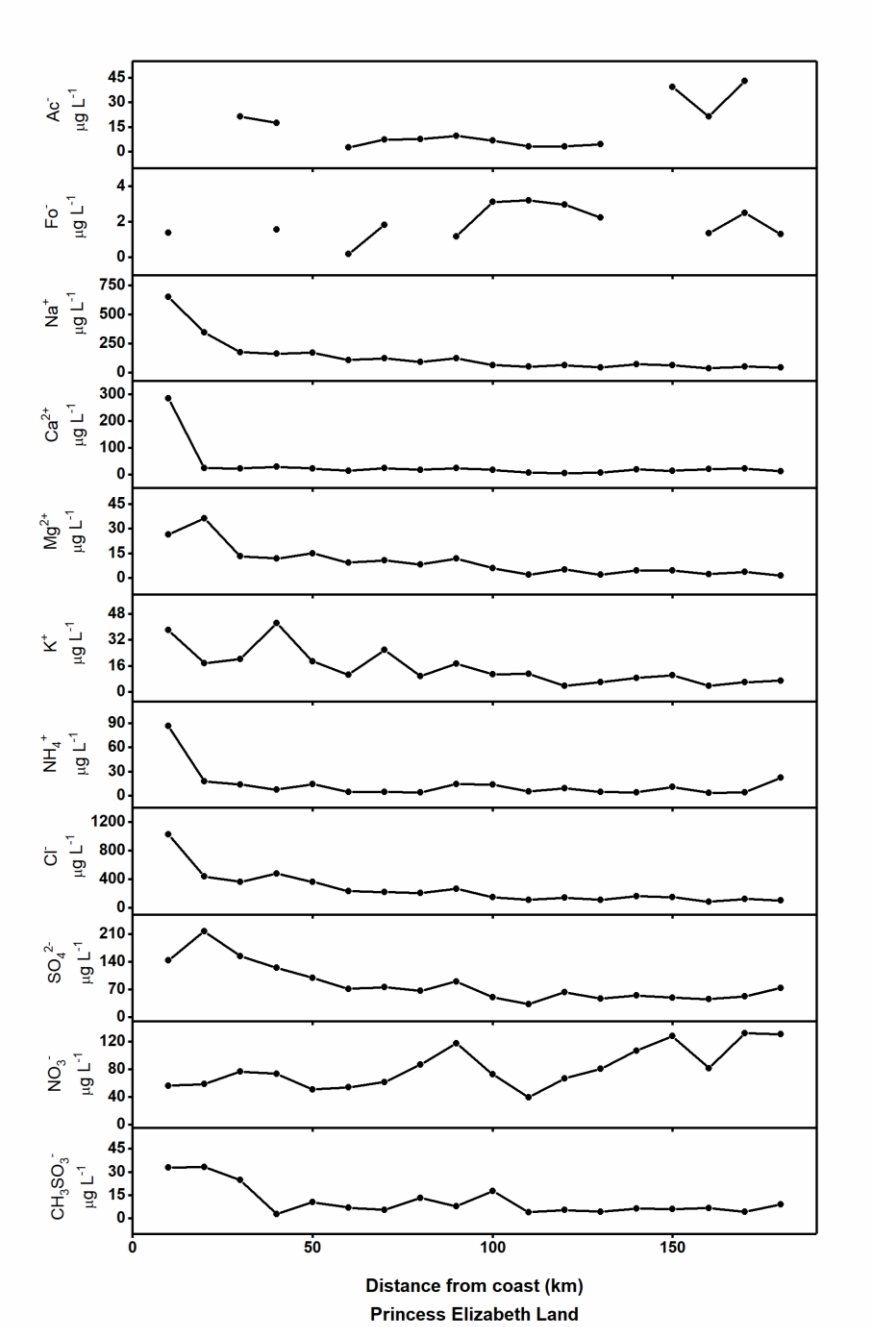

Fig. 3.1. Spatial trend of major ions and carboxylate ions in Princess Elizabeth Land.

At PEL, the inorganic ion composition was dominated by Cl^- (30%), followed by Na^+ (23%), SO_4^{2-} (9%), NO_3^- (8%), Ca^{2+} (5%) and other ions (3%). Concentration of sea salt Na^+ ($ssNa^+$), a conservative proxy for sea spray in coastal Antarctica (Traversi et al., 2004), was estimated using **equation 3.1** (Röthlisberger et al., 2002):

$$ssNa^+ = \frac{[R_t \times Na^+ - Ca^{2+}]}{[R_t - R_m]} \qquad \textit{equation 3.1}$$

where, R_t (average ratio of Ca^{2+}/Na^+ in crustal system) is assumed to be 1.78 and R_m (average ratio of Ca^{2+}/Na^+ in marine system) is assumed to be 0.038. In PEL, $ssNa^+$ (24 - 501 μg L^{-1}, mean - 121 μg L^{-1}) contributed to 89% of the total Na^+ (36 - 650 μg L^{-1}, mean - 137 μg L^{-1}). In addition, $ssNa^+$ showed a strong negative correlation ($n = 18$; $p<0.001$) with the increasing distance from the sea coast, suggesting a strong marine contribution to the snow chemistry at PEL. Concentration of non sea salt Ca^{2+} ($nssCa^{2+}$), a proxy for mineral dust (Ruth et al., 2008), was estimated using **equation 3.2** (Röthlisberger et al., 2002):

$$nssCa^{2+} = Ca^{2+} - (Ca^{2+}/\ Na^+)_{\text{sea water}} \times Na^+ \qquad \textit{equation 3.2}$$

where, $(Ca^{2+}/\ Na^+)_{\text{sea water}}$ is the ratio of Ca^{2+} and Na^+ in sea water and is assumed to be 0.038 (Chester, 2003). The $nssCa^{2+}$ (3 - 59 μg L^{-1}) contributed to 77% of the total Ca^{2+} concentration (6 - 284 μg L^{-1}), indicating a significant contribution from crustal sources. Acidity (or alkalinity) in the samples was estimated using the ionic balance equation (**equation 3.3**) as:

$$H^+ = (Cl^- + SO_4^{2-} + NO_3^- + CH_3SO_3^- + Ac^- + Fo^-) - (Na^+ + K^+ + Ca^{2+} + Mg^{2+} + NH_4^+)$$

equation 3.3

Estimation of H^+ concentration showed that the majority of the samples were acidic except for two coastal samples (10 and 20 km) which were alkaline in nature (HCO_3^-: 17.3 and 2.6 μeq L^{-1}, **Table 3.1**). Total organic carbon (TOC) concentration in the surface snow samples ranged from 88±6 to 271±3 μg L^{-1} (Antony et al., 2011, **Table 3.2**).

Table 3.2. Concentrations of Ac^-, Fo^- and total organic carbon (TOC) in surface snow samples at Princess Elizabeth Land and Amery Ice Shelf.

Distance from Coast (km)	Princess Elizabeth Land			Amery Ice Shelf		
	Ac^-	Fo^-	TOC*	Ac^-	Fo^-	TOC
	μg L^{-1}					
10	bDL**	1.38±1.04	115±5	bDL	0.61±0.08	96.0±2.8
20	bDL	bDL	158±4	1.88±0.61	6.66±0.09	54.0±2.3
30	21.47±0.61	bDL	156±5	15.23±0.84	21.00±0.31	26.7±1.1
40	17.47±2.00	1.56±0.27	164±9	bDL	bDL	56.7±1.1
50	bDL	bDL	207±9	0.29±1.07	3.24±0.21	bDL
60	2.60±1.51	0.20±0.00	128±8	4.04±0.06	7.11±0.07	52.4±1.4
70	7.40±0.87	1.82±0.12	137±7	3.93±0.93	6.21±0.03	50.5±0.9
80	7.67±0.83	bDL	166±5	5.96±0.11	8.36±0.04	51.8±2.4
90	9.67±1.17	1.17±0.11	123±15	bDL	0.14±0.06	15.7±0.5
100	6.79±0.41	3.12±0.11	202±4	bDL	0.74±0.07	49.2±2.3
110	3.09±0.24	3.19±0.04	88±6	bDL	0.69±0.11	117.6±2.9
120	3.30±0.14	2.95±0.08	210±15	1.05±0.19	2.52±0.06	110.6±1.8
130	4.60±0.20	2.23±0.15	271±3	bDL	5.43±0.04	65.5±0.2
140	bDL	bDL	158±15	.	.	.
150	39.20±1.20	bDL	171±11	.	.	.
160	21.47±0.00	1.36±0.07	158±4	.	.	.
170	42.93±0.00	2.48±0.96	214±8	.	.	.
180	bDL	1.31±0.11	269±6	.	.	.

*TOC concentration at PEL is from Antony et al., 2011; **below detection limit.

The concentration of carboxylate ions, Ac^- and Fo^-, along the 180 km coastal-inland transect ranged from below detection limit (bDL) to 42.93±0.00 μg L^{-1} (mean, 14.4 μg L^{-1}) and bDL to 3.19±0.04 μg L^{-1} (mean, 1.90 μg L^{-1}), respectively (**Table 3.2**). Acetate concentration varied widely along the 180 km transect, while Fo^- exhibited a narrow range over the entire transect. In the coastal region (10 - 50 km) of the 180 km transect, Ac^- concentration varied significantly from bDL to 21.47±0.61 μg L^{-1} (mean, 19.47 μg L^{-1}). In the inland region from 50 to 130 km, Ac^- concentration showed only a narrow variation ranging between 2.60±1.51 and 9.67±1.17 μg L^{-1} (mean, 5.64 μg L^{-1}), while beyond 130 km, a wide variation in Ac^- concentrations ranging from bDL to 42.93±0.00 μg L^{-1} (mean, 34.53 μg L^{-1}) was observed.

3.2.1.2 Amery Ice Shelf (AIS)

Major inorganic ion (Na^+, Ca^{2+}, Mg^{2+}, K^+, NH_4^+, Cl^-, SO_4^{2-} and NO_3^-) concentrations in the surface snow samples are given in **Table 3.3**.

Table 3.3. Major ion (Na^+, Ca^{2+}, Mg^{2+}, K^+, NH_4^+, Cl^-, SO_4^{2-}, NO_3^-) and H^+ concentrations in surface snow samples at Amery Ice Shelf.

Distance from coast (km)	Na^+	Ca^{2+}	Mg^{2+}	K^+	NH_4^+	Cl^-	SO_4^{2-}	NO_3^-	H^+
	μg L^{-1}								μeq L^{-1}
10	150	17	7	8	13	291	29	6	0.1
20	523	35	72	30	bDL*	646	167	13	-9.2**
30	239	24	52	13	bDL	467	162	17	1.3
40	85	9	11	3	10	141	28	9	-1
50	134	16	25	5	12	231	53	13	-1.6
60	578	56	165	31	bDL	753	302	18	-14.5
70	254	26	58	12	16	393	90	15	-4.9
80	85	14	19	4	7	151	55	14	-0.5
90	292	12	18	5	bDL	430	36	5	-2.4
100	117	17	23	10	bDL	240	48	12	-0.2
110	118	20	21	7	10	238	47	12	-0.8
120	59	20	5	5	5	119	15	6	-0.6
130	77	17	11	7	15	162	25	9	-0.8

*below detection limit; **Negative values of H^+ represent alkalinity (or HCO_3^- concentration).

Along the coastal transect, all the ions except NO_3^- showed a slight decreasing trend with the increasing distance from the coast (**Fig. 3.2**). Sea salt Na^+ (49 - 514 μg L^{-1}, mean - 201 μg L^{-1}) contributed to >94% of the total Na^+ (59 - 523 μg L^{-1}, mean - 208 μg L^{-1}) indicating high sea spray influence along the coastal transect of AIS. Non sea salt Ca^{2+} (1 - 34 μg L^{-1}, mean - 14 μg L^{-1}) contributed to 64% of the total Ca^{2+} (9 - 56 μg L^{-1}, mean - 22 μg L^{-1}) indicating a substantial crustal influence to the study region. This concurs with the high dust concentrations ranging between 10 - 48 mg L^{-1} in the snow samples. Ionic balance shows the dominance of Cl^- (36%) followed by Na^+ (32%), Mg^{2+} (10%), SO_4^{2-} (6%) and Ca^{2+} (5%). Estimation of H^+ concentration showed that majority of the samples were alkaline except for the samples at 10 and 30 km which were acidic (H^+: 0.1 and 1.3 μeq L^{-1} respectively, **Table 3.3**).

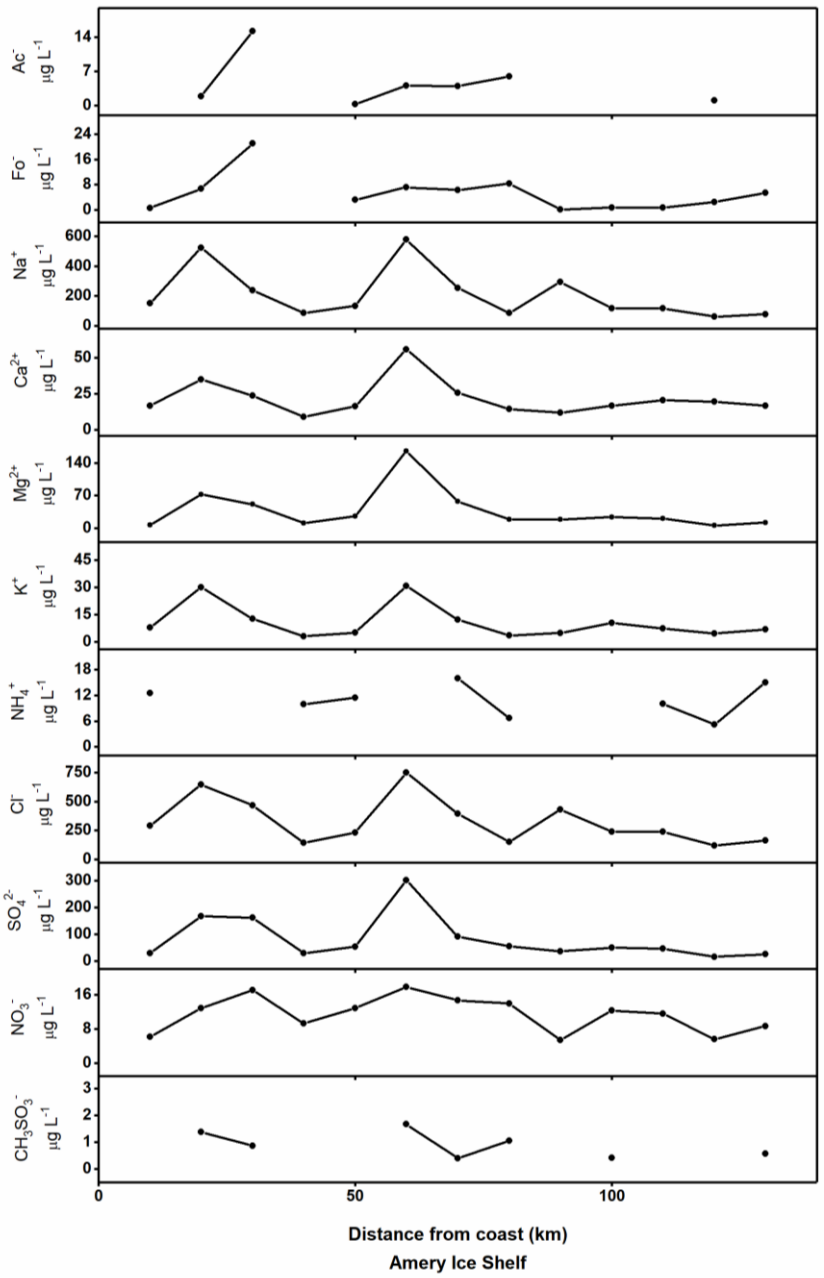

Fig. 3.2. Spatial trend of major ions and carboxylate ions in Amery Ice Shelf.

The concentration of Ac^- and Fo^- along the 130 km coastal transect at AIS ranged from bDL to 15.23±0.84 µg L^{-1} (mean, 4.63 µg L^{-1}) and bDL to 21.00±0.31 µg L^{-1} (mean,

5.23 μg L^{-1}), respectively (**Table 3.2**). Both the carboxylate ions showed a slight decrease with increasing distance. Total organic carbon concentration ranged from bDL to 117.6±2.9 μg L^{-1} (mean, 57.83 μg L^{-1}) (**Table 3.2**). Microbial cell densities in the AIS samples ranged between 0.16 × 10^4 and 10.34 × 10^4 cells mL^{-1}. Microscopic examination revealed the presence of bacteria and diatom frustules (**Fig. 3.3**).

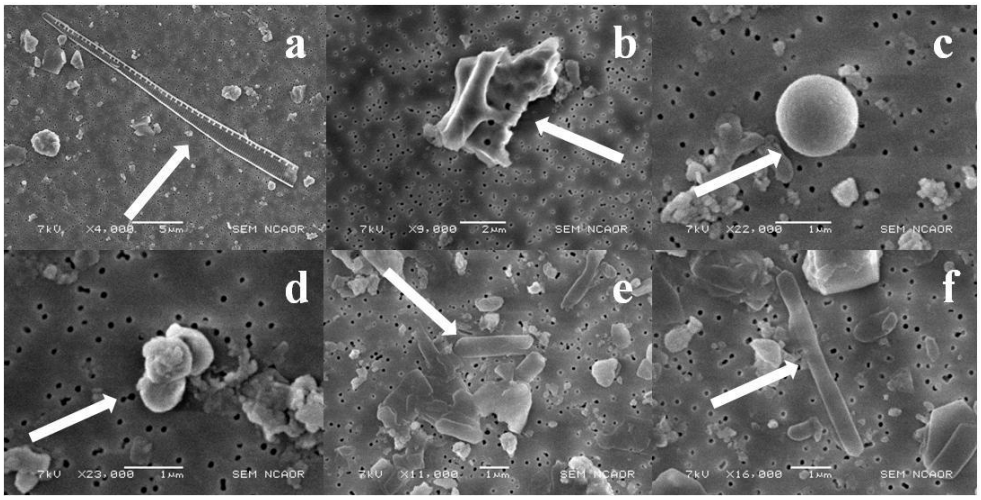

Fig.3.3. Microscopy images of diatom frustules (a, b), bacteria (cocci) (c, d) and rod shaped bacteria (e, f) found in the surface snow samples from Amery Ice Shelf.

3.2.2 Blue ice

Concentration of major ions (Na^+, K^+, Ca^{2+}, Mg^{2+}, Cl^-, SO_4^{2-} and NO_3^-), carboxylate ions (Ac^- and Fo^-) and TOC, in the blue ice samples from LHS and AIS are as given in **Table 3.4**. Two/three sub-samples from each core were analyzed to ensure repeatability of the measurements in a core. To understand the trend of ionic composition in blue ice, ion concentrations in blue ice were compared to annual snow deposits (1 m depth) from the same study regions by estimating the enrichment factor (EF) of the ions using **equation 3.4** as:

$$\mathrm{EF(i)} = \mathrm{C(i)}_{\text{Blue Ice}} / \mathrm{C(i)}_{\text{Snow Deposit}} \qquad \textit{equation 3.4}$$

where, $C(i)_{Blue\ Ice}$ and $C(i)_{Snow\ Deposit}$ are the ion concentrations in blue ice and snow deposit, respectively. Estimated EFs of the ions are as given in **Table 3.5**. Total cell density in the blue ice samples ranged from 0.46×10^4 to 0.90×10^4 cells mL^{-1}.

Table 3.4. Major ion (Na^+, K^+, Mg^{2+}, Ca^{2+}, Cl^-, SO_4^{2-} and NO_3^-), carboxylate ion (Ac^- and Fo^-) and TOC concentration in the blue ice samples from Larsemann Hills and Amery Ice Shelf.

Sample ID	Na^+	K^+	Mg^{2+}	Ca^{2+}	Cl^-	SO_4^{2-}	NO_3^-	Ac^-	Fo^-	TOC
	μg L^{-1}									
Larsemann Hills										
BI 1-1	979	33	38	374	257	43	181	5.78±0.10	13.76±0.44	46.0
BI 1-2	961	93	55	905	295	54	302	13.67±0.33	10.24±0.12	289.4
BI 1-3	1518	62	37	366	402	73	204	10.56±0.45	17.34±0.33	71.6
BI 4-1	1031	21	16	197	65	12	233	22.67±0.56	20.35±0.67	81.0
BI 4-2	1069	11	20	281	89	17	145	13.53±0.10	19.80±0.28	85.4
BI 7-1	3818	19	36	317	1019	38	125	9.22±0.22	10.45±0.85	49.5
BI 7-2	3382	23	91	422	800	26	71	15.01±0.44	17.25±0.12	78.3
BI 7-3	1198	51	88	340	488	123	191	14.58±0.01	5.54±0.03	45.6
Amery Ice Shelf										
BI8-1	834	11	50	107	567	104	337	11.23±0.25	9.58±0.83	78.3
BI8-2	638	23	91	122	483	98	382	10.34±0.54	9.34±0.65	108.0
BI10-1	374	8	40	68	467	60	144	3.58±0.72	10.98±0.35	107.3
BI10-2	547	31	29	116	615	63	66	6.54±0.03	10.01±0.26	135.5

3.3 Discussion

3.3.1 Ionic balance

Majority of the surface snow samples in the PEL transect were found to be acidic (H^+: 0.4 - 6.4 μeq L^{-1}), except for two samples at 10 and 20 km (HCO_3^-: 17.3 and 2.6 μeq L^{-1}) which were alkaline. In contrast, majority of the samples at AIS were alkaline (HCO_3^-: 0.2 - 14.5 μeq L^{-1}), except for two samples at 10 and 30 km, which were estimated to be acidic (H^+: 0.1 and 1.3 μeq L^{-1}). The ions, SO_4^{2-}, Cl^- and NO_3^- that are associated with the inorganic acids H_2SO_4, HCl and HNO_3 respectively,

determine the acidity (or alkalinity) of snow (Delmas and Gravenhorst, 1982; Legrand, 1987).

Table 3.5. Enrichment factor of Na^+, K^+, Mg^{2+}, Ca^{2+}, Cl^-, SO_4^{2-} and NO_3^- in blue ice samples from Larsemann Hills and Amery Ice Shelf.

	EF						
Sample ID	**Na^+**	**K^+**	**Mg^{2+}**	**Ca^{2+}**	**Cl^-**	**SO_4^{2-}**	**NO_3^-**
Larsemann Hills							
BI 1-1	3.4	1.9	1.1	8.1	0.4	0.3	1.3
BI 1-2	3.3	5.2	1.5	19.7	0.5	0.4	2.2
BI 1-3	5.3	3.5	1.0	8.0	0.7	0.5	1.5
BI 4-1	3.6	1.2	0.4	4.3	0.1	0.1	1.7
BI 4-2	3.7	0.6	0.6	6.1	0.1	0.1	1.0
BI 7-1	13.2	1.1	1.0	6.9	1.7	0.3	0.9
BI 7-2	11.7	1.3	2.5	9.2	1.3	0.2	0.5
BI 7-3	4.1	2.8	2.4	7.4	0.8	0.9	1.4
Amery Ice Shelf							
BI 8-1	0.4	0.1	0.3	2.3	0.9	0.9	3.2
BI 8-2	0.3	0.2	0.5	2.6	0.8	0.8	3.6
BI 10-1	0.2	0.1	0.2	1.5	0.7	0.5	1.4
BI 10-2	0.2	0.2	0.2	2.5	1.0	0.5	0.6

In Antarctic surface snow, apart from the contribution of the sea salt aerosols to the total SO_4^{2-} concentration (Rankin et al., 2000), oxidation of SO_2 originated from biogenic, anthropogenic and volcanic emissions in the atmosphere contributes to the $nssSO_4^{2-}$ content in the form of H_2SO_4 (Legrand and Pasteur,1998). However, in the remote marine atmosphere of Antarctica, oxidation of dimethyl sulphide (DMS) (sourced from marine biogenic emissions) leads to production of H_2SO_4 together with methanesulphonic acid (CH_3SO_3H) and is considered the major source of $nssSO_4^{2-}$ (Legrand and Pasteur, 1998; Udisti et al., 1999). In coastal Antarctica, $nssSO_4^{2-}$ was estimated using **equation 3.5** (Maupetit and Delmas, 1992):

$$nssSO_4^{2-} = SO_4^{2-} - (SO_4^{2-}/\ Na^+)_{\text{sea water}} \times Na^+ \qquad \textit{equation 3.5}$$

where, $(SO_4^{2-}/ Na^+)_{sea\ water}$ is the ratio of SO_4^{2-} and Na^+ in seawater and is assumed to be 0.252 (Chester, 2003). At PEL, $nssSO_4^{2-}$ (23 - 130 μg L^{-1}, mean - 54 μg L^{-1}) was found to contribute to 67% of the total SO_4^{2-} concentration (33 - 216 μg L^{-1}, mean - 84 μg L^{-1}), indicating its possible contribution to the acidity of surface snow at PEL. However, interaction between H_2SO_4 and salts like NaCl leading to the neutralisation of the acid is a well known process occurring in the Antarctic atmosphere (Legrand and Delmas, 1988). At PEL, significant correlation observed between SO_4^{2-} and major cations (Na^+, Mg^{2+}, Ca^{2+} and K^+) ($n = 18$; $p<0.01$) suggests the presence of SO_4^{2-} as salts of these cations (Na^+, Mg^{2+}, Ca^{2+} and K^+) in the surface snow. In addition, estimations from ionic balance revealed that SO_4^{2-} contributes to only 8.5% of the total ion concentration in the surface snow samples. Of this, only 1.5% contributes to the acidity of snow, while the rest is present in the form of salts of NH_4^+ (3.0%), Na^+ (2.2%), Mg^{2+} (1.5%) and Ca^{2+} (0.1%).

Similarly, in addition to a major sea salt aerosol contribution to Cl^- in coastal Antarctica (Thamban et al., 2010), an additional source of Cl^- in the form of HCl results from the interaction between NaCl and HNO_3/H_2SO_4 (Benassai et al., 2005; Udisti et al., 1999), which can contribute to the acidity of snow. Concentration of excess Cl^- derived from such non sea-salt sources was estimated using **equation 3.6** (Legrand and Delmas, 1988):

$$\text{Excess } Cl^- = Cl^- - (Cl^-/Na^+)_{sea\ water} \times Na^+ \qquad \textit{equation 3.6}$$

where, $(Cl^-/Na^+)_{sea\ water}$ is the ratio of Cl^- and Na^+ in sea water and is assumed to be 1.8 (Chester, 2003). In the surface snow samples at PEL, Cl^-/Na^+ ratio ranged from 1.3 to 2.9 (mean, 2.1, **Table 3.6**), where values > 1.8 suggest an additional source of Cl^-. The excess Cl^- (39 - 280 μg L^{-1}, mean - 98 μg L^{-1}) comprised 42% of the total Cl^- concentration indicating that it can appreciably contribute to the acidity of surface snow. However, only a small deviation of Cl^-/Na^+ (mean, 2.1, **Table 3.6**) from the sea salt ratio of 1.8 in the snow samples suggest that only a small fraction of Cl^- contributes to the acidity in surface snow. This is also corroborated by the ionic balance estimations showing that Cl^- contributes to 30% of the total ionic concentration of

which only 3.6% contributes to the acidity in snow and the rest is present in form of salts of Na^+ (19%), Ca^{2+} (5.2%), K^+ (1.7%) and Mg^{2+} (1.5%). This is further supported by the strong correlation (n = 18; $p<0.005$) observed between the cations (Na^+, Mg^{2+}, Ca^{2+} and K^+) and Cl^-.

Unlike $nssSO_4^{2-}$ and excess Cl^-, NO_3^- is thought to have multiple sources in the Antarctic environment. In Antarctic snow, it predominantly results from stratospheric and tropospheric transport of HNO_3 and subsequent deposition in the surface snow (Michalski et al., 2005). Nitrate concentrations ranged from 39 to 132 μg L^{-1} in the snowpack and did not show any systematic trend with changes in distance from the coast. Due to multiple sources of NO_3^- in snow, its distribution does not show any relation with the proximity to the ocean, elevation or with other ions (Bertler et al., 2005). But certain studies have observed higher NO_3^- concentration in the interior regions of Antarctica (Erbland et al., 2013, 2015). Similarly, the inland region at PEL in this study was characterized by relatively higher values of NO_3^- (**Table 3.1, Fig. 3.1**). Nitrate concentration at PEL ranged between 39 and 132 μg L^{-1}. No significant correlation was observed between the cations (Na^+, Mg^{2+}, Ca^{2+} and K^+) and NO_3^-, which indicates weak or insignificant interaction between the dust minerals and NO_3^-. Thus, it is suggested that NO_3^- which comprises 8% of the total ion concentration is majorly present in the form of HNO_3 and significantly contributes to the total acidity of surface snow. An exception is the coastal sample at 10 km which was highly alkaline (HCO_3^-: 17.3 μeq L^{-1}), possibly due to the proximity to the sea and absence of $nssSO_4^{2-}$. In addition, the high dust and $nssCa^{2+}$ (77% of total Ca^{2+}) concentrations in this sample indicate the possibility that salts like $Ca(NO_3)_2$ could be formed (Mahalinganathan et al., 2016), thereby neutralising HNO_3 (Gibson et al., 2006).

Table 3.6. Cl^-/Na^+ ratio in the surface snow samples at Princess Elizabeth Land and Amery Ice Shelf.

Distance from coast (km)	Cl^-/Na^+	
	Princess Elizabeth Land	**Amery Ice Shelf**
10	1.6	1.9
20	1.3	1.2
30	2	2
40	2.9	1.7
50	2.1	1.7
60	2.1	1.3
70	1.7	1.5
80	2.2	1.8
90	2.1	1.5
100	2.2	2
110	2	2
120	2.2	2
130	2.3	2.1
140	2.2	.
150	2.2	.
160	2.3	.
170	2.2	.
180	2.3	.

In AIS, majority of the samples were alkaline possibly due to the proximity to the sea. Sea salt Na^+ concentrations (49 - 514 μg L^{-1}, mean - 201 μg L^{-1}) comprised 94% of the total Na^+ indicating high sea spray influence over the coastal transect. This is supported by Cl^-/Na^+ of ~1.8 for these samples demonstrating a dominant marine source for Cl^- **(Table 3.6)**. Further, high concentrations of $ssSO_4^{2-}$ (12 - 141 μg L^{-1}, mean - 47 μg L^{-1}), constituting 62% of the total SO_4^{2-}, also indicates a substantial marine influence. High dust inputs ($nssCa^{2+}$: 1 - 34 μg L^{-1}, mean - 14 μg L^{-1}) comprising 64% of total Ca^{2+} suggest that the interaction between dust minerals and the anions ($nssSO_4^{2-}$, excess Cl^- and NO_3^-) could result in the neutralization of the acids, thereby contributing to the alkalinity of snow. This is further supported by the

strong correlation (n = 13; $p<0.001$) observed between the anions ($nssSO_4^{2-}$, excess Cl^- and NO_3^-) and the cations (Na^+, Ca^{2+}, Mg^{2+} and K^+).

In the case of blue ice, ionic composition was dominated by Na^+ (36%), Ca^{2+} (10%) and Cl^- (11%) followed by K^+, Mg^{2+}, SO_4^{2-}, Ac^-, Fo^- and NO_3^-. Ionic concentration measured in the blue ice samples varied significantly from the annual snow deposits and surface snow samples from the same regions (**Table 3.7**). A previous study carried out in the Vestfold Hills region reports the ionic concentration of glacier ice collected from a blue ice area (Hodson et al., 2013). Concentration of Na^+ and Ca^{2+} obtained in this study are consistent with the blue ice studied in the Vestfold Hills region, while Cl^- and SO_4^{2-} concentrations were lower and NO_3^- concentration was higher in this study compared to the Vestfold Hills values (**Table 3.7**). Dominance of Ca^{2+} (11%) over Cl^- (5%) was observed in LHS, while Cl^- (22%) dominated Ca^{2+} (7%) in AIS. Few ions such as Na^+ and Ca^{2+} were present in higher concentrations in LHS than AIS which may be attributed to coastal influence of sea salt aerosol deposition. Enrichment factor of ions estimated with respect to annual snow deposit concentrations showed significant enrichment of Na^+ (mean EF, 6.0) and Ca^{2+} (mean EF, 8.7), while Cl^- (mean EF, 0.7) and SO_4^{2-} (mean EF, 0.3) were depleted (**Table 3.5**). However, no significant difference was observed in Mg^{2+} (mean EF, 1.3), K^+ (mean EF, 2.2) and NO_3^- (mean EF, 2.2). On the other hand, in AIS, all the ions except Ca^{2+} (mean EF, 2.2) and NO_3^- (mean EF, 2.2), showed depletion. Surface and subglacial melting in the blue ice region and subsequent drainage of the melt water and associated ions (Bell et al., 2017; Kingslake et al., 2017; Liston et al., 1999) may result in a depletion of ions as observed in few blue ice samples in this study. On the other hand, proximity of blue ice region to the nunataks (exposed land mass) may result in high dust concentration in some samples and therefore, result in enrichment of dust associated ions such as Na^+ and Ca^{2+} through dissolution of dust minerals. Freeze thaw cycles associated with the blue ice may also result into the accumulation and enrichment of ions as observed for few ions (Ca^{2+}, Na^+ and NO_3^-) in this study.

Table 3.7. Ion (Na^+, K^+, Mg^{2+}, Ca^{2+}, Cl^-, SO_4^{2-}, NO_3^-, Ac^- and Fo^-) and TOC concentration in blue ice, annual snow deposits and surface snow from different regions in Antarctica.

Samples	Na^+	Ca^{2+}	Cl^-	SO_4^{2-}	NO_3^-	TOC	Ac^-	Fo^-
	μg L^{-1}							
Larsemann Hills								
Blue ice	598	103	533	81	232	107.3	7.92	9.98
Snow deposit	289	46	613	141	140	.	.	.
Surface snow	137	33	530	84	82	172	5.64	1.90
Amery Ice Shelf								
Blue ice	1745	400	427	48	181	93.4	22.50	15.59
Snow deposit	2199	280	641	121	107	170.6	15.16	6.94
Surface snow	208	22	328	81	11	57.8	3.79	2.86
Vestfold Hills (Hodson et al., 2013)								
Glacier ice	631	567	1048	203	50	.	.	.

3.3.2 Carboxylate ions

3.3.2.1 Atmospheric deposition of carboxylic acids on surface snow

Carboxylate ion (Ac^- and Fo^-) concentrations obtained in this study are consistent with the data for surface snow (mean, 10.07±5.87 μg L^{-1}) along a ~1200 km transect from Zongshan station to Dome A in East Antarctica (Li et al., 2015) and with that measured in snow and ice from various remote sites worldwide (**Table 3.8**).

Table 3.8. Concentrations of Fo^- and Ac^- observed in snow and ice from glaciers worldwide.

Sampling site	Fo^- (µg L^{-1})	Ac^- (µg L^{-1})	Sample	Reference
Princess Elizabeth Land (East Antarctica)	1.90	14.44	Surface Snow	This study
Amery Ice Shelf (East Antarctica)	5.23	4.63	Surface Snow	This study
Concordia (central Antarctica)	1.15	2.25	Snow (annual)	Legrand et al. (2013)
Summit (central Greenland)	9.20	18.01	Snow (summer)	Legrand and Mayewski (1997)
Summit (central Greenland)	10.7±1.7	9.3±1.4	Ice core (1310 m, Holocene)	Legrand and de Angelis (1995)
Mt Blanc (French Alps)	187.93	20.16	Snow (summer)	Legrand et al. (2013)
Col du Dôme (French Alps)	.	30.6	Firn core (summer)	Maupetit and Delmas (1994)
Northern Victoria Land (East Antarctica)	16.9± 15.9	17.4± 13	Firn core (22 m, 63 yr)	Udisti et al. (1998)
Lambert glacier (East Antarctica)	2.93±1.72	10.07±5.87	Snow (summer)	Li et al. (2015)
Central East Antarctic Plateau	0.22±0.14	0.32 ± 0.24	Ice core (Holocene)	De Angelis et al. (2012)
Dronning Maud Land (East Antarctica)	0.55±0.24	0.86±0.67	Ice core (Holocene)	De Angelis et al. (2012)
Berkner Island (West Antarctica)	0.1 ± 0.08	0.11 ± 0.09	Ice core	De Angelis et al. (2012)
Talos Dome (East Antarctica)	0.3 ±0.33	1.2 ±1.6	Ice core	De Angelis et al. (2012)
Vostok (Central East Antarctica)	0.16 ±0.07	0.16 ±0.16	Ice core	De Angelis et al. (2012)
Glacier de la Girose (French Alps)	40.02	31.80	Snow (early spring)	Maupetit and Delmas (1994)
South Pole	2.30 - 13.81	3.6 – 15.6	Snow (annual)	Dibb and Arsenault (2002)

In remote areas like Antarctica, natural sources of carboxylic acids such as biomass burning are likely to contribute through long range atmospheric transport (Udisti et al., 1998). Previous studies have shown long range transport of terrestrial organic matter and biomass burning emissions to the PEL region of Antarctica (Antony et al., 2014;

Hu et al., 2013), indicating that long range transport of carboxylic acids to this region is possible. Enhanced concentrations of Ac^- over Fo^- documented in non-polar ice core records have been attributed to atmospheric transport of anthropogenic emissions, particularly coal combustion, to the glaciers (Lee et al., 2003). In addition, anthropogenic inputs like vehicular and biomass burning have been found to contribute to higher concentrations of HAc over HFo in Antarctic snow (Udisti et al, 1998). Thus, the higher concentration of Ac^- over Fo^- observed in both the study regions could possibly be attributed to long range transport of anthropogenic emissions to PEL and AIS.

Direct marine emissions and atmospheric oxidation of compounds emitted from the marine environment are also considered as important sources of carboxylic acids (Legrand and De Angelis, 1996). For instance, in Dumont d'Urville, Legrand et al. (2004) observed enhanced HAc mixing ratios in marine air masses (630 pptV) compared to katabatic air masses (168 pptV). A recent study carried out over a ~1200 km coastal - inland transect in East Antarctica found that marine emissions governed the Ac^- and Fo^- supply up to 600 km from the coast, while different sources and mechanisms were responsible for their deposition in the rest of the transect (Li et al., 2015). Although in the present study, Ac^- and Fo^- did not show any correlation with $ssNa^+$, an indirect marine contribution cannot be eliminated, as a previous study in the same region has shown that the ocean is an important source of dissolved organic matter (DOM) to these sites and that a number of compounds detected in the snow samples are from secondary processing of biogenic organic matter in the atmosphere (Antony et al., 2014).

A major sink of HAc and HFo derived from long range atmospheric transport or secondary sources in the atmosphere is considered to be wet and dry deposition (Chebbi and Carlier, 1996; Paulot et al., 2011; Talbot et al., 1988). The incorporation and preservation of Fo^- and to a lower extent Ac^- in snow is favoured by lower acidity (Legrand and De Angelis, 1995, 1996). Thus, considering atmospheric deposition and subsequent uptake as a major source of carboxylate ions in the surface snow samples, a

negative correlation between acidity and carboxylate ions could be expected. On the contrary, Fo^- and Ac^- concentrations were relatively high in highly acidic samples and low in weakly acidic or highly alkaline samples in both the transects. Variations in both Fo^- and Ac^- concentrations in the surface snow seem to be unrelated to the acidity of snow. Thus, snowpack concentrations of Ac^- and Fo^- may have additional sources other than direct atmospheric deposition of these species.

3.3.2.2 Snowpack production of carboxylate ions

A previous study on carboxylic acids (HAc and HFo) conducted in Greenland and South Pole, observed higher mixing ratios in firn air (5 - 7 times) than in ambient air indicating that atmospheric deposition of these acids alone cannot give rise to such high concentrations of carboxylic acids (Dibb and Arsenault, 2002). Dibb and Arsenault (2002) further suggests that photo-oxidation of various organic compounds such as carbonyls and alkenes can produce monocarboxylic acids within the snowpack. In the atmosphere, alkenes and carbonyls are known to produce carboxylic acids via $^{\cdot}OH$ and O_3 oxidation (Jacob, 1986; Legrand and Saigne, 1988; Sanhueza et al., 1996). Furthermore, such precursors are known to be produced within the snowpack. For example, in a previous study carried out in Arctic, higher mixing ratios of alkenes such as ethene and propene were obtained in firn air than the ambient which is attributed to photochemical production of the alkenes within the snowpack (Bottenheim et al., 2002; Swanson et al., 2002). Similarly, studies carried out in Arctic and South Pole report higher mixing ratios of carbonyl compounds such as formaldehyde (HCHO) in firn air than ambient air. The positive flux of the carbonyl compounds from the snow surface indicates photochemical production of carbonyl compounds within the snowpack via O_3 and $^{\cdot}OH$ oxidation (Couch et al., 2000; Hutterli et al., 2004; Sumner and Shepson, 1999).

In the present study, significant concentrations of organic carbon were measured in the surface snow samples at AIS (mean, 57.8 μg L^{-1}) and PEL (172.0 μg L^{-1}, Antony et al., 2011). Molecular characterization of this organic matter indicates that it is comprised of materials derived from microbial biomass, as well as, lignin-like,

tannin-like and unsaturated hydrocarbon compounds (Antony et al., 2014). Photo-degradation of complex organic compounds such as lignin can contribute to the production of low-molecular weight organic compounds (Gold et al., 1983; Grannas et al., 2004; Opsahl and Benner, 1998) that are precursors of carboxylate ions. In addition, some microbes can also degrade lignin and generate $^{\cdot}OH$ (Frick and Crawford, 1983) which in turn could contribute to *in-situ* production of monocarboxylic acids through $^{\cdot}OH$ oxidation of organic compounds within the snowpack (Anastasio et al., 2007). This together with the fact that microbes identified in these samples are capable of degrading lignin-like molecules (Antony et al., 2016) indicate that snowpack microbes could potentially impact the concentration of monocarboxylic acids.

Rate of photochemical production of HAc and HFo vary with the availability of reactants/hydrocarbons (Souza and Carvalho, 2001). Hydroxyl radical is considered a vital photochemical reactor capable of oxidizing complex organic carbon compounds to produce simpler compounds like mono-carboxylic acids (Anastasio et al., 2007) and results from multiple sources in the snowpack. Within the snowpack, 90% of $^{\cdot}OH$ production was found to be occurring from hydrogen peroxide (H_2O_2) and NO_3^- within the top 10 cm of snowpack (Anastasio et al., 2007). In Antarctic sea ice, King et al. (2005) determined higher depth integrated production rate of $^{\cdot}OH$ from NO_3^- (0.06 - 2 μmol m^{-2} h^{-1}) as compared to H_2O_2 (0.01 - 0.3 μmol m^{-2} h^{-1}) suggesting that photolysis of NO_3^- is an efficient pathway for production of $^{\cdot}OH$ and could result in an oxidizing environment within the ice. Additionally, significant production of $^{\cdot}OH$ from NO_3^- under acidic conditions has been observed in earlier studies (Bock and Jacobi, 2010; Boxe and Saiz-Lopez, 2008; Jacobi et al., 2006).

Ionic balance estimation in the surface snow samples from PEL showed acidic conditions in the surface snow where NO_3^- was the major contributor to the surface snow acidity. Thus, NO_3^- can appreciably undergo photolysis producing an oxidising environment within the snowpack via formation of $^{\cdot}OH$, which can further oxidize the

organic matter to produce carboxylic acids. In addition, strong correlation observed between NO_3^- and Ac^- also indicate the possibility of Ac^- production through $^{\cdot}OH$ oxidation of organic matter. This trend is concurrent with the multiple year round observations made in Dumont d'Urville indicating that $^{\cdot}OH$ oxidation is an efficient pathway for the production of Ac^- (Legrand et al., 2004). Considering this production pathway, higher Ac^- in the interior region of PEL transect is concordant with the high NO_3^- concentration in these samples. In contrast, majority of samples in the AIS, were alkaline. Strong correlation of NO_3^- with $nssCa^{2+}$ and other cations ($n = 13$; $p<0.05$) indicates non-availability of NO_3^- for photolysis and subsequent production of $^{\cdot}OH$ at AIS. Correspondingly, Ac^- concentrations in the coastal section of the ice shelf were found to be low in AIS compared to PEL.

On the other hand, negative correlation between Fo^- and NO_3^- probably indicates that sources other than $^{\cdot}OH$ oxidation of organic matter could be dominant in the case of Fo^-. Higher Fo^- concentrations were observed in AIS compared to PEL. Previous studies show that Fo^- (and Ac^- to a lower extent) is majorly produced from ozonolysis of alkenes (Legrand et al., 2004; Souza and Carvalho, 2001). Although their possible contribution could not be directly/ definitively determined in this study, oxidation of alkenes by O_3 and other peroxy radicals could be a possible source of HAc and HFo in the snowpack.

3.3.2.3 Post depositional changes of carboxylate ions within snowpack

Studies suggest that mineral dust containing Ca^{2+} may interact with organic ions and stabilize the organic ions against photochemical decomposition (Müller-Tautges et al., 2016). Experimental studies have shown irreversible uptake of Ac^- and Fo^- by calcerious aerosols to form calcium acetate ($Ca(Ac)_2$) and calcium formate ($Ca(Fo)_2$) respectively (Al-Hosney et al., 2005; Prince et al., 2008). Similarly, irreversible uptake of Ac^- by other mineral particles such as SiO_2 (Prince et al., 2008; Usher et al., 2003) can lead to the stability of the acids which would subsequently prevent desorption of

Ac^- from snow surface. In both the study regions, high dust concentration and significant fraction of $nssCa^{2+}$ comprising 77% (PEL) and 64% (AIS) of the total Ca^{2+} indicate the possibility of strong interaction between carboxylate ions and mineral dust particles which would further prevent their desorption.

In addition, microbial activity can significantly affect the carboxylate ion concentrations in snow. Experimental studies have shown significant degradation of carboxylic acids such as Ac^-, Fo^-, Oxy^{2-} and $Succ^{2-}$ in cloud water via photochemical as well as microbial activity (Vaïtilingom et al., 2011). Diverse and active microorganisms have been recovered from snow in Antarctica (Carpenter et al., 2000; Lopatina et al., 2013; Michaud et al., 2014; Yan et al., 2012), including snow samples in the study region (Antony et al., 2016). Among the several available organic compounds, carboxylic acids are one of the carbon sources for microorganisms in snow. Resident microbial communities in snow have been shown to be capable of utilizing a wide diversity of carboxylic acids including Ac^- and Fo^- (Amato et al., 2007; Antony et al., 2016). Therefore, biological activity may also influence the budget of the carboxylic acids in snow.

3.3.2.4 Blue ice

Carboxylate ions (Ac^-, mean: 11.39 µg L^{-1}; Fo^-, mean: 12.89 µg L^{-1}) did not show any specific trend in the blue ice samples (**Table 3.4**). TOC concentration in the blue ice samples from LHS (93.4 µg L^{-1}) and AIS (107.3 µg L^{-1}) were found to be consistent with concentrations observed in surface snow and annual snow deposits (**Table 3.7**). A previous study has reported that the penetration of photosynthetically active radiation within blue ice provides a conductive environment for photosynthetic activity (Hodson et al., 2013). Microbial cells (0.46×10^4 - 0.90×10^4 cells mL^{-1}) were documented in the blue ice samples from LHS and AIS in this study. However, due to the severely limited data on microbial communities and organic and inorganic constituents in blue ice, the impacts of melt water discharge from blue ice areas to downstream environments is not known.

Chapter 4

Chemical characteristics of cryoconite holes in coastal Antarctica

4.1 Introduction

Cryoconite holes are cylindrical depressions found on glacier surfaces and are filled with water overlying a thin layer of sediment. They are formed when windblown dust and organic matter gets accumulated on glacier surface and due to lower albedo, the ice beneath starts melting forming a cylindrical hole (McIntyre, 1984; Podgrony and Grenfell, 1996). They are common in ablation regions (Fountain et al., 2004; Hodson et al., 2013) and in temperate regions with low melt rates and deficient runoffs incapable of washing the sediments off the glacier surface (Anesio et al., 2010). Depending on air temperature, cryoconite holes can remain open to atmosphere or develop an ice lid. Open cryoconite holes allow for atmospheric exchange of gases, while closed cryoconite holes remain isolated to the atmosphere (Foreman et al., 2007; Stibal and Tranter, 2007). Further, depending on the hydrological connectivity with any nearby stream, other cryoconite holes or channels below the ice surface, cryoconite holes can be differentiated into hydrologically connected and hydrologically isolated holes. Decay of cryoconite holes occur through shrinkage caused by accumulation of ice on the walls of the cryoconite hole, as well as, by the intrusion of water through the walls in the events of increased meltwater drainage (McIntyre, 1984). In the hydrologically connected cryoconite holes, there is significant exchange of water, microbes and chemical components with each other and the surrounding area (MacDonnell and Fitzsimons, 2012). Contrastingly, there is an accumulation of chemical constituents due to the dissolution of debris, as well as, due to the photochemically and biologically driven reactions in the hydrologically isolated cryoconite holes (Fountain et al., 2004; Telling et al., 2014). Cryoconite holes cover upto 0.1 – 10% of the glacier surface (Anesio et al., 2010) and are significant

contributors to regional carbon cycling (Bagshaw et al., 2016). Due to the high abundance and diversity of microorganisms inoculated by the sediments forming the cryoconite hole, these environments are important sites for biogeochemical cycling of carbon, nitrogen and other nutrients on otherwise relatively passive glaciers and ice sheets (Anesio et al., 2009; Cook, 2016; Fountain and Tranter, 2008; Hodson et al., 2010; Stibal et al., 2008; Säwström et al., 2002; Telling et al., 2014). Cryoconite holes can store chemical and microbial constituents on the glacier surface until they decay and contribute to the transfer of nutrients, carbon and microbes to the supraglacial or subglacial drainage systems. Given the significance of cryoconite holes in biogeochemical cycling on the glacier surface (Anesio et al., 2009) and potential to impact downstream ecosystems through exchange of chemical (Foreman et al., 2004; Fountain et al., 2004; Tranter et al., 2005) and microbial constituents (Stanish et al., 2013; Yallop and Anesio, 2010), characterizing the chemical composition of cryoconite holes and understanding their hydrology is of importance.

In this chapter, trends in the distribution of inorganic ions (Na^+, Ca^{2+}, Mg^{2+}, K^+, Cl^-, SO_4^{2-}, NO_3^- and F^-), organic ions (Ac^-, Fo^-, Oxy^{2-} and Lc^-), total organic carbon (TOC) and dissolved inorganic carbon (DIC) in cryoconite hole samples collected from Larsemann Hills (LHS, 7 samples), central Dronning Maud Land (cDML, 7 samples) and Amery Ice Shelf (AIS, 7 samples), together with their possible sources have been discussed.

4.2 Results

4.2.1 Larsemann Hills (LHS)

The major ions detected in the seven cryoconite hole water samples were: Na^+ (705 - 4198 μg L^{-1}), K^+ (17 - 313 μg L^{-1}), Mg^{2+} (87 - 715 μg L^{-1}), Ca^{2+} (99 - 1692 μg L^{-1}), Cl^- (105 - 1531 μg L^{-1}), SO_4^{2-} (98 - 458 μg L^{-1}), NO_3^- (below detection limit (bDL) - 158 μg L^{-1}), F^- (2 - 21 μg L^{-1}), Ac^- (4.75±0.45 - 27.83±1.25 μg L^{-1}), Fo^- (2.42±0.08 - 13.25±0.04 μg L^{-1}), Lc^- (1.72±0.04 - 18.31±0.87 μg L^{-1}) and Oxy^{2-} (16.57±5.62 - 41.10±1.70 μg L^{-1}) (**Table 4.1 and 4.2**). Dissolved inorganic carbon

represented as HCO_3^- was estimated using the ionic balance equation **(equation 4.1)** as:

$$HCO_3^- = (Na^+ + Ca^{2+} + Mg^{2+} + K^+) - (Cl^- + SO_4^{2-} + NO_3^- + F^- + Ac^- + Fo^- + Lc^- + Oxy^{2-})$$

equation 4.1

The DIC concentration ranged between 44 and 268 μeq L^{-1} (mean, 112 μeq L^{-1}) (**Table 4.1**). Total organic carbon concentration ranged from 7.1±2.7 to 167.5±2.5 μg L^{-1} (mean, 62.3 μg L^{-1}) (**Table 4.2**). Ionic concentration in the cryoconite holes can be significantly affected by the hydrological connectivity/isolation of the holes (Bagshaw et al., 2016; Tranter et al., 2004). Therefore, to understand the sources/sinks of the ions within the cryoconite holes, enrichment factor (EF) was estimated using **equation 4.2** as:

$$EF(i) = (C_i)_{\text{cryoconite hole}} / (C_i)_{\text{snow}}$$ *equation 4.2*

where, $(C_i)_{\text{cryoconite hole}}$ and $(C_i)_{\text{snow}}$ are the concentration of ions in the cryoconite holes and surface snow, respectively. Enrichment factors for the major ions ranged from 0.0 - 0.3 for Cl^- (mean, 0.1), 0.0 - 0.2 for Na^+ (mean, 0.1), 0.0 - 0.4 for K^+ (mean, 0.1), 0.2 - 1.3 for Mg^{2+} (mean, 0.5), 0.3 - 4.4 for Ca^{2+} (mean, 1.1), 0.1 - 0.4 for SO_4^{2-} (mean, 0.2), 0.0 - 0.8 for NO_3^- (mean, 0.3) and 0.0 - 0.4 for TOC (mean, 0.2) (**Table 4.3**). EF(i)>1 represents the enrichment of ion (*i*) mainly due to the accumulation of the ion "*i*" during isolation and aging of the cryoconite hole (Telling et al., 2014). Conversely, EF(i)<1 indicates water exchange with other melt-water implying that the cryoconite hole is hydrologically connected. The abundance of microbial cells in the cryoconite hole water ranged from 0.47×10^4 - 11.8×10^4 cells mL^{-1}. In the cryoconite sediments, TOC concentration ranged from 0.4 to 1.8 mg C g^{-1}. X-Ray diffraction analysis showed the presence of major minerals like quartz, orthoclase, plagioclase, feldspar, biotite, spinel and magnetite in the cryoconite sediments.

Table 4.1. Major ion (Na^+, K^+, Mg^{2+}, Ca^{2+}, Cl^-, SO_4^{2-}, NO_3^- and F^-) and dissolved inorganic carbon (DIC) concentrations in the cryoconite holes from Larsemann Hills, central Dronning Maud Land and Amery Ice Shelf.

Sample ID	Na^+	K^+	Mg^{2+}	Ca^{2+}	Cl^-	SO_4^{2-}	NO_3^-	F^-	DIC
	µg L^{-1}								µeq L^{-1}
Larsemann Hills									
LHS C1	2550	55	102	142	974	120	48	4	96
LHS C2	2324	54	141	110	955	160	58	2	88
LHS C3	3724	313	715	1692	1129	458	158	21	268
LHS C4	705	17	203	280	105	98	35	6	55
LHS C6	902	28	117	326	152	199	bDL*	7	56
LHS C8	1060	26	87	99	370	119	48	3	44
LHS C10	4198	89	411	253	1531	457	90	20	175
Central Dronning Maud Land									
MIS C6	1839	20	41	379	71	120	107	16	95
MIS C8	785	38	44	356	47	112	94	9	49
MIS C9	850	14	38	368	77	66	182	56	49
MIS C16	732	6	24	139	66	79	19	bDL	35
MIS C18	718	5	11	52	53	63	38	29	29
MIS C19	1124	426	113	1890	120	28	24	55	156
MIS C20	1148	10	24	135	78	58	61	8	54
Amery Ice Shelf									
AIS C1	6669	190	1056	603	2359	636	27	5	331
AIS C2	2035	40	211	234	727	256	52	4	92
AIS C3	1271	22	93	149	310	66	77	5	58
AIS C4	1135	22	49	240	224	97	36	8	56
AIS C5	1007	27	28	77	259	64	42	7	40
AIS C6	823	14	22	184	96	46	41	4	42
AIS C7	1241	15	45	215	211	115	93	5	59

* below Detection Limit

4.2.2 Central Dronning Maud Land (cDML)

The major ions detected in the seven cryoconite hole water samples were: Na^+ (718 - 1839 µg L^{-1}), K^+ (5 - 426 µg L^{-1}), Mg^{2+} (11 - 113 µg L^{-1}), Ca^{2+} (52 - 1890 µg L^{-1}), Cl^- (47 - 120 µg L^{-1}), SO_4^{2-} (28 - 120 µg L^{-1}), NO_3^- (19 - 182 µg L^{-1}), F^- (bDL - 55 µg L^{-1}), Ac^- (0.57 - 22.67±0.94 µg L^{-1}), Fo^- (0.86 - 11.53±0.04 µg L^{-1}), Lc^-

(3.15±1.00 - 10.94±0.44 μg L^{-1}) and Oxy^{2-} (bDL - 54.48±18.28 μg L^{-1}) (**Table 4.1 and 4.2**). DIC concentration ranged from 29 - 156 μeq L^{-1} (mean, 67 μeq L^{-1}) (**Table 4.1**), while TOC concentration ranged between 140.3±3.4 and 1213.5±6.3 μgL^{-1} (mean, 498.7 μg L^{-1}) (**Table 4.2**). Total cell density ranged from 0.07 × 10^4 - 1.62 × 10^4 cells mL^{-1}. Enrichment factors ranged from 0.1 - 0.3 for Cl^- (mean, 0.2), 3.6 - 9.2 for Na^+ (mean, 5.2), 0.2 - 19.3 for K^+ (mean, 3.4), 0.8 - 8.1 for Mg^{2+} (mean, 3.0), 4.0 - 55.6 for Ca^{2+} (mean, 13.9), 0.2 - 0.7 for SO_4^{2-} (mean, 0.4), 0.1 - 1.3 for NO_3^- (mean, 0.5) and 0.9 - 9.1 for TOC (mean, 3.7) (**Table 4.3**).

4.2.3 Amery Ice Shelf (AIS)

Major ions detected in the seven cryoconite holes from Amery Ice Shelf were: Na^+ (823 - 6669 μg L^{-1}), K^+ (14 - 190 μg L^{-1}), Mg^{2+} (22 - 1056 μg L^{-1}), Ca^{2+} (77 - 603 μg L^{-1}), Cl^- (96 - 2359 μg L^{-1}), SO_4^{2-} (46 - 636 μg L^{-1}), NO_3^- (27 - 93 μg L^{-1}), F^- (4 - 8 μg L^{-1}), Ac^- (1.56±0.28 - 26.38±1.02 μg L^{-1}), Fo^- (2.03±0.57 - 30.69±0.10 μg L^{-1}), Lc^- (3.43±0.42 - 6.56±0.92 μg L^{-1}) and Oxy^{2-} (bDL - 41.19±4.24 μg L^{-1}) (**Table 4.1 and 4.2**). DIC concentration ranged between 40 and 331 μeq L^{-1} (mean, 97 μeq L^{-1}) (**Table 4.1**) and TOC concentration ranged between 141.3±5.0 and 996.1±10.6 μgL^{-1} (mean, 581.4 μg L^{-1}) (**Table 4.2**). Cell density ranged from 0.13 × 10^4 - 9.57 × 10^4 cells mL^{-1}. Enrichment factor of the major ions were: 0.6 - 14.7 for Cl^- (mean, 3.7), 10.7 - 86.6 for Na^+ (mean, 26.3), 2.0 - 27.2 for K^+ (mean, 6.7), 2.0 - 96.0 for Mg^{2+} (mean, 19.5), 4.5 - 35.5 for Ca^{2+} (mean, 14.3), 2.7 - 37.4 for SO_4^{2-} (mean, 10.8), 3.0 - 10.3 for NO_3^- (mean, 5.9) and 1.9 - 15.2 for TOC (mean, 8.8) (**Table 4.3**).

Table 4.2. Carboxylate ion (Ac^-, Fo^-, Lc^- and Oxy^{2-}) and total organic carbon (TOC) concentrations in the cryoconite holes.

Sample ID	Ac^-	Fo^-	Lc^-	Oxy^{2-}	TOC
			µg L^{-1}		
Larsemann Hills					
LHS C1	4.75±0.45	10.75±0.09	9.90±0.54	25.09±0.58	7.2±2.7
LHS C2	7.79±0.36	6.56±0.17	1.72±0.04	18.14±3.85	113.3±2.3
LHS C3	21.29±1.51	2.42±0.08	18.31±0.87	16.57±5.62	167.5±2.5
LHS C4	6.94±2.74	9.17±0.39	11.04	31.14±5.11	21.5±0.3
LHS C6	6.17±0.38	4.72±0.06	12.51±0.25	23.38±8.14	25.0±1.8
LHS C8	8.33±0.4	6.58±0.05	2.87±0.09	26.67±2.00	35.5±1.8
LHS C10	27.83±1.25	13.25±0.04	7.51±1.62	41.10±1.70	66.3±0.4
Central Dronning Maud Land					
MIS C6	3.18	2.70	10.94±0.44	7.28±5.76	564.7±5.7
MIS C8	22.67±0.94	11.53±0.04	5.84±1.40	54.48±18.28	140.3±3.4
MIS C9	3.41	6.35	11.34	11.21	1213.5±6.3
MIS C16	18.71±0.07	11.44±0.63	3.15±1.00	48.29±16.42	170.4±0.9
MIS C18	14.29±0.36	11±0.02	4.15±0.35	30.90±0.93	614.4±8.4
MIS C19	0.8±0.21	1.51±0.11	6.53±0.20	bDL*	364.7±18.9
MIS C20	0.57	0.86	5.73	bDL	422.9±14.5
Amery Ice Shelf					
AIS C1	26.38±1.02	30.69±0.04	5.69±0.40	15.19±3.77	141.3±5.0
AIS C2	3.35±0.37	8.12±1.0	6.33±0.92	bDL	996.1±10.6
AIS C3	20.62±2.28	16.58±1.34	3.43±0.42	41.19±4.24	161.0±5.9
AIS C4	4.44±1.03	4.49±1.25	7.19	28.67±3.82	872.8±5.3
AIS C5	3.48±1.14	4.92±2.08	5.69	16.19±10.42	626.8±15.3
AIS C6	1.56±0.28	2.03±0.57	6.28±0.55	9.42±5.05	501.9±5.1
AIS C7	2.29±0.57	2.42±0.30	6.56±0.92	bDL	769.8±4.9

*below Detection Limit

Table 4.3. Enrichment factor (EF) of Na^+, K^+, Mg^{2+}, Ca^{2+}, SO_4^{2-}, NO_3^-, TOC and Cl^- in the cryoconite holes.

	EF							
	(Na^+)	**(K^+)**	**(Mg^{2+})**	**(Ca^{2+})**	**(SO_4^{2-})**	**(NO_3^-)**	**(TOC)**	**(Cl^-)**
Larsemann Hills								
LHS C1	0.2	0.1	0.2	0.4	0.1	0.3	0.0	0.2
LHS C2	0.1	0.1	0.3	0.3	0.1	0.3	0.3	0.2
LHS C3	0.2	0.4	1.3	4.4	0.4	0.8	0.4	0.2
LHS C4	0.0	0.0	0.4	0.7	0.1	0.2	0.1	0.0
LHS C6	0.1	0.0	0.2	0.9	0.2	0.0	0.1	0.0
LHS C8	0.1	0.0	0.2	0.3	0.1	0.3	0.1	0.1
LHS C10	0.2	0.1	0.8	0.7	0.4	0.5	0.2	0.3
CentralDronning Maud Land								
MIS C6	9.2	0.9	2.9	11.1	0.7	0.7	4.2	0.2
MIS C8	3.9	1.7	3.1	10.5	0.6	0.7	4.4	0.1
MIS C9	4.3	0.6	2.7	10.8	0.4	1.3	0.9	0.2
MIS C16	3.7	0.3	1.7	4.1	0.4	0.1	9.1	0.2
MIS C18	3.6	0.2	0.8	1.5	0.3	0.3	1.1	0.1
MIS C19	5.6	19.3	8.1	55.6	0.2	0.2	2.7	0.3
MIS C20	5.8	0.4	1.7	4.0	0.3	0.4	3.2	0.2
Amery Ice Shelf								
AIS C1	86.6	27.2	96.0	35.5	37.4	3.0	1.9	14.7
AIS C2	26.4	5.7	19.2	13.7	15.0	5.8	15.2	4.5
AIS C3	16.5	3.2	8.5	8.8	3.9	8.6	2.2	1.9
AIS C4	14.7	3.2	4.4	14.1	5.7	4.0	13.3	1.4
AIS C5	13.1	3.9	2.6	4.5	3.8	4.7	9.6	1.6
AIS C6	10.7	2.0	2.0	10.8	2.7	4.6	7.7	0.6
AIS C7	16.1	2.1	4.1	12.6	6.8	10.3	11.8	1.3

4.3 Discussion

4.3.1 Hydrological connectivity within cryoconite holes

Chloride ion (Cl^-) behaves as a relatively conservative tracer ion in nearly all hydrological streams with high sea salt input of Cl^- (Gooseff et al., 2004; Svensson et al., 2012; Zellweger, 1994). Similarly, Cl^- in cryoconite holes, which is primarily sourced from sea salt aerosols present in the snowmelt, is considered to behave conservatively as long as they are hydrologically isolated and is only affected by the

deepening and aging of the holes (Fountain et al., 2004). In the present study, the calculated enrichment factor indicate a depletion of Cl^- in LHS (mean EF, 0.1) and cDML (mean EF, 0.2), indicating the possibility of hydrological connectivity which results in the dilution of Cl^- within the cryoconite holes. In order to confirm the hydrological connectivity at LHS, age of the cryoconite holes was estimated using **equation 4.3** (Fountain et al., 2004) as:

$$\Delta t = [(M_t/(a \times i)) - h] / (dz/dt) \qquad \textit{equation 4.3}$$

where, Δt indicates the elapsed time (or age of the cryoconite holes), "M_t" is the amount of Cl^- concentration in the hole at time "*t*", "*a*" is the cross-sectional area of the cryoconite hole, "*i*" is the Cl^- concentration in the surrounding ice, "*h*" represents the depth of the cryoconite hole and "*dz/dt*" represents the melt rate of the ice which is assumed to be equal to the ablation rate of the ice surface. The estimated value of $\Delta t>0$ indicates the age of isolation of the cryoconite holes, while $\Delta t<0$ indicates the exchange of water with meltwater (Fountain et al., 2004). The average value of ablation rate "*dz/dt*" determined for this region in LHS was 1.8 cm a^{-1} (Mohd. Yunus Shah, personal communication). In LHS, the obtained $\Delta t<0$ for the cryoconite hole samples indicates the hydrological connectivity of the cryoconite holes with the nearby streams. Hydrological connectivity of the cryoconite holes in LHS also explains the depletion observed in the estimated enrichment factors of other ions (Na^+, Ca^{2+}, Mg^{2+}, K^+, SO_4^{2-} and NO_3^-) and TOC (**Table 4.3**). These results corroborate the field observations on water exchange between the cryoconite holes and the surrounding streams during the sampling.

While no obvious conduits were visible at cDML and AIS, during the cryoconite hole sampling, hydrological connectivity between the cryoconite holes through melt water channels and/or fractures cannot be ruled out. Previous studies have reported annual occurrence of surface melting at cDML during the warming season (Boggild et al., 1995). The observed depletion of Cl^- (mean EF, 0.2) at cDML indicates a dilution of the ion within the cryoconite holes. On the other hand, enrichment observed for mineral associated ions like Na^+ (EF: 3.6 - 9.2, mean - 5.2); K^+ (EF: 0.2 -

19.3, mean - 3.4); Mg^{2+} (EF: 0.8 - 8.1, mean - 3.0) and Ca^{2+} (EF: 1.5 – 55.6, mean - 13.9) suggests the interaction between the cryoconite hole water and the underlying sediment (**Table 4.3**). This further suggests a limited and slow rate of water exchange between the cryoconite holes and the surface meltwater allowing the cryoconite sediment to interact with the overlying water, thereby influencing the ionic concentration.

At AIS, enrichment of Cl^- (mean EF, 3.7) observed in the cryoconite holes from AIS suggests hydrological isolation of the holes leading to an accumulation of the conservative tracer ion. This is corroborated by the strong positive correlation ($r^2>0.9$) between EF(Cl^-) and EF(Na^+, Ca^{2+}, Mg^{2+}, K^+ and SO_4^{2-}) suggesting that similar ion accumulation trend was followed by other ions within the cryoconite holes possibly due to the hydrological isolation. In addition, significant correlation ($p<0.001$) was observed between Na^+, Ca^{2+}, Mg^{2+}, K^+ and SO_4^{2-} together with a higher enrichment (EF) of ions (Na^+, Ca^{2+}, Mg^{2+}, K^+ and SO_4^{2-}) than EF(Cl^-). This suggests that the cryoconite debris are possibly composed of minerals consisting these ions and the dissolution of such mineral material results into ion enrichment in the overlying water.

Apart from the major ions, higher concentration of TOC was also observed in the cryoconite hole water samples from cDML and AIS. Previous studies in Taylor Valley, Antarctica observed an increase in organic carbon concentration with the deepening and aging of the isolated cryoconite holes which is attributed to the increased biomass within the cryoconite sediments during the isolation (Bagshaw et al., 2007, 2013). Thus, in the present study, higher organic carbon concentration in the cryoconite holes than surface snow, as well as, the significant TOC enrichment observed in the cryoconite holes at AIS (EF: 1.9 - 15.2, mean - 8.8) and cDML (EF: 0.9 - 9.1, mean - 3.7) are possibly a result of dissolution of the organic matter from the cryoconite debris. However, apart from sediment dissolution, microbial synthesis of organic matter could also contribute to the higher TOC concentration in cryoconite holes, as observed in previous studies (Anesio et al., 2009, 2010).

4.3.2 Ionic concentration trend and possible sources

Ionic concentrations obtained in the cryoconite holes from the three study regions are consistent with few previous studies carried out in Antarctica (**Table 4.4**).

Table 4.4. Ionic concentration of various ions in cryoconite holes from different regions of Antarctica.

Study Area	Na^+	K^+	Mg^{2+}	Ca^{2+}	Cl^-	SO_4^{2-}	NO_3^-	DIC	References
	μeqL^{-1}								
Larsemann Hills	96	2	21	21	21	5	1	111	this study
Central Dronning Maud Land	45	2	4	24	2	2	1	67	this study
Amery Ice Shelf	88	1	18	12	17	4	1	96	this study
Commonwealth glacier	138	21	101	203	187	57	6	212	Bagshaw et al., 2013
Canada Glacier	57	16	50	231	92	51	7	202	Bagshaw et al., 2013
Taylor Valley	19	4	23	56	19	18	2	64	Bagshaw et al., 2013
McMurdo Dry Valley	65	12	41	84	123	.	9	.	MacDonell et al., 2016
McMurdo Dry Valley	24	6	6	83	27	6	2	242	Telling et al., 2014
Canada Glacier	57	16	50	2	92	51	4	202	Bagshaw et al., 2011
Mc Murdo Dry Valleys	.	.	.	230	106	63	24	150	Tranter et al., 2004

Ionic composition in the cryoconite hole water samples from all three regions was dominated by Na^+. At LHS, the dominance of Na^+ in cryoconite holes is similar to the trend shown in surface snow samples at the coast (Antony et al., 2011). This similarity could be due to the hydrological connectivity of the cryoconite holes preventing longer interaction between cryoconite water and sediments within the holes which further leads to Na^+ depletion (**Table 4.3**). In contrast, surface snow samples at cDML and AIS were dominated by Cl^- followed by Na^+. Previous studies have observed higher enrichment of Na^+ over Cl^- within the isolated cryoconite holes due to mineral dissolution from the cryoconite hole sediments (Bagshaw et al., 2007; Telling et al., 2014; Tranter et al., 2004). Similarly, in a previous study carried out on meltwater

streams in dry valleys of Antarctica, an increase in the concentration of ions like Na^+ and K^+ was considered to be a result of sediment dissolution (Gooseff et al., 2004). Rock promontories near the cryoconite hole sites in AIS and in the Schrimacher Oasis at cDML are found to be comprised of Na^+ containing minerals such as plagioclase feldspar (Joshi and Pant, 1995; Malton et al., 1992; Mikhalsky et al., 2001; Sengupta, 1986; Ravich and Kamanev, 1975). Thus, eolian deposition of these sediments on surface snow could influence the sediment composition in the cryoconite holes in these study regions. The dissolution of such minerals in sediment particles within the cryoconite holes could result in higher enrichment of Na^+ over Cl^- in both the regions (**Table 4.3**). In addition to plagioclase feldspar, NaCl in the sediments can also influence the Na^+ concentration in the overlying water. The cDML and AIS regions, which recieve high sea salt inputs from marine sea-spray (Antony et al., 2011; Samui et al., 2017), could have significant contribution of NaCl in the cryoconite sediments, thereby resulting in an enrichment of Na^+ in the cryoconite water.

Calcium (Ca^{2+}) ion enrichment factors in cryoconite holes at cDML (mean EF, 13.9) and AIS (mean EF, 14.3) exhibited a similar trend as that of Na^+ (**Table 4.3**), suggesting possible dissolution of minerals like plagioclase feldspar rich in Ca^{2+} (Joshi and Pant, 1995; Malton et al., 1992; Mikhalsky et al., 2001; Ravich and Kamanev, 1975; Sengupta, 1986). Additionally, presence of $CaCO_3$ in the promontories at cDML (Bauer and Fitzner, 2003; Sengupta, 1986) and AIS (Malton et al., 1992) supports its possible presence in the cryoconite sediments, thereby contributing to the enrichment of Ca^{2+} in the overlying water. Possible presence of minerals like gypsum containing Ca^{2+} and SO_4^{2-} at AIS is also indicated by a significant correlation ($p < 0.001$) between these ions. The presence of such minerals could also contribute to the enrichment of Ca^{2+} in the cryoconite hole.

Sulphate enrichment observed in cryoconite holes and lakes in previous studies is attributed to the dissolution of evaporite minerals like gypsum (Bagshaw et al., 2013; Lyons et al., 2003; Tranter et al., 2004). Similarly, in the isolated cryoconite holes at AIS, dissolution or oxidation of sulphur rich minerals (like gypsum) may have resulted in higher enrichment of SO_4^{2-} (mean EF, 10.8) than Cl^- enrichment (mean EF, 3.7). In

contrast, SO_4^{2-} in cDML was found to be depleted (mean EF, 0.4) (**Table 4.3**). Depletion of SO_4^{2-} was also accompanied by depletion in Cl^- indicating the possibility of dilution during the melt season. In earlier studies, lower concentration of SO_4^{2-} in some frozen holes compared to other cryoconite holes was attributed to lower initial concentration of minerals rich in sulphur in the cryoconite sediments (Bagshaw et al., 2007). Similarly, in cDML, lower initial concentration of sulphur rich minerals in the sediments may result in depletion of SO_4^{2-}. This is also supported by a weak correlation between SO_4^{2-} and the cations (Na^+, Ca^{2+}, Mg^{2+} and K^+). However, limited information on sediment composition at this site precludes any inferences on the depletion of SO_4^{2-} at cDML. Similar to Na^+ and Ca^{2+}, significant enrichment of Mg^{2+} and K^+ were observed at both AIS and cDML. This is most likely a result of dissolution of Mg^{2+} and K^+ containing sediment minerals like biotite, feldspar, corderite, and spinel commonly present near the cryoconite hole sites in the AIS (Malton et al., 1992; Mikhalsky et al., 2001) and cDML (Musta and Tahir, 2012; Sengupta, 1986). However, at LHS, higher Mg^{2+} contribution to the total ionic concentration is possibly a result of Mg^{2+} salts resulting from the stream water intrusion.

Enrichment of NO_3^- observed in AIS (mean EF, 5.9) may be attributed to microbial activity occurring within the cryoconite holes as observed in previous studies in Antarctica (Bagshaw et al., 2013) and Svalbard (Hodson et al., 2008) where, NO_3^- enrichment was attributed to nitrification processes occurring in these environments (Porazinska et al., 2004). On the other hand, a depletion of NO_3^- was observed in cDML (mean EF, 0.5). Earlier studies have suggested that NO_3^- depletion is majorly a result of microbial uptake (Tranter et al., 2004). In contrast, NO_3^- depletion in cDML is possibly a result of local drainage via near-surface channels during the melt season which is also consistent with the depletion observed in SO_4^{2-} and Cl^-. Similarly, at LHS, observed depletion in SO_4^{2-} and NO_3^- could be attributed to the hydrological connectivity and ensuing dilution of cryoconite hole water.

On the other hand, organic ion (Ac^-, Fo^-, Lc^- and Oxy^{2-}) concentrations in the cryoconite holes did not show any significant variation between the three study regions.

Unlike the major inorganic ions, concentration of organic ions seem to be influenced by biogeochemical processes occurring within the cryoconite holes instead of the accumulation/discharge of the ions due to hydrological connectivity. Laboratory experiments show that microbial communities within the cryoconite holes in this study are capable of metabolizing carboxylate ions such as Ac^{-}, Fo^{-}, Lc^{-} and Oxy^{2-} (Sanyal et al., 2018). Further, as discussed in **chapter 5**, *in-situ* photo-biochemical processes also influence carboxylate ion concentrations within the cryoconite holes.

4.3.3 Influence of Microbial activity

Dissolved inorganic carbon concentrations estimated in the three study regions were: LHS - 44 to 268 μeq L^{-1} (mean, 112 μeq L^{-1}); cDML - 29 to 156 μeq L^{-1} (mean, 67 μeq L^{-1}) and AIS - 40 to 331 μeq L^{-1} (mean, 97 μeq L^{-1}) (**Table 4.1**). In a previous study, a significant fraction of the carbon (60 - 76%) in the cryoconite holes was found to be present as DIC (Bagshaw et al., 2013). Likewise, in the present study, concentration of DIC (HCO_3^{-}: 1742 - 20197 μg L^{-1}) is significantly higher compared to the TOC concentration (7 - 1214 μg L^{-1}) in all the samples.

In spite of a considerable difference in the ion concentration in the three study regions, DIC concentration was found to be comparable between the sites. Previous studies suggest that due to pH increase and $CaCO_3$ saturation during the process of photosynthesis, dissolution and hydrolysis of $CaCO_3$ result in an increase in DIC concentrations (Tranter et al., 2004). Also, release of CO_2 during heterotrophic microbial activity within the cryoconite holes cause weathering of carbonate and silicate minerals, thereby increasing the concentration of ions such as Ca^{2+}, K^{+} and Mg^{2+} (Bagshaw et al., 2016). Several other studies from the Arctic (Anesio et al., 2010; Hodson et al., 2010), Antarctic (Anesio et al., 2010; Foreman et al., 2007; Telling et al., 2014) and Alpine (Anesio et al., 2010) regions have reported microbial activity within the cryoconite holes. The cryoconite hole samples in this study have been found to harbour diverse heterotrophic bacteria and eukarya that are metabolically active (Sanyal et al., 2018), and can significantly influence the chemical composition within the cryoconite holes. These findings are corroborated by other studies which show that

microbial activity in cryoconite holes can appreciably affect the nutrient cycling within the holes (Anesio et al., 2009; Bagshaw et al., 2016). Thus, in spite of isolation and resulting accumulation of the ions in isolated holes, charge balance is most likely preserved due to the continued heterotrophic activity within the cryoconite holes.

Chapter 5

Biogeochemical cycling in surface snow and cryoconite holes

5.1 Introduction

Carbon cycling on glaciers and ice sheets, has received a lot of attention over the past decade because they harbour microbial communities that interact with their physical and chemical environment resulting in distinct processes and feedbacks that impacts glacier nutrient availability, glacier albedo and melt rates, as well as, regional atmospheric carbon concentrations. Snow and cryoconite holes are particularly active and diverse microbial habitats on the glacier surface in which carbon is both fixed and respired (Hodson et al, 2010), akin to "factories that sequester organic carbon from the atmosphere and recycle recalcitrant organic carbon from various sources into more labile carbon substrates" (Stibal et al., 2012). Carbon fixed on glacier surfaces can be redistributed to other supraglacial zones and downstream environments through melt water streams thereby seeding and providing nutrients/energy sources for downstream ecosystems (Foreman et al., 2004; Hood et al., 2015).

Limited studies around the globe have recorded a wide range of rates of carbon uptake and release on glaciers and ice sheets (Anesio et al., 2012) reflecting differences in the geographical locations studied, carbon and energy sources, and physical factors. Whether a supraglacial environment is a net sink or source of carbon, can be inferred depending on the balance between the activities of primary producers, which convert carbon dioxide into organic carbon and rates of community respiration, that is, the conversion of organic carbon into carbon dioxide (Stibal et al., 2012). Thus, a common approach to understand the DOM cycling on the glacier surface has been to study DOM processing or CO_2 production from microbial respiration of labile DOM. However, recent research on DOM degradation highlights

the importance of photo-degradation (Kieber et al., 1999; Larsen et al., 2007; Ward and Cory, 2016) and the interactions between photochemistry and biology in DOM cycling (Cory et al., 2013; Moran and Zepp, 1997).

Photo-degradation by sunlight could result in complete oxidation of DOM to CO_2 or partial oxidation of DOM resulting in altered chemical composition (Cory et al., 2007, 2010; Larsen et al., 2007; Stubbins et al., 2010). Because exposure to sunlight can have a direct, harmful effect on microbial cells (Bagshaw et al., 2016) and also alter the chemical composition of DOM which in turn influence microbial activity and community composition (Bertilsson and Tranvik, 1998; Cory et al., 2010, 2013; Tranvik and Bertilsson, 2001; Ward et al., 2016; Wetzel et al., 1995), it follows that photochemical activity is likely a critical, control on microbial DOM uptake and thus, DOM fate. Thus measuring the coupled 'photo-biological' degradation of DOM is critical to understand the DOM cycling.

The present study aims to: 1) quantify the rates of primary production and bacterial production within the Antarctic snow and cryoconite holes, 2) advance the understanding of how photochemistry and biology interact to determine the fate of DOM on the glacier surface, and 3) assess the relative importance of photo-degradation versus microbial degradation. In order to address these, we present results from two *in-situ* field experiments conducted during the austral summer to test the combined effects of microbes and solar radiation on DOM and nutrient cycling. In the first experiment (experimental system), surface snow and cryoconite hole water samples collected in quartz tubes were incubated in the field (for approximately 30 days) under light and dark (wrapped in aluminium foil) conditions, both in the presence and absence (biocide amended/passed through 0.2 μm filter) of microbes. In the second experiment (natural system), two cryoconite holes, located adjacent to each other and of similar dimension and hydrological characteristics, were subjected to different light conditions, i.e. one was left as is and the other was shaded to restrict light penetration, but allowed gas exchange with the atmosphere.

The experimental system **(Fig. 5.1)** was designed to understand the effect of light and/or microbes acting individually or in concert, on DOM cycling through incubations where, 1) quartz tubes with snow/cryoconite hole water samples containing resident microbial communities were wrapped in aluminium foil to prevent penetration of light in order to study

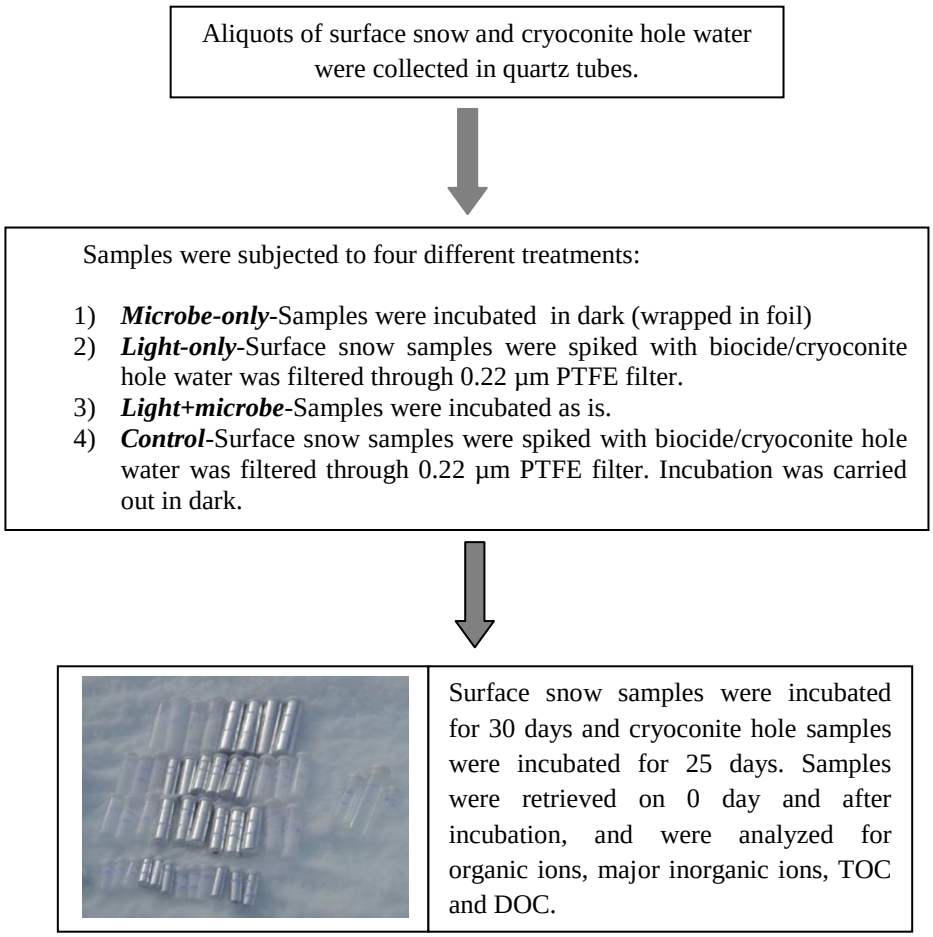

Fig. 5.1. Schematic of the incubation setup in the experimental system.

the effect of microbes alone on DOM degradation and nutrient cycling, 2) quartz tubes with snow/cryoconite hole water samples spiked with a biocide/filtered through 0.2 µm PTFE filter to eliminate microbial activity and exposed to ambient light conditions to study the effect of light alone on DOM degradation and nutrient cycling, 3) snow/cryoconite hole water samples containing natural microbial assemblages

incubated in the field under ambient light conditions to study the effect of light and microbes, and 4) sterile snow (biocide treated)/cryoconite hole water (0.2 µm filtered) were incubated in the field under dark conditions to serve as the control. All incubations were carried out in triplicate.

Because the simulation of the natural environmental conditions (such as new DOM inputs, gas exchange, concomitant autotrophic production) and physical conditions (such as precipitation, wind, hydrological connectivity, etc.), in the experimental set up is challenging, the second experiment was conducted where cryoconite holes in the natural environment **(Fig. 5.2)** subjected to different light conditions (sunlight-exposed and shaded) and were monitored over a period of 25 days in order to obtain a more representative understanding of how DOM is cycled in these environments. Samples retrived after incubations (experimental and natural system) were analyzed for major inorganic ions, carboxylate ions and dissolved organic carbon (DOC).

5.2 Results

5.2.1 Carbon fluxes

Primary production rates in two surface snow samples were 0.15±0.04 and 0.23±0.01 µgC L^{-1} h^{-1} as determined from *in-situ* incubations of 72 h duration using ^{14}C-$NaHCO_3$. Primary production measurements in the cryoconite hole water and sediment samples from *in-situ* incubations of 48 h duration ranged from 0.13±0.06 to 0.47±0.08 µgC L^{-1} d^{-1} and 0.15±0.01 to 1.05±0.43 µgC g^{-1} d^{-1}, respectively (**Table 5.1**). Bacterial production rates were measured using methyl-^{3}H-Thymidine incorporation through the heterotrophic bacterial community. Bacterial production rates were non-detectable in surface snow samples. Bacterial production in six cryoconite hole water samples ranged between 4.70±0.23 and 35.35±1.25 ngC L^{-1} d^{-1}, while in cryoconite hole sediments, it ranged from 0.42±0.19 to 3.63±5.49 ngC g^{-1} d^{-1} (**Table 5.1**).

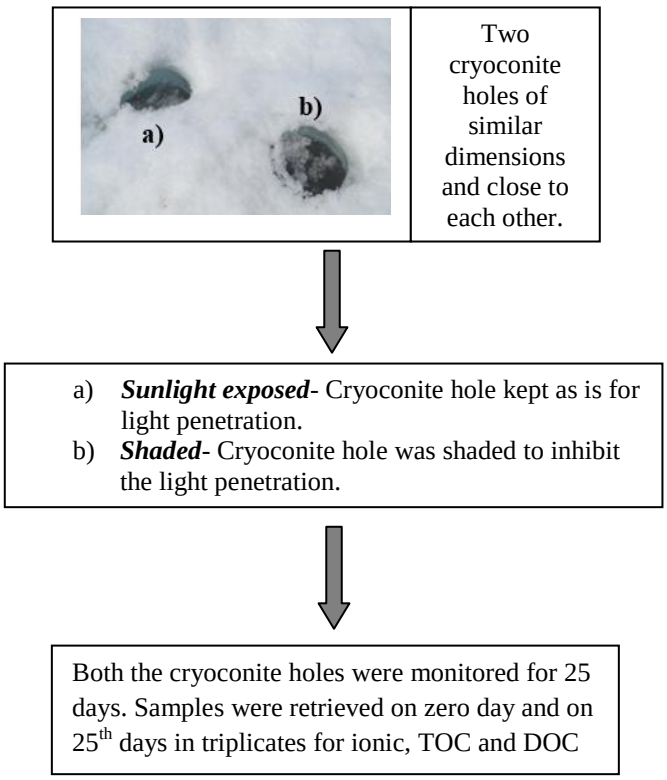

Fig. 5.2. Schematic of the incubation setup in the natural system.

Major ion (Na^+, K^+, Ca^{2+}, Mg^{2+}, Cl^-, SO_4^{2-} and NO_3^-) and carboxylate ions (Ac^-, Fo^-, Oxy^{2-}) concentrations in the surface snow and cryoconite hole samples are as given in **Table 5.1**. Dissolved inorganic carbon (HCO_3^-) concentrations estimated by using **equation 5.1** are as given in **Table 5.1**.

$$HCO_3^- = (Na^+ + Ca^{2+} + Mg^{2+} + K^+) - (Cl^- + SO_4^{2-} + NO_3^- + Ac^- + Fo^- + Oxy^{2-}) \qquad \textit{equation 5.1}$$

Mean total organic carbon (TOC) concentrations in the surface snow samples was 17.6±7.9 µg L^{-1}, while DOC was below detection limit (bDL). In cryoconite hole samples, TOC concentration ranged from 52.3±1.0 to 132.8±2.9 µg L^{-1}, while DOC concentrations ranged from 13.2±1.4 to 129.7±0.5 µg L^{-1}. Total organic carbon concentration in the cryoconite sediments ranged from 0.9 to 2.8 mgC g^{-1}.

Table 5.1. Rates of primary and bacterial production in surface snow and cryoconite holes together with their chemical composition. Concentration of ions, DOC and TOC are represented in µg L^{-1} and DIC concentration is represented in µeq L^{-1}.

System	Snow		Cryoconite hole					
	A	B	A	B	C	D	E	F
Primary Production water (µgC L^{-1} d^{-1})	0.15± 0.04	0.23± 0.01	0.24± 0.05	0.35± 0.02	0.25± 0.08	0.31± 0.05	0.13± 0.06	0.47± 0.08
sediment (µgC g^{-1} d^{-1})	.	.	1.02± 0.02	0.77± 0.32	0.15± 0.01	0.33± 0.03	0.55± 0.34	1.05± 0.43
Bacterial Production water (ngC L^{-1} d^{-1})	nd*	nd	11.00± 0.46	35.35± 1.25	4.70± 0.23	7.54± 1.35	27.15± 0.88	30.64± 2.00
sediment (ngC g^{-1} d^{-1})	.	.	1.14± 0.37	1.88± 0.38	0.42± 0.19	0.44± 0.13	3.63± 5.49	1.22± 0.27
Ac^-	1.74	2.48	1.04	2.7	1.93	0.89	3.37	4.19
Fo^-	2	2.48	3.62	4.4	7.5	4.5	5.26	4.21
Oxy^{2-}	7.66	8.92	6.19	6.68	8.07	6.93	6.2	5.33
Na^+	755	383	1268	1868	884	1327	620	1933
K^+	46	39	67	107	97	373	81	114
Mg^{2+}	59	228	167	139	167	215	139	58
Ca^{2+}	86	133	239	149	191	211	171	120
Cl^-	270	97	532	736	411	566	268	433
NO_3^-	29	15	29	34	38	37	34	25
SO_4^{2-}	42	33	186	242	178	285	118	246
DIC	2082	2408	3855	4665	2939	4455	2341	4870
DOC	bDL**	bDL	13.2	45.6	51	61.7	24.3	129.7
TOC	11.1	24.8	52.3	60.1	70.8	81.2	92	132.8

*not detected; **below detection limit

5.2.2 Nutrient cycling

5.2.2.1 Experimental system

In control, accumulation of Ac^- (27 times), Fo^- (42 times), Oxy^{2-} (19 times) and DOC (3 times) were observed at the end of incubation in surface snow samples. In cryoconite hole water samples, large accumulation of Ac^- (102 times) and Fo^- (64 times) were observed, while Oxy^{2-} (0.6 times) and DOC (0.5 times) concentrations decreased.

Under the influence of microbial activity, DOC concentrations declined to below detection limit (<10 μg L^{-1}) at the end of the incubation, while an overall increase in carboxylate ion concentration were observed in the surface snow samples at the end of the incubation, with an increase in Ac^- by 3 times, Fo^- by 8 times and Oxy^{2-} by 2 times. Similarly, in cryoconite hole water samples, a small decrease in DOC (0.9 times) and an accumulation in carboxylate ions was observed with an increase in Ac^- by 25 times, Fo^- by 8 times and Oxy^{2-} by 2 times.

Incubations carried out in the presence of light alone showed a decrease in DOC (0.6 times) and an increase in Oxy^{2-} (11.1 times) concentrations in surface snow at the end of the experiment. Changes in Ac^- and Fo^- could not be observed in surface snow due to some technical issues during the sample analysis. In cryoconite hole water samples, light mediated reactions resulted in an increase in Ac^- (68 times) and Fo^- (39 times), while a decrease in Oxy^{2-} (0.6 times) and DOC (0.9 times) concentrations were observed.

Under the influence of both light and microbes, DOC concentration at the end of the incubation depleted by 0.6 times, while carboxylate ion concentrations increased by 3 times for Ac^-, 4 times for Fo^- and 2 times for Oxy^{2-} in surface snow. In cryoconite hole water samples, accumulation was observed in Ac^- (65 times), Fo^- (171 times), Oxy^{2-} (3 times) and DOC concentrations (1.1 times).

Changes in inorganic ion concentration showed large variations in surface snow and cryoconite hole water samples. In control incubation in the surface snow samples,

an increase in inorganic ion concentration (2 to 35 times) was observed. In other treatments, depletion in Na^+, K^+, Mg^{2+}, Ca^{2+}, Cl^- was observed at the end of incubation except an increase in K^+ and Ca^{2+} in microbe-only treatment. Sulphate showed an increase ranging from 2 to 7 times and NO_3^- showed an increase ranging from 2 to 14 times at the end of experiment in surface snow. In cryoconite hole water, Na^+, Mg^{2+} and Ca^{2+} showed an average depletion of 0.8 times, while K^+, Cl^-, SO_4^{2-} and NO_3^- showed an average increase of 1.3 times in control treatment. In the other treatments, Na^+, K^+, Mg^{2+}, Ca^{2+}, Cl^- and SO_4^{2-} showed an average depletion by 0.5 times except an increase observed in K^+ concentration (3 times) in light+microbe treatment and an average increase of 3 times observed in K^+, Mg^{2+}, Ca^{2+} concentration in microbe-only treatment. Sulphate showed no change in microbe-only treatment, while NO_3^- showed an average increase of 3 times in all the treatments.

5.2.2.2 Natural System

In the natural system, an accumulation of Ac^- (1.7 times), Fo^- (1.1 times) and Oxy^{2-} (1.2 times) was observed in the cryoconite hole that are exposed to direct sunlight when compared to the initial sample. In the shaded cryoconite hole, a decrease in Ac^- (0.2 times) and an increase in Oxy^{2-} (2.0 times) were observed, while Fo^- concentration remained same. Dissolved organic carbon concentrations increased in both sunlight exposed (9.3 times) and shaded (5.6 times) cryoconite holes, with a higher increase in the sunlight exposed cryoconite hole. Total organic carbon concentration in the cryoconite sediments in sunlight-exposed cryoconite hole increased by 1.2 times and by 1.4 times in shaded cryoconite hole.

In sunlight exposed cryoconite hole, significant accumulation of Mg^{2+} (14 times) and Ca^{2+} (7 times) was observed, while decrease was observed in Na^+, K^+ and NO_3^-. Change in SO_4^{2-} could not be studied due to technical issues. In shaded cryoconite hole, slight increase was observed in K^+ (1.2 times), Mg^{2+} (1.8 times) and Ca^{2+} (1.1 times) and decrease was observed in Na^+ and NO_3^-. Sulphate did not show any change in the shaded cryoconite hole.

5.3 Discussion

5.3.1 Carbon flux

Primary production rates measured in surface snow (0.19±0.05 µgC L^{-1} d^{-1}) and cryoconite hole water samples (0.29±0.11 µgC L^{-1} d^{-1}) were comparable, while significantly higher (1110 times) primary productivity rates were observed in the cryoconite sediments (321.96±211.91 mgC m^{-3} d^{-1}) (**Fig. 5.3, Table 5.1**). Bacterial production in the sediments (0.53±0.28 mgC m^{-3} d^{-1}) was observed to be 26 times higher compared to overlying cryoconite water (19.40±12.07 ngC L^{-1} d^{-1}) (**Fig 5.3**). Bacterial production in snow was not detectable (most likely due to insufficient incubation period). Studies reporting bacterial production in surface snow are scarce except, a study by Carpenter et al. (2000) reported low rates of bacterial production measured at South Pole (reported as thymidine incorporation, 0.13 pmol L^{-1} h^{-1}).

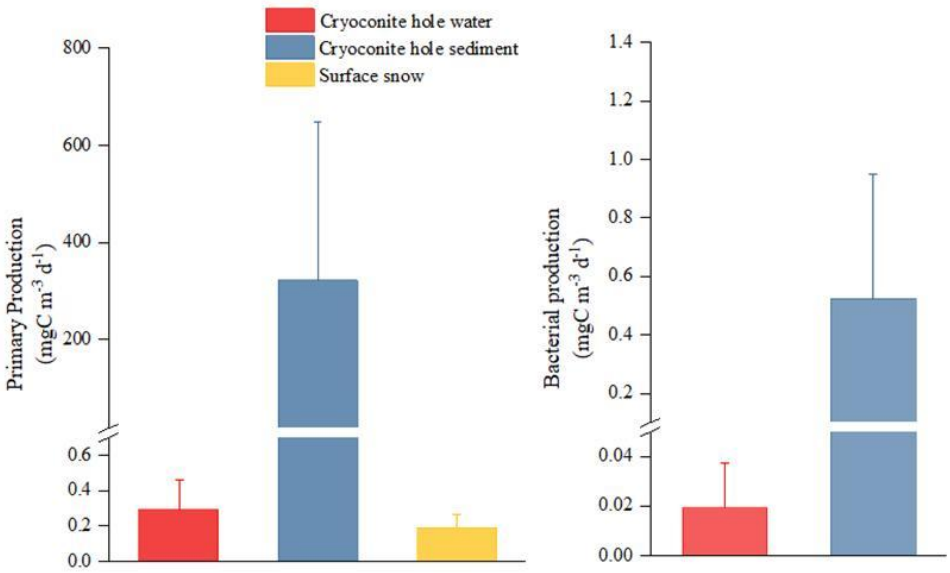

Fig. 5.3. Mean primary and bacterial production in cryoconite hole water (6 samples), cryoconite hole sediment (6 samples), and surface snow (2 samples).

Overall, the rate of DOC utilization by heterotrophic bacterial activity was lower than the rate of DOC generated during primary production. Higher rates of primary and bacterial production in the cryoconite sediments than the overlying water are consistent

with that of previous studies (Anesio et al., 2010). The rates of primary and bacterial production in Larsemann Hills were at the lower end of the range documented for the cryoconite hole water samples from other regions of Antarctica (Hodson et al., 2010; Telling et al., 2014).

On comparing the primary production rates in Larsemann Hills to non-Antarctic regions, a large difference was observed with 70 to 550 times higher production rates in the non-Antarctic glaciers (**Table 5.2**). Bacterial production rates in Larsemann Hills on the other hand, showed some similarities with non-Antarctic regions with few exceptions (**Table 5.3**). In this study, primary productivity rates between different cryoconite holes in the Larsemann Hills region varied widely (**Table 5.1**). The potential primary production in cryoconite holes over the period of 25 days is estimated to be 16 µgC g^{-1} of wet debris. This is 10 times lower than the TOC content of the debris (161 µgC g^{-1} debris). This simple calculation and comparison suggests that bulk of the organic carbon present in the debris may not be produced *in-situ* and are likely derived from other sources. For instance, viral lysis is believed to be an important contributor to the total DOC pool in various environments (Fuhrman and Suttle, 1993; Hodson et al., 2008; Wilhelm and Suttle, 1998). Other sources include marine emissions and long range transport of aerosols.

5.3.2 Nutrient cycling - experimental system

5.3.2.1 Microbially driven changes

In surface snow, DOC concentrations declined to below detection limit (<10 µg L^{-1}) at the end of the incubation in the microbe-only treatment, while in the control treatment, DOC concentration showed a 2.8 times increase (**Fig. 5.4**). The significant decrease in DOC concentration in the microbe-only treatment suggests that bulk of the DOC in snow is bio- available and utilized by microbes even though some DOC might be abiotically produced as observed in the control treatment.

Table 5.2. Comparison of primary production in surface snow and cryoconite holes obtained in this study with that of previous studies.

Study Area	Sample type	Primary production	Reference
Larsemann Hills	Surface snow	0.19±0.05 (0.15 - 0.23) µgC L^{-1} d^{-1}	This study
	Cryoconite hole water	0.29±0.11 (0.13 - 0.47) µgC L^{-1} d^{-1}	This study
	Cryoconite hole sediment	0.64±0.42 (0.15 – 1.05) µgC g^{-1} d^{-1}	This study
Svalbard	Cryoconite hole water	79.8±75.9 (5.38 - 234) µgC L^{-1} d^{-1}	Anesio et al., 2009
		87.5±56 (24.8 - 158) µgC L^{-1} d^{-1}	
	Cryoconite hole sediment	353±248 (72.2 - 756) µgC g^{-1} d^{-1}	Anesio et al., 2009
		48±35.9 (11.2-125) µgC g^{-1} d^{-1}	
		208±106 (101 - 368) µgC g^{-1} d^{-1}	
Greenland	Cryoconite hole water	53.5±59.7 (7.97 - 183) µgC L^{-1} d^{-1}	Anesio et al., 2009
	Cryoconite hole sediment	115±56.3 (35.5 - 205) µgC g^{-1} d^{-1}	
Alpines	Cryoconite hole sediment	147±78.3 (2.83 - 205.9) µgC g^{-1} d^{-1}	Anesio et al., 2009
Dry Valleys	Cryoconite hole	0.3 µgC g^{-1} d^{-1}	Telling et al., 2014
Dry Valleys	Cryoconite hole	0.4 - 1.4 µgC g^{-1} d^{-1}	Hodson et al., 2010
Vestfold	Cryoconite hole	2 µgC g^{-1} d^{-1}	Hodson et al., 2013

Table 5.3. Rates of bacterial production in surface snow and cryoconite holes obtained in this study with that of previous studies.

Study Area	Sample type	Bacterial production	Reference
Larsemann Hills	Cryoconite hole water	0.81±0.50 (0.20 – 1.47) ngC L^{-1} h^{-1}	Present study
	Cryoconite hole sediment	0.04±0.02 (0.02 - 0.08) ngC g^{-1} h^{-1}	
Arctic	Cryoconite hole water	3.26±2.62 (0.5 - 7.44) ngC L^{-1} h^{-1}	Anesio et al., 2010
	Cryoconite hole water	5.27±1.75 (2.88 - 7.9) ngC L^{-1} h^{-1}	
	Cryoconite hole sediment	8.62±6.4 (2.06 - 21.6) ngC g^{-1} h^{-1}	
	Cryoconite hole sediment	39.7±17.9 (16.9 - 70.3) ngC g^{-1} h^{-1}	
Alpines	Cryoconite hole water	16.7±15.8 (1.2 - 43) ngC L^{-1} h^{-1}	Anesio et al., 2010
	Cryoconite hole water	0.05±0.02 (0.03 - 0.07) ngC L^{-1} h^{-1}	
	Cryoconite hole sediment	24.6±21.4 (6 - 67) ngC g^{-1} h^{-1}	
	Cryoconite hole sediment	0.13±0.14 (0.02 - 0.38) ngC g^{-1} h^{-1}	
Dry Valleys	Cryoconite hole water	0.22±0.31 (0.02 - 0.78) ngC L^{-1} h^{-1}	Anesio et al., 2010
	Cryoconite hole water	0.04±0.02 (0.01 - 0.06) ngC L^{-1} h^{-1}	
	Cryoconite hole sediment	11.2±4.11 (8.62 - 19.4) ngC g^{-1} h^{-1}	
	Cryoconite hole sediment	23.4±11.8 (9.2 - 37.1) ngC g^{-1} h^{-1}	
Dry Valleys	Cryoconite hole	2.4±1.6 ngC g^{-1} h^{-1}	Telling et al., 2014

In cryoconite holes, a decrease in DOC concentration was observed in the microbe-only and control treatment following incubation (**Fig. 5.4**). However, the decrease in DOC in the microbe-only treatment was much lower than that in the control suggesting that the observed decline in concentrations in the microbial incubation cannot be ascertained due to microbial activity. This is contrary to that observed in a previous study where 55% (Antony et al., 2017) of the DOC in supraglacial environment was found to be bioavailable.

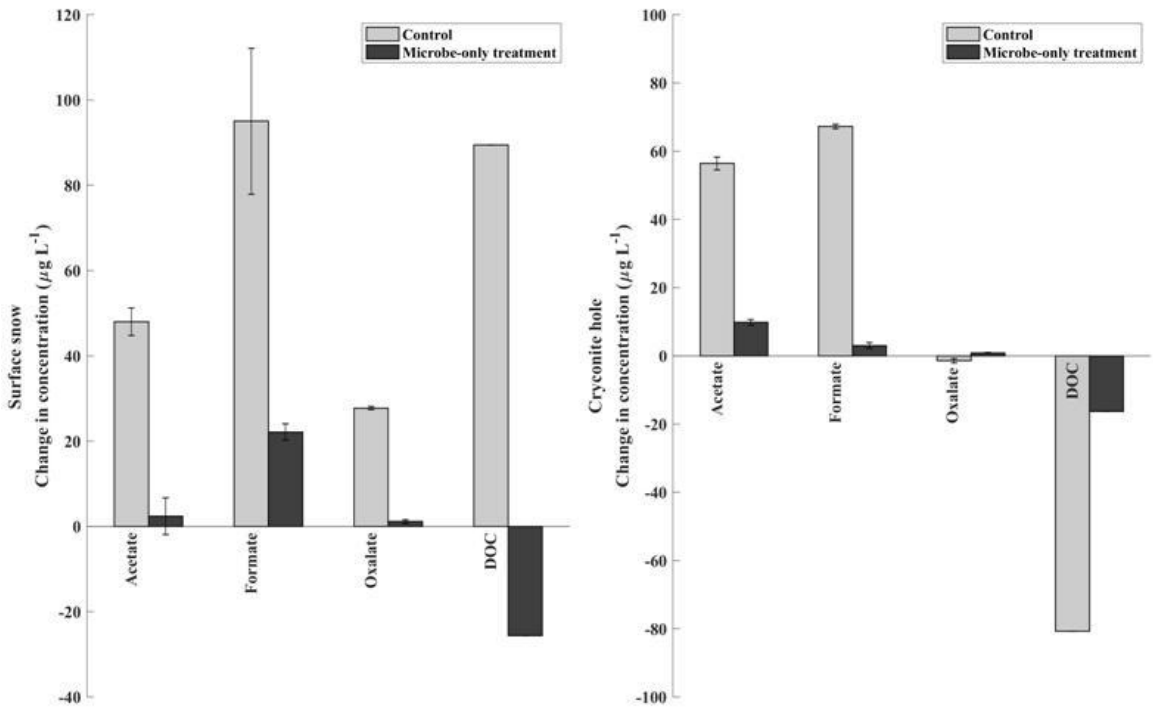

Fig. 5.4. Changes in Ac^{-}, Fo^{-}, Oxy^{2-} and DOC in microbe-only treatment over a period of 30 days in surface snow and 25 days in cryoconite holes in experimental system. Negative values represent utilization/degradation and positive values represent production/accumulation.

A possible explanation for the relatively low decline in DOC concentrations in cryoconite hole water despite the presence of microbes (approximately 11.0 cells ml^{-1}) and possible microbial uptake of DOC is the presence of viral communities. Previous studies have shown that viruses are abundant in cryoconite holes and play an important

role in controlling bacterial mortality and hence, the cycling of carbon and nutrients in these environments through the release of cellular lysates (Anesio et al., 2007, 2010; Bellas et al., 2013; Hodson et al., 2008; Säwström et al., 2007; Williams et al., 2016).

Carboxylate ion concentrations following incubation of surface snow in the microbe-only treatment were found to be 2 to 8 times higher (Fo^-) than that in the initial sample (**Fig. 5.4**). Carboxylate ion concentrations in the control treatment however, showed higher (19 to 43 times) increases from the initial concentration following the incubation (**Fig. 5.4**). Accumulation of carboxylate ions at the end of the control incubation suggests possibility of abiotic production of these carboxylate ions in dark. Such abiotic production of carboxylate ions are also expected to occur in the microbe-only treatment resulting in similar increases in concentrations as in the control. However, the lower carboxylate ion accumulation in the presence of microbes indicates that these abiotically generated carboxylate ions are possibly bioavailable, and are utilized by the microbial community. Previous studies have also demonstrated the degradation of carboxylate ions by supraglacial microbial communities (Amato et al., 2007; Sanyal et al., 2018; Vaïtilingom et al., 2011), which supports the observed degradation of carboxylate ions in this work. Similarly, in cryoconite hole water, lower accumulation of Ac^- (25 times) and Fo^- (8 times) was observed in the microbe-only treatment than control treatment (Ac^-, 102 times; Fo^-, 64 times) indicating microbial uptake of Ac^- and Fo^- (**Fig. 5.4**). In the case of Oxy^{2-}, an increase in concentration (1.5 times) was observed in the microbe-only treatment, whereas, a depletion (0.6 times) was observed in the control treatment (**Fig. 5.4**). It is not clear why an opposing trend of Oxy^{2-} increase was observed in the microbe-only treatment compared to the control where, Oxy^{2-} concentrations were found to decrease. However, there is evidence that microbes are capable of producing oxalic acids (Frey et al., 2010; Nataka and He, 2010), and that such an ability is beneficial in the acquisition of nutrients (Dutton and Evans, 1996; Gharieb, 2000; Munir et al., 2001; Shimada et al., 1994).

In surface snow, an increase in SO_4^{2-} (2 times) and NO_3^- (3 times) concentrations was observed in the microbe-only treatment (**Table 5.4**). However,

higher accumulation of SO_4^{2-} (3 times) and NO_3^- (14 times) concentrations were observed in control treatment indicating abiotic production (**Table 5.4**). The lower accumulation of NO_3^- (3 times) in the microbe-only treatment compared to that of the control may be attributed to microbial transformation or uptake of the NO_3^- (Carpenter and Dunhem, 1985; Cochlan, 1989) that is abiotically produced. This is supported by the presence of denitrifying bacteria and associated denitrification processes documented in the snowpacks (Larose et al., 2013). Similarly, lower accumulation of SO_4^{2-} in the microbe-only treatment compared to that of the control may be attributed to microbial uptake of SO_4^{2-} (Hodson et al., 2005, 2008; Mikucki and Priscu, 2007) by resident microbial communities in snow. In cryoconite hole water, NO_3^- showed higher accumulation in the microbe-only treatment (1.6 times) compared to the control (1.3 times) (**Table 5.4**) suggesting microbial production of NO_3^-. Earlier studies have identified nitrification to result in accumulation of NO_3^- in cryoconite holes (Telling et al., 2014). In addition, mineralization of organic nitrogen to NH_4^+ followed by nitrification is also attributed to accumulation of NO_3^- (Hodson et al., 2008; Wynn et al., 2007). Rock weathering-derived NH_4^+, liberated during sediment dissolution is also considered as a potential source of NH_4^+ for nitrification (Wynn et al., 2007). Thus, accumulation of NO_3^- in cryoconite hole water may be attributed to mineralization of organic nitrogen followed by nitrification. Differences observed in the NO_3^- cycling between surface snow and cryoconite hole water is most likely a result of differences in microbial communities and activity in the cryoconite holes and the surrounding surface snow. In cryoconite hole water, SO_4^{2-} concentrations following incubation remained nearly similar to that of the initial concentration in microbe-only treatment, while an accumulation was shown in control treatment (**Table 5.4**).

5.3.2.2 Light driven changes

In surface snow, light mediated activities resulted in a decrease in DOC concentration from 50 to 30 μg L^{-1} while the control showed a 3 times increase from 50 to 139 μg L^{-1} (**Fig. 5.5**). This shows an overall decrease in DOC content in surface snow in presence of the light which is consistent with that of other studies which show

that DOC can be partially or fully photo-oxidized to CO_2 (Ward and Cory, 2016). Study of CO_2 records in ice cores also suggests that simpler organic compounds (like HCHO and HFo) undergo oxidation with potential oxidants such as hydrogen peroxide (H_2O_2) to produce CO_2 (Peel, 1992; Tschumi and Stauffer, 2000). In cryoconite hole water, although a similar trend of decline in DOC concentrations in the light-only treatment was observed, the extent of DOC decrease was much lower than that in the control (**Fig. 5.5**). Therefore, no conclusions can be drawn on light mediated degradation of DOC in cryoconite hole water.

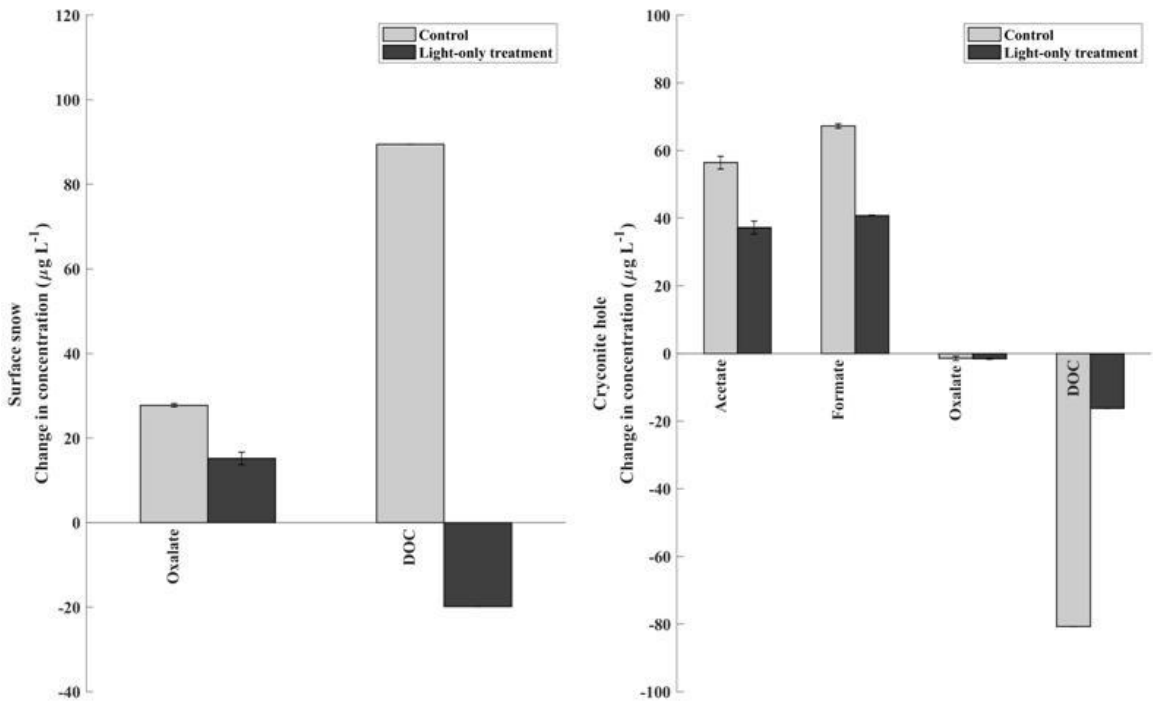

Fig. 5.5. Changes in Ac^-, Fo^-, Oxy^{2-} and DOC in light-only treatment over a period of 30 days in surface snow and 25 days in cryoconite holes in experimental system. Negative values represent utilization/degradation and positive values represent production/accumulation.

Light mediated activities resulted in a 11 times increase in Oxy^{2-} concentrations in surface snow, while the control surface snow incubation showed a 19 times increase in Oxy^{2-} values (**Fig. 5.5**). The increase in Oxy^{2-} concentrations in both treatments

suggests abiotic production of Oxy^{2-} under both light and dark conditions. However, a lower increase in concentrations in the light-only treatment compared to the control indicates that photochemical production may be occurring at rates lower than that of abiotic dark production of Oxy^{2-} or that photochemical degradation of Oxy^{2-} may be occurring together with abiotic production. This is supported by previous study reporting photochemical decomposition of Oxy^{2-} (Vaïtilingom et al., 2011). Changes in Ac^- and Fo^- could not be detected in snow samples due to technical issues during the sample analysis. In cryoconite hole water, accumulation of Ac^- (68 times) and Fo^- (39 times) were observed in light-only treatment, while in the control incubation, a higher accumulation of these ions (Ac^-, 102 times and Fo^-, 64 times) were observed (**Fig. 5.5**). Lower accumulation of Fo^- and Ac^- in light-only treatment than control suggests that production of these ions may be slightly inhibited in the presence of light or that photochemical degradation of Fo^- and Ac^- could be occurring concurrently. Photochemical degradation of Fo^- has been previously demonstrated (Vaïtilingom et al., 2011). Oxalate concentrations on the other hand were found to be lower than initial in both light-only and control treatments with nearly similar extent of decline (**Fig. 5.5**)

Higher accumulation of SO_4^{2-} (7 times) was observed in the light-only treatment than control incubation (3.3 times) (**Table 5.4**). Photochemical oxidation of sulphide present in the dust particles on surface snow might explain the accumulation of SO_4^{2-} in presence of light as observed in previous studies (Toom-Sauntry and Barrie, 2002). Nitrate was found to accumulate in both light-only and control treatments indicating, photochemical and dark abiotic production of NO_3^- respectively. While the mechanism of NO_3^- production in the dark is not clear, photochemical production of NO_3^- has been reported in snowpacks (Dibb et al., 2002; Honrath et al., 2000). In cryoconite hole, NO_3^- showed higher accumulation (3 times) in presence of light than the control (1.3 times) (**Table 5.4**). This is attributed to photochemical mineralization of organic nitrogen compounds to NH_4^+ (Bushaw-Newton and Moran, 1999; Wilhelm and Suttle, 1998; Wynn et al., 2007) followed by photochemical nitrification, that is oxidation of NH_4^+ to NO_3^- (Zobell, 1933). In the case of SO_4^{2-}, a minor depletion (0.8 times) was observed in the light-only treatment, while a minor accumulation (1.2 times)

was observed in the control treatment (**Table 5.4**). The depletion of SO_4^{2-} in presence of light is not clear.

5.3.2.3 Combined effect of light and microbes

Dissolved organic carbon concentration in the light+microbe incubation of snow was found to be lower than the initial, while that in the control, it was found to be higher. The low DOC concentration under the combined influence of light and microbes is suggestive of photochemical and microbial degradation of organic carbon (**Fig. 5.6**). On the other hand, in cryoconite hole, a slight increase in DOC concentrations in the light+microbe treatment (**Fig. 5.6**) indicates light stimulated microbial production of DOC which is supported by the presence of cyanobacteria and algae (**Fig. 5.7**), as well as, the high primary production rates observed in cryoconite holes in the present study (**Table 5.1 and Fig. 5.3**). It is not clear why DOC concentrations in the control were lower than initial over the same time period.

In the incubations with snow, an increase in the concentration of carboxylate ions was observed in both light+microbe and control treatments indicating that carboxylate ions are produced in the presence of light and/or microbes, as well as, abiotically in the dark. A 2 to 4 times increase in Ac^-, Fo^- and Oxy^{2-} were observed in the light+microbe treatment, while higher increase in concentrations of Ac^- (27 times), Fo^- (42 times) and Oxy^{2-} (19 times) were observed in the control (**Fig. 5.6**). This suggests that carboxylate ion production in the presence of light and microbes occurs to a lower extent than that in the dark. A lower extent of increase in carboxylate ion concentrations in the light+microbe treatment compared to that in the light-only and microbe-only indicates an inhibitory effect of light on microbial activity or vice versa.

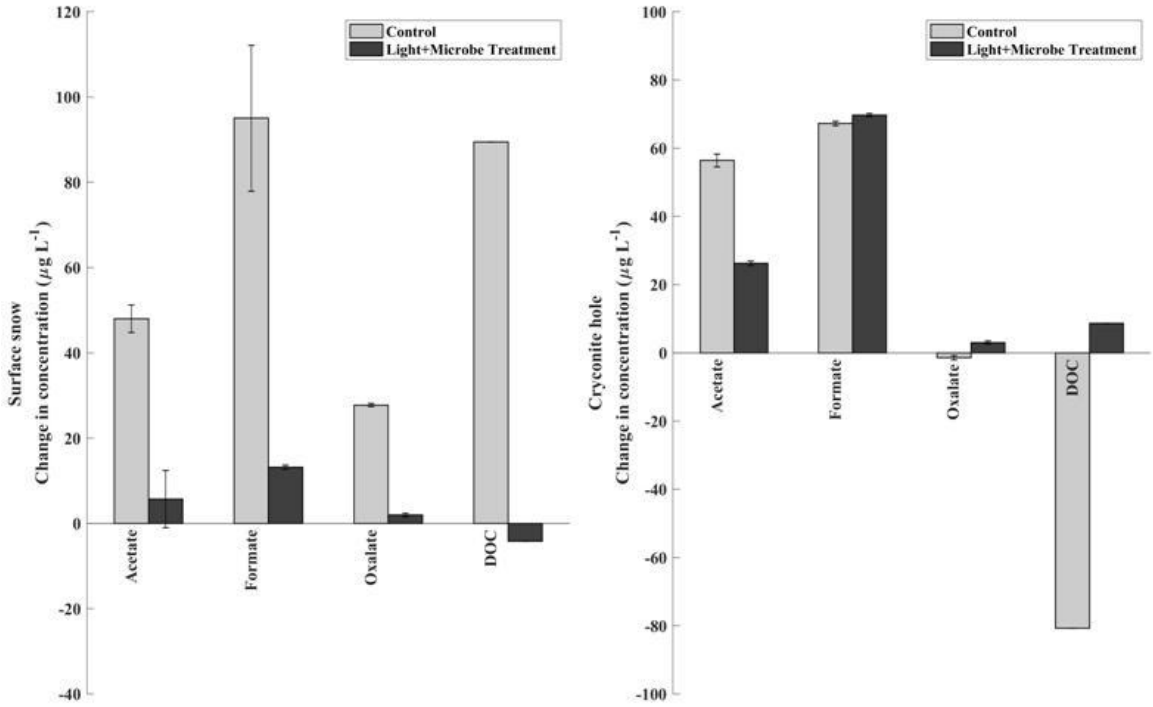

Fig. 5.6. Changes in Ac^-, Fo^-, Oxy^{2-} and DOC in light+microbe treatment over a period of 30 days in surface snow and 25 days in cryoconite holes in experimental system. Negative values represent utilization/degradation and positive values represent production/accumulation.

A similar trend of lower accumulation of Ac^- (65 times) in the light+microbe treatment than control (102 times) was observed in the cryoconite hole water. However, in cryoconite hole, higher accumulation of Fo^- (171 times) and Oxy^{2-} (3 times) in light+microbe treatment than control (Fo^-, 64 times; Oxy^{2-}, 0.6 times) (**Fig. 5.6**) indicates production of carboxylate ions driven by microbial and/or photochemical activity. It is not clear why opposing trends in Fo^- and Oxy^{2-} concentrations are observed in snow and cryoconite holes under the combined influence of light and microbes. Several studies have shown that organic compounds on the glacier surface can act as important precursors for the photochemical production of carboxylic acids (Dibb and Arsenault, 2002; Legrand et al., 2004). DOC produced by the primary producers in snow and cryoconite holes could provide some of the organic precursors

for the formation of carboxylate ions. However, the nature of carboxylate ions generated would depend on the concentration and types of organic carbon precursors (Souza and Carvalho, 2001). Therefore, differences in photosynthetic activity and in the nature of organic material present in snow and cryoconite holes could possibly contribute to differences in the nature and concentration of carboxylate ions observed in snow and cryoconite holes.

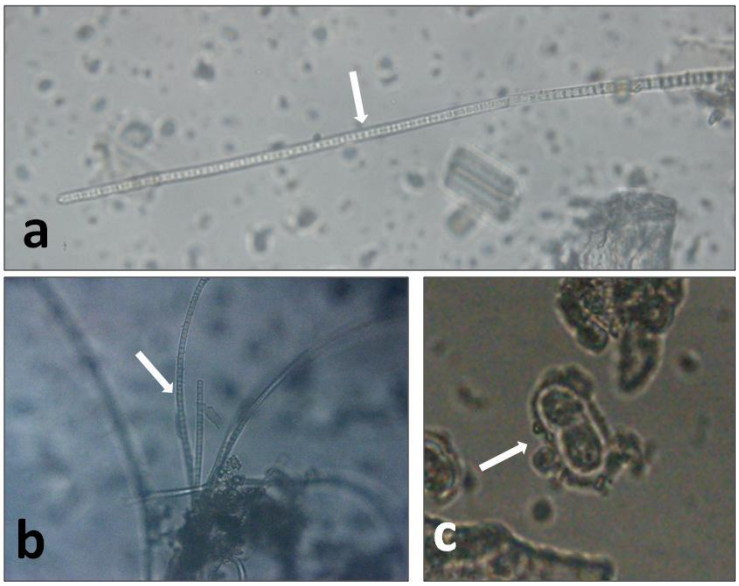

Fig. 5.7. Microscopy images of the cryoconite water samples showing cyanobacteria (a and b) and algae (c).

In surface snow, higher accumulation of NO_3^- in the light-only (2.6 times) and microbe-only (13.5 times) treatments compared to the light+microbe treatment (2.3 times) (**Table 5.4**) suggests that photochemical and microbial activity occurring independantly had a higher influence on surface snow NO_3^- concentrations compared to the combined effect of light and microbes. In contrast, in cryoconite hole water, a higher accumulation in NO_3^- concentrations (4.0 times) in the light+microbe incubation compared to that in control (1.3 times), the light-only (2.6 times) and microbe-only (1.6 times) (**Table 5.4**) incubation suggest that photochemical production of NO_3^- occurring

concomitantly with sunlight stimulated microbial production of NO_3^- (nitrification) influence cryoconite hole NO_3^- concentrations to a greater extent than these processes occurring individually.

Table 5.4. Concentration of major inorganic ions (Na^+, K^+, Mg^{2+}, Ca^{2+}, Cl^-, SO_4^{2-} and NO_3^-) on 0 day and 30th day in surface snow, and on 0 day and 25th day in cryoconite hole water.

	Na^+	K^+	Mg^{2+}	Ca^{2+}	Cl^-	SO_4^{2-}	NO_3^-
				μg L^{-1}			
Surface Snow							
Microbe-only treatment							
0 day	4932	179	813	912	792	118	30
30 day	3766	204	630	1289	650	215	80
Light-only treatment							
0 day	1713	88	234	526	336	38	21
30 day	nd*	nd	nd	nd	nd	255	284
Light+microbe treatment							
0 day	4932	179	813	912	792	118	30
30 day	2799	169	180	680	468	359	69
Control							
0 day	1713	88	234	526	336	38	21
30 day	2544	557	541	1943	11770	126	300
Cryoconite hole water							
Microbe-only treatment							
0 day	7587	198	1246	1204	1068	378	19
25 day	5917	574	683	1855	964	366	30
Light-only treatment							
0 day	7632	224	949	1187	1079	384	17
25 day	3661	133	398	658	681	293	44
Light+microbe treatment							
0 day	7587	198	1246	1204	1068	378	19
25 day	980	606	154	820	243	122	78
Control							
0 day	7632	224	949	1187	1079	384	17
25 day	6432	366	842	926	1148	468	23

*Not detected

5.3.2.4 Overview of carbon and nutrient cycling in the experimental system

Changes in DOC concentrations in each of the incubation treatments showed similar trends of depletion in surface snow and cryoconite hole water samples except a slight accumulation observed in light+microbe treatment in the cryoconite hole water **(Fig. 5.6)**. Decrease in DOC concentrations in Antarctic surface snow following microbial (Antony et al., 2017) and/or photochemical activity has been previously observed (unpublished data). The highest depletion in DOC concentration in the surface snow samples was observed in microbe-only treatment where DOC concentration dropped to below detection limit at the end of the incubation. Decrease in DOC concentrations occurred to a lower extent (0.6 times) in both light-only and light+microbe treatments. This shows that light independant microbial activity plays an important role in DOC degradation in surface snow compared to that of photo-degradation. A lower depletion of DOC in the light+microbe treatment compared to the microbe-only treatment may be a result of either inhibitory effect of light on microbial activity or light induced DOC production (primary production) occurring concommitanly with microbial degradation resulting in higher DOC concentrations in the light+microbe treatment. A similar trend is observed in the cryoconite hole water wherein, there is an increase in DOC concentrations in the light+microbe treatment (1.6 times) in comparison to the light-only and microbe-only treatment indicating light stimulated microbial production of DOC, that is primary production. Thus, light could have an inhibitory effect on heterotrophic microbial activity and a positive effect on autotrophic microbial activity. The net effect of these two processes will determine the fate of DOC in these environments.

The lower depletion of DOC concentration in the cryoconite hole than surface snow could be due to differences in the concentration and composition of initial DOM, as well as, differences in microbial abundance, diversity and activity. For example, a previous study has shown that cryoconite hole organic matter is highly bio-available and readily utilized by heterotrophic microbial communities (Sanyal et al., 2018). Thus, microbial processing of the high initial organic matter load in the cryoconite hole water

(150 and 162.2 µg L^{-1}) compared to surface snow samples (11 to 50 µg L^{-1}) could result in higher accumulation of inorganic nutrients in the cryoconite hole water. In the light+microbe treatment, this increase in inorganic nutrient concentrations would stimulate phytoplankton growth and therefore, photosynthetic activity, consequently increasing the DOC concentration in the sample despite the simultaneous decrease in DOC due to heterotrophic activity. This is supported by significantly higher inorganic nutrient concentrations in cryoconite hole water samples compared to the surface snow samples, likely resulting in an increase in phytoplankton biomass and activity towards the end of the experiment.

In general, following incubation, carboxylate ion concentrations were found to be higher than initial in the snow samples in all treatments. However, lower accumulation in light-only, microbe-only and light+microbe treatments than control are attributed to concurrent photochemical and/or microbial degradation of these organic species in surface snow as has been shown in several studies (Vaïtilingom et al., 2011). In contrast, carboxylate ion concentrations in the cryoconite hole water showed varying trends in concentrations in the different treatments. This is attributed to variability in microbial community composition and organic matter sources that are reactive precursors to carboxylic acids in cryoconite holes.

Following incubation, lower accumulation of NO_3^- concentrations were observed in surface snow in all treatments than control incubation **(Table 5.4)**. The increase in NO_3^- concentrations in the control treatment indicates abiotic production of NO_3^-. The much lower extent of NO_3^- increase in the light and microbe treatments occurring individually and in combination suggests that despite abiotic production of NO_3^-, photochemical decomposition (Dibb et al., 2002; Honrath et al., 2000), and/or microbial uptake (Carpenter and Dunhem, 1985; Cochlan, 1989) of NO_3^- may be simultaneously occurring. While, in cryoconite hole water, higher accumulation of NO_3^- was observed in all treatments compared to the control incubation suggesting photochemical and/or microbial production of NO_3^- in the light and microbe treatments. Sulphate showed accumulation in surface snow in all treatments **(Table 5.4)**. Higher

accumulation of SO_4^{2-} in light-only treatment in surface snow is attributed to sulphide oxidation as observed in previous studies reporting the presence of reduced sulphur compounds in snow overridden with dust which can undergo oxidation to SO_4^{2-} (Hasnain and Thayyen, 1999; Hodson et al., 2010; Mikucki and Priscu, 2007; Sharp et al., 1999). Since the snow samples in this study had significant dust inputs from surrounding nunataks (exposed land mass), it is possible that these samples have associated reduced sulphur species which undergo photochemical and/or microbial oxidation resulting in high SO_4^{2-} in these samples following incubation when compared to the initial sample. The higher accumulation of sulphate observed in the light-only treatment (4.4 times) compared to the microbe-only treatment (1.1 times) indicates that photochemical processes may play a more important role than microbial processes.

In surface snow, depletion of inorganic ions (Na^+, K^+, Mg^{2+}, Ca^{2+} and Cl^-) were observed in all the treatments except an increase observed in K^+ and Ca^{2+} concentrations in microbe-only treatment (**Table 5.4**). In cryoconite hole water, depletion was observed in the concentrations of Na^+, K^+, Mg^{2+}, Ca^{2+} and Cl^- in the light-only treatment. Whereas, in light+microbe treatment in cryoconite water, depletion in Na^+, Mg^{2+}, Ca^{2+} and Cl^-, while an accumulation in K^+ concentrations was observed. Similarly, in microbe-only treatment in cryoconite water, depletion of Na^+ and Cl^- was observed and an accumulation of K^+, Mg^{2+} and Ca^{2+} was observed (**Table 5.4**). Heterotrophic activity has been identified to reduce the pH within the cryoconite holes via generation of CO_2 (Tranter et al., 2004; Telling et al., 2014). In turn, reduction in pH causes a dissolution of salts and minerals like carbonates and silicates, thereby resulting in an increase in ion concentrations such as Ca^{2+}, Mg^{2+} and K^+ (Bagshaw et al., 2016; Telling et al., 2014; Tranter et al., 2004). In the cryoconite hole water, accumulation of Ca^{2+} (1.5 times), Mg^{2+} (3.5 times) and K^+ (2.9 times) in light+microbe and accumulation of K^+ (3.1 times) in microbe-only treatment is credited to the heterotrophic activity occurring in the cryoconite hole water (**Table 5.4**). Similarly, in surface snow, accumulation of K^+ (1.1) and Ca^{2+} (1.4) in microbe-only treatment is attributed to heterotrophic activity (**Table 5.4**). Depletion observed in the inorganic ions in both surface snow and cryoconite holes is not clear. However, an ion

imbalance caused by significant changes in carboxylate ions, as well as, in NO_3^- and SO_4^{2-} may cause depletion in inorganic ions.

5.3.3 Nutrient cycling - Natural System

Dissolved organic carbon was found to accumulate in both sunlight-exposed and shaded cryoconite holes. Higher accumulation in the sunlight-exposed (9.3 times) than shaded (5.6 times) cryoconite hole is attributed to the enhanced primary production in the sunlight-exposed cryoconite hole (**Fig 5.8**). Taking into account the *in-situ* primary productivity rates measured in the cryoconite hole and the DOC accumulation in the sunlight-exposed cryoconite hole, 15% of DOC accumulation in the cryoconite water is contributed by the primary production. Similarly, considering the accumulation observed in sediment in the sunlight-exposed cryoconite hole (0.16 mg C g^{-1}), 10% of TOC accumulation is contributed by the primary production. This indicates that a significant fraction of DOC in the cryoconite holes is contributed by sources other than primary production.

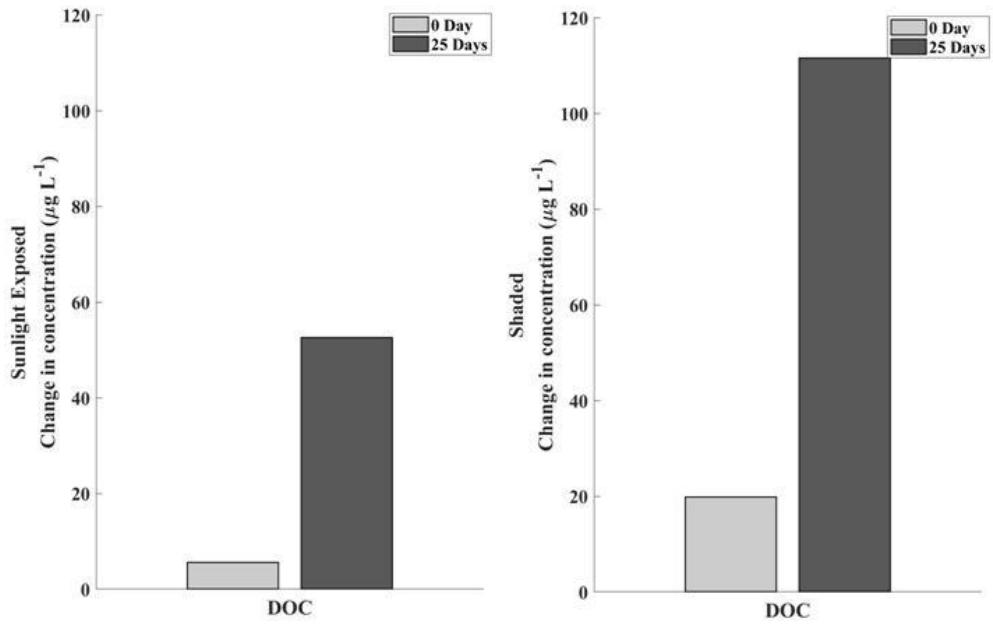

Fig. 5.8. Changes in DOC concentration in sunlight exposed and shaded cryoconite hole.

The results from this study concur with previous findings from an Arctic glacier which show that microbial primary production contributes to only a small fraction of the DOC on the glacier surface and that most of the organic carbon in the cryoconite hole most likely comes from allochthonous sources (Stibal et al., 2008) such as marine emissions and long range transports of aerosols. Various studies on viral induced bacterial lysis suggest that disintegration of bacteria can increase the DOC pool in the environment (Hodson et al., 2008; Wilhelm and Suttle, 1998). In the present study, an increase in DOC/TOC ratio from initial to final day was observed in both sunlight-exposed (initial, 0.09; final, 0.86) and shaded (initial, 0.39; final, 0.95) cryoconite hole. This shows that by the end of the experiment, an average of 90% of organic carbon was consisted of the DOC fraction in both sunlight exposed and shaded cryoconite holes compared to only 9% (sunlight-exposed hole) and 35% (shaded hole) of DOC observed in the initial sample. This trend supports the idea that viral induced microbial lysis could possibly contribute to some of the DOC content in the cryoconite holes.

Accumulation of DOC (9.3 times) in the sunlight-exposed cryoconite hole in the natural system, where concomittant photochemical and microbial activity occurs, was consistent with the trend observed in the light+microbe treatment in the experimental system (1.1 times). Higher accumulation of DOC observed in the natural system is attributed to: 1) Concomitant influx of atmospheric CO_2 which can be utilised by microbes for production of DOC, and 2) Interaction of sediments and the overlying water resulting in dissolution of organic matter from the sediments. Similarly, accumulation of DOC in the shaded cryoconite hole (5.6 times) in the natural system where photochemical activity is restricted and only microbial activity occurs, was consistent with the lower DOC accumulation observed in the microbe-only treatment (0.9 times) than control (0.5 times) in the experimental system.

Accumulation in Ac^- (1.7 times) was observed in sunlight-exposed cryoconite hole, while depletion (0.3 times) was observed in shaded cryoconite hole (**Fig. 5.9**). The observed increase in Ac^- in the sunlight-exposed cryoconite hole is most likely

attributed to photochemical degradation of DOM as has been observed in several studies (Backlund, 1996; Brinkmann et al., 2003) resulting in production of Ac^- (Dibb and Arsenault, 2002, Legrand et al., 2004). Similarly, in the experimental system, higher accumulation of Ac^- was observed in light+microbe treatment than microbe-only treatment suggesting production of Ac^- via photo-degradation of DOM. The decrease observed in shaded cryoconite hole is attributed to microbial uptake of Ac^-. Similarly, an increase in Fo^- concentration was observed in the sunlight-exposed cryoconite hole in natural system (**Fig. 5.9**) and is consistent with the trend observed in light+microbe treatment in the experimental system (**Fig. 5.6**), thereby suggesting a production of Fo^- via photochemical degradation of organic matter. In the shaded cryoconite hole, Fo^- concentration remained unchanged (**Fig. 5.9**).

In the natural system, accumulation of Oxy^{2-} (1.2 times) in the sunlight-exposed cryoconite hole (**Fig. 5.9**) where concomitant microbial and photochemical activity occurs is consistent with the trend observed in the light+microbe treatment in the experimental system (2.8 times) (**Fig. 5.6**) suggesting accumulation of Oxy^{2-} in environment during the melt season. Similarly, a small increase in Oxy^{2-} in shaded cryoconite hole in natural system (2.0 times) (**Fig. 5.9**) is consistent with accumulation in the microbe-only treatment (1.5 times) in the experimental system (**Fig. 5.4**) which indicates microbial production of Oxy^{2-} in dark. Higher accumulation of Oxy^{2-} in shaded cryoconite hole than sunlight exposed cryoconite holes suggests photochemical degradation of Oxy^{2-}. In contrast, in the experimental system, higher accumulation of Oxy^{2-} in light+microbe treatment (2.8 times) than microbe-only treatment (1.5 times) was observed. The opposing trend observed in both the systems is not clear. However, it is suggested that variability in microbial community composition and organic matter sources that are reactive precursors to carboxylic acids are important factors determining the final composition and concentration of carboxylate ions.

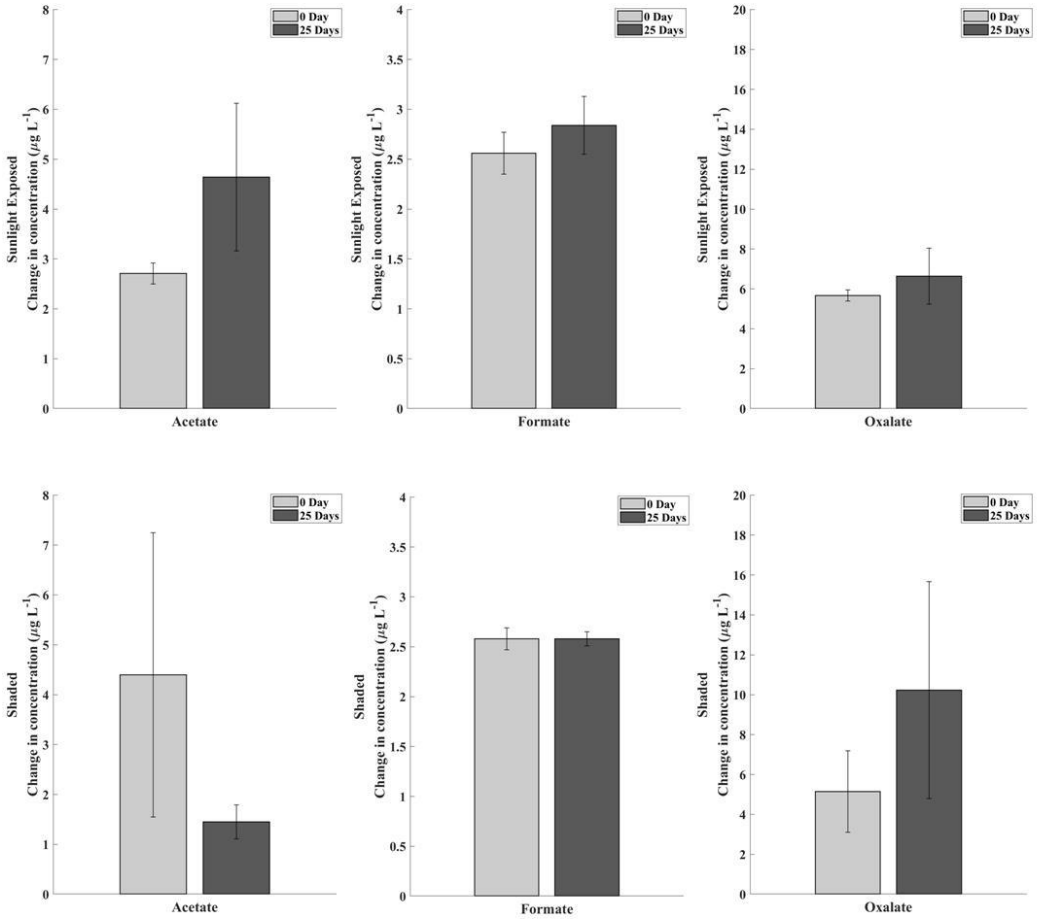

Fig. 5.9. Changes in Ac^-, Fo^- and Oxy^{2-} in sunlight exposed and shaded cryoconite hole.

Reduction in NO_3^- was observed in both sunlight-exposed and shaded cryoconite holes with higher depletion in sunlight-exposed cryoconite hole (13.1 times) than shaded cryoconite hole (2.3 times) (**Table 5.5**), which is attributable to the photochemical decomposition of NO_3^- in sunlight-exposed cryoconite hole. In contrast, accumulation of NO_3^- was observed in the cryoconite hole water in the experimental system in both light+microbe treatment and microbe-only treatment with higher accumulation observed in light+microbe treatment. The opposing trend is attributed to higher dissolved organic nitrogen (DON) concentration in the experimental system (10 μg L^{-1}) compared to natural system (bDL), which through mineralization followed by

nitrification may contribute to higher NO_3^- content in the sample. This NO_3^- production compensates any reduction in its content caused by photochemical decomposition.

Accumulation of Mg^{2+} and Ca^{2+} were observed in sunlight-exposed cryoconite hole, while accumulation of K^+, Mg^{2+} and Ca^{2+} were observed in shaded cryoconite hole **(Table 5.5)**. The accumulation of these cations is attributed to dissolution of minerals such as silicates and carbonates as a result of heterotrophic activity reducing the pH of the cryoconite hole water. Higher accumulation of Mg^{2+} (14.2 times) and Ca^{2+} (7.3 times) in sunlight-exposed cryoconite hole than shaded cryoconite hole (Mg^{2+}, 1.3 times; Ca^{2+}, 1.1 times) may be attributed to changes in pH and ionic balance due to: 1) higher extent of heterotrophic activity and respiration of DOC generated through primary production (Cory et al., 2013, 2018), and 2) CO_2 produced through photochemical degradation of DOM (Ward and Cory, 2016).

Table 5.5. Inorganic ion concentrations in sunlight-exposed and shaded cryoconite holes on 0 and 25 day.

	Na^+	**K^+**	**Mg^{2+}**	**Ca^{2+}**	**Cl^-**	**SO_4^{2-}**	**NO_3^-**
	µg L^{-1}						
Sunlight exposed cryoconite hole							
0 day	4268	157	20	29	nd*	nd	1750
25 day	1448	80	279	217	230	14	134
Shaded cryoconite hole							
0 day	1771	59	121	313	nd	14	897
25 day	1342	70	213	351	750	15	391

* Not detected

Results obtained from the study of DOM and nutrient cycling in snow and cryoconite holes through *in-situ* incubations in an experimental and/or natural set up indicate that photochemical and/or microbial processes result in a continuous exchange of nutrients, CO_2, and DOC, thereby playing an important role in the final composition and concentration of DOC and nutrients in these environments. The experimental system provided a focused view to understand the effect of light and/or microbes acting

individually or in concert, on DOM cycling, while the natural system provides a snap shot of DOM cycling in the natural environment. Thus, both the sampling strategies need to be implemented together to understand the variation in DOC and nutrient cycling due to microbial and/or photochemical activities.

5.3.4 Overview of nutrient cycling in the environment

An accumulation of organic carbon was observed in the cryoconite holes in this study over the melt season. DOC inputs from *in-situ* primary production appears to be a small but an important contributor to the organic carbon pool in these cryoconite holes resulting in about 2.5% of TOC accumulation in cryoconite sediments and about 15% of the DOC accumulation in cryoconite water. Thus, a large fraction of organic matter in cryoconite holes may be derived *largely from allochthonous sources as has been demonstrated in previous studies (Stibal et al., 2008).* In addition, viral lysis of bacterial cells could also contribute to the release of cellular contents and DOC from bacterial cells, thereby impacting DOC concentrations in these environments. Higher DOC accumulation in the sunlight-exposed cryoconite hole compared to shaded hole is attributed to the light induced production of DOC, i.e. primary production.

Carboxylate ions which constitute an important fraction of the DOC pool appears to accumulate in cryoconite hole meltwater as by-products of photochemical decomposition of organic matter. Under dark conditions, microbial uptake/degradation seems to deplete the pool of carboxylate ions. Among the major carboxylate ions, Ac^- and Fo^- are more readily utilized by microbes, while Oxy^{2-} appears to be produced during microbial activity. Photochemical production of Ac^-, Fo^- and Oxy^{2-} appears to compensate for any loss due to photochemical decomposition of these ions.

Depletion in NO_3^- in the natural system appears to be due to microbial uptake and photochemical decomposition together with atmospheric exchange. However, accumulation trend of NO_3^- observed in the experimental system is most likely attributed to higher DON concentrations observed in the experimental system which in turn contributes to high NO_3^- concentrations through mineralization of DON to NH_4^+, followed by nitrification.

Apart from direct impact of microbial activity or photochemical activity on the nutrient content, these activities may indirectly cause various changes in the major ion concentrations. For instance, accumulation of K^+, Ca^{2+}, and Mg^{2+} have been observed in the samples resulting from dissolution of silicates and carbonates which in turn could be triggered by reduction of pH caused by heterotrophic activity. Similarly, generation of CO_2 during photochemical decomposition of DOM may also cause dissolution of salts and minerals comprising silicates and carbonates due to reduction in pH. In addition, various changes in concentration of ions such as carboxylate and NO_3^- may affect the concentration of other ions in order to compensate the ion imbalance.

Overall, in the present study, both photochemical and microbial activies seem to control the nutrient cycling. Although, it is difficult to elucidate the individual effects of each activity, but the behavioural trend of the nutrients due to each of the activities could be determined. In addition to photochemical and microbial activties, initial inoculums of various nutrients and atmospheric exchange of gases also seem to play a determining role in the final chemical composition. A schematic diagram showing the DOM cycling in the supraglacial environments in glaciers and ice sheets as depicted from this study is given in **Fig. 5.10**.

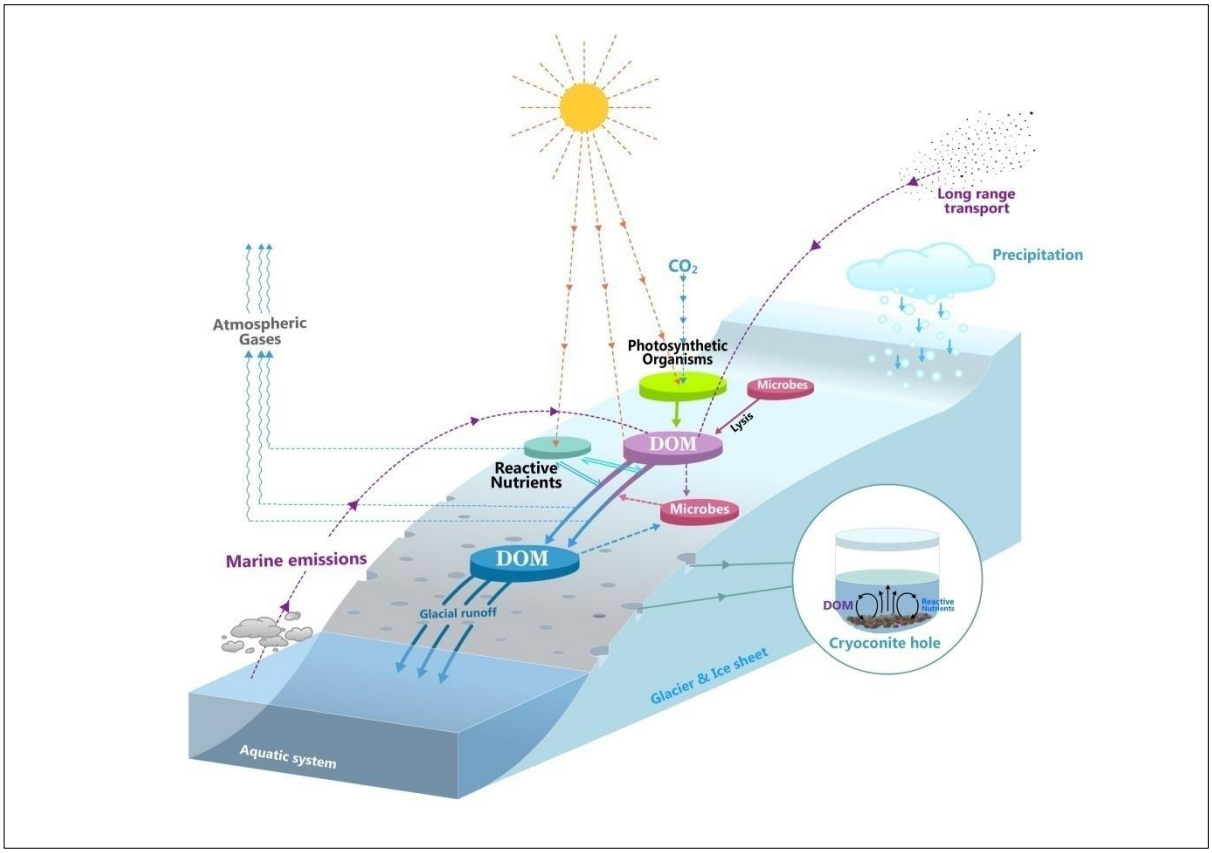

Fig. 5.10. Schematic diagram depicting dissolved organic matter (DOM) cycling in supraglacial environments (like snow and cryoconite holes) of glaciers and ice sheets. Source of DOM (indicated with purple colour) include photosynthesis, microbial lysis and allochthonous sources (like marine emissions and long range transportation of aerosols). The DOM (purple) is further consumed by microbes such as heterotrophic organisms. Photochemical activity on this DOM (purple) may produce DOM (indicated with blue colour) with different composition. Additionally, microbial activity also causes transformation in the DOM composition before getting transported to downstream. Involvement of nutrients and atmospheric gases in these processes are represented in the diagram. Cryoconite hole sediments contributing to the DOM cycling is also depicted.

Chapter 6

Summary and conclusions

Antarctic ice sheet, which hosts about 90% of world's ice, contains a globally relevant pool of dissolved organic matter (DOM) and therefore, can significantly affect the downstream ecological functioning as a result of the ongoing climate warming. The glaciers and ice sheets harbor a wide range of microbial communities that interact with their physical and chemical environments resulting in distinct processes and feedbacks that impact nutrient cycling, surface albedo, melt rates and regional atmospheric carbon concentrations. However, studies dealing with biogeochemical cycling and information on the sources and distribution of OC within these supraglacial environments are scarce and limited. Additionally, changes observed in the composition and concentration of DOM and nutrients due to various complex environmental processes is still not well understood. Therefore, this doctoral research was aimed to: 1) understand the characteristics of different supraglacial ecosystems; 2) gain insights into how DOM and nutrients are transformed through photochemical and microbial activity in supraglacial environments.

To meet these goals, biogeochemical characteristics were studied in surface snow, cryoconite holes and blue ice samples from three geographically distinct study areas within the East Antarctica. Surface snow samples were systematically collected along a 180 km coastal-inland transect at Princess Elizabeth Land (PEL) (18 samples) and along a 130 km coastal transect at Amery Ice Shelf (AIS) (13 samples). Cryoconite holes were sampled from AIS (7 samples), central Dronning Maud Land (cDML) (7 samples) and Larsemann Hills (LHS) which lies within the PEL region (7 samples). Blue ice samples were collected from LHS (3 samples) and AIS (2 samples). Biogeochemical parameters studied in these ecosystems include major inorganic ions, carboxylate ions, total organic carbon (TOC), dissolved organic carbon (DOC), bacterial cell density, microbial morphology, mineralogy of cryoconite hole sediments,

dust concentration (surface snow), primary production and bacterial production. More importantly, *in-situ* field experiments were carried out together with laboratory measurements to understand the DOM and nutrient cycling through photochemical and microbial activity in these selected environments. *In-situ* experiments consisted of an experimental system and a natural system. In the experimental system, surface snow and cryoconite hole water samples collected in quartz tubes were incubated in the field for approximately 30 days under light and dark conditions, both in the presence and absence of microbes. In the natural system, two adjacent cryoconite holes in the natural system subjected to different sunlight conditions (light-exposed and shaded), were monitored over a period of 25 days in order to better understand how DOM is cycled in these environments. Salient findings of this study are:

- Surface snow chemistry at both PEL and AIS is significantly influenced by sea spray as demonstrated by sea salt (ss)Na^+ contribution (89% in PEL and 94% in AIS) to total Na^+ concentration. Significant crustal input in surface snow was demonstrated by non sea salt (nss)Ca^{2+} contribution (77% in PEL and 64% in AIS) to total Ca^{2+} concentration. Ionic balance estimations showed that majority of surface snow samples in the PEL region were acidic, while at AIS, majority of surface snow samples were alkaline. Acidity in the surface snow samples was majorly contributed by NO_3^- (which contributes to 8% of the ionic composition and was majorly present in form of HNO_3 in the samples) followed by SO_4^{2-} and Cl^-. Alkalinity in the surface snow samples at AIS is attributed to the interaction of anions (SO_4^{2-}, Cl^- and NO_3^-) with the salts and dust minerals leading to neutralization of acids.

- Total organic carbon concentration at PEL ranged from 88±6 to 269±6 µg L^{-1} and at AIS, it ranged from below detection limit (bDL) to 117.6±2.9 µg L^{-1}. Acetate concentration measured in surface snow ranged from bDL to 42.93±0.00 µg L^{-1} and 15.23±0.84 µg L^{-1} at PEL and AIS, respectively. Formate concentration ranged from bDL to 3.19±0.04 µg L^{-1} and 21.00±0.31 µg L^{-1} at PEL and AIS, respectively. Carboxylate ion concentration in surface snow at PEL and AIS was consistent with

data reported in a previous study in East Antarctica. Microbial cell densities in the AIS samples ranged between 0.16×10^4 and 10.34×10^4 cells mL^{-1}.

- Major sources of carboxylate ions (Ac^- and Fo^-) include marine aerosols and long range transport. Additionally, photochemical activity within snowpack is found to be a significant source of these ions. It is suggested that photochemical production of Ac^- occurs via photolysis of NO_3^- producing hydroxyl radical ($^{\bullet}OH$) which further oxidizes the organic matter to produce carboxylate ions. Oxidation of organic matter with $^{\bullet}OH$ could not explain the spatial trend of Fo^- in this study, suggesting that other sources could be dominant for Fo^- content in surface snow.
- In blue ice, average TOC concentration was 93.4 µg L^{-1} at LHS and 107.3 µg L^{-1} at AIS. Bacterial cell density ranged from 0.46×10^4 and 0.94×10^4 cells mL^{-1}. Studies providing the chemical composition and TOC concentration in blue ice are limited or not available. This work therefore provides a valuable data on blue ice chemistry.
- This study presents chemical characteristics of cryoconite holes from the regions in the East Antarctica, where there is limited or no data available. Total organic carbon concentration in cryoconite hole water ranged from 7.2±2.7 to 1213.5±6.3 µg L^{-1}, while in cryoconite hole sediments, TOC concentration ranged from 0.4 to 1.8 mg C g^{-1}. Bacterial cell density ranged from 0.07×10^4 and 11.8×10^4 cells mL^{-1}.
- In cryoconite hole samples, Cl^- concentration and Cl^- enrichment factor [EF(Cl^-)] was used as the proxy to determine the hydrological isolation/connectivity of the cryoconite holes. Cryoconite holes at LHS were found to be hydrologically connected [EF(Cl^-)<1] and cryoconite holes at AIS were isolated [EF(Cl^-)>1]. Depletion occurs in major ions and TOC concentration in the hydrologically connected cryoconite holes at LHS. This depletion is attributed to flushing of the ions and organic matter from the cryoconite holes via the interconnected streams and melt water channels. In contrast, major ions and TOC in the isolated cryoconite holes at AIS were enriched by 7 to 26 times. This accumulation is attributed to the dissolution of salts, minerals and DOM resulting from the interaction between

sediment and overlying water in a cryoconite hole during the period of isolation. In addition, microbial activity also contributes to the TOC enrichment in a cryoconite hole. Cryoconite holes at cDML were partially connected as revealed from depletion of Cl^- and accumulation of other major ions and TOC. At cDML, variations observed in the enrichment trend shown by Cl^- and other ions (and TOC) are attributed to increased interaction between sediments and the overlying water within a cryoconite hole due to limited and slower rate of water exchange. It is further inferred from the study that isolated holes store an abundance of nutrients and carbon compared to connected holes which may further affect the extent of microbial activity within the holes and also their impact on nutrient and carbon transport to the downstream environments.

- Primary production rates (measured using ^{14}C-$NaHCO_3$) in two surface snow samples were 0.15±0.04 and 0.23±0.01 µgC L^{-1} d^{-1}. Primary production in cryoconite hole water and sediment samples ranged from 0.13±0.06 to 0.47±0.08 µgC L^{-1} d^{-1} and 0.15±0.01 to 1.05±0.43 µgC g^{-1} d^{-1}, respectively. Primary production measured in surface snow and cryoconite hole water samples were comparable, while the rates were approximately 1110 times higher in the cryoconite sediments. Between different cryoconite holes in the LHS, primary production rates varied widely. Primary production rates measured in LHS were at the lower end of the range documented for the cryoconite hole water samples from other regions of Antarctica. Rates reported for non-Antarctic regions are approximately 70 to 550 times higher than that measured at LHS.
- Bacterial production rates (measured using methyl-^3H-Thymidine) in cryoconite hole water and sediment samples ranged from 4.70±0.23 to 35.35±1.25 ngC L^{-1} d^{-1} and 0.42±0.19 to 3.63±5.49 ngC g^{-1} d^{-1}, respectively. Bacterial production rates in the sediment samples were 26 times higher compared to the overlying water. Bacterial production rates measured at LHS were at the lower end of the range documented for the cryoconite hole water samples from other regions of Antarctica. Rates measured at LHS showed few similarities with non-Antarctic regions.

- Primary production contributed to 15% of DOC accumulation in cryoconite hole water and 10% in cryoconite hole sediments. Thus, significant amount of DOC in cryoconite holes is probably derived from allochthonous sources. Additionally, it is suggested that bacterial lysis may contribute to the DOC concentration within the cryoconite holes.
- Microbial and photochemical degradation of DOC in surface snow and cryoconite hole water was inferred from the decrease in DOC concentration following different incubations (light-only, microbe-only and light+microbe treatment) in experimental system. Higher depletion of DOC occurs in light independent microbial activity than photochemical activity (occurring individually). In light+microbe treatment, lowest depletion of DOC in surface snow and an accumulation of DOC in cryoconite holes is attributed to inhibitory effect of light on microbial activity and primary production occurring concomitantly with microbial degradation. Lower depletion of DOC concentration in the cryoconite hole than surface snow is attributed to the higher concentration of initial DOM and nutrients in cryoconite hole, as well as, differences in microbial abundance, diversity and activity. It is suggested that higher inorganic nutrient and DOC concentrations in cryoconite hole water samples compared to the surface snow sample, likely result in an increase in phytoplankton biomass and activity towards the end of the experiment.
- Higher accumulation of DOC was observed in the natural system than experimental system due to the concomitant input of CO_2 required for primary production and the interaction between the cryoconite hole water and the underlying sediment. Further, higher accumulation of DOC occurs in presence of sunlight than dark conditions as a result of primary production. This was supported by higher accumulation of DOC observed in sunlight-exposed cryoconite hole (9.3 times) than shaded cryoconite hole (5.6 times).
- Among the carboxylate ions, Ac^- and Fo^- are readily utilized by microbes, while Oxy^{2-} production occurs due to microbial activity under dark conditions. In presence of sunlight, photochemical production of Ac^-, Fo^- and Oxy^{2-} compensates for any loss due to photochemical decomposition of these ions. Additionally, it is

suggested that variability in microbial community composition and organic matter sources that are reactive precursors to carboxylic acids are important factors determining the final composition and concentration of carboxylate ions.

- Depletion of NO_3^- in the natural system, appears to be due to microbial uptake and photochemical decomposition together with atmospheric exchange. However, accumulation trend of NO_3^- observed in the experimental system may be attributed to higher DON concentrations observed in the experimental system which in turn contributes to high NO_3^- concentrations through mineralization of DON to NH_4^+, followed by nitrification.
- Apart from the direct impact on the nutrient concentrations, the microbial and/or photochemical activities may indirectly cause various changes in the ionic concentrations. For instance, heterotrophic activity reduces pH in the system, which further causes dissolution of silicates and carbonates, and results in accumulation of K^+, Ca^{2+}, and Mg^{2+}. Similarly, generation of CO_2 during photochemical decomposition of DOM may also results in accumulation of ions.

Perspectives and future scope of study

This study shows that supraglacial ecosystems such as surface snow, cryoconite holes and blue ice are potential sites of important biogeochemical cycling as they hold a significant pool of nutrients and organic carbon that is constantly engaged in complex environmental processes. Surface snow chemistry in the coastal regions of Antarctica is significantly influenced by sea spray. Microbes observed in these supraglacial ecosystems include cyanobacteria, algae, cocci, rod shaped bacteria and diatoms. Allochthonous sources of the organic carbon include marine emissions and long range transport of aerosols. Cryoconite holes, in particular the isolated holes, contain 7 to 26 times higher concentration of ions and TOC as compared to surrounding surface snow. Additionally, cryoconite hole sediments contain much higher concentration of TOC as compared to the overlying water in the cryoconite holes. Thus, cryoconite holes provide a natural mechanism for the storage of chemical and microbial constituents on the glacier surface and can significantly affect the rate of their transfer to the supraglacial

or subglacial drainage systems. Primary production contributes about 15% to the DOC content in the cryoconite hole water and about 10% to the cryoconite hole sediment. Bacterial lysis is a likely source of organic carbon in cryoconite holes.

This study provides critical information on how photochemistry and biology interact to determine the fate of DOM and nutrient cycling in supraglacial environments. Depletion in the concentration of supraglacial DOM is attributed to microbial as well as photochemical degradation. Light independent microbial degradation leads to higher depletion in the DOC concentration as compared to photochemical degradation. Furthermore, accumulation in DOC in light+microbe treatment in the experimental system suggests that light possibly has an inhibitory effect on heterotrophic activity and a positive effect on autotrophic activity. Higher accumulation of DOC in cryoconite holes in a natural system as compared to experimental system is attributed to: 1) Concomitant input of atmospheric CO_2, which can be utilised by microbes for production of DOC, and 2) Interaction of sediments and the overlying water resulting in dissolution of organic matter from the sediments. Overall, both photochemical and microbial activities seem to control the nutrient cycling. Additionally, apart from microbial and photochemical activities, initial inoculums of various nutrients and atmospheric exchange of gases also play a determining role in the final chemical composition of DOM and nutrients.

Present study provides valuable information on the biogeochemical cycling in different supraglacial ecosystems in the Antarctic ice sheet. However, to understand the global impact of the supraglacial ecosystems to the environment, a more detailed work is still required. Biogeochemical parameters and rates of microbial production in supraglacial ecosystems may differ due to geographical location, carbon sources and various physical parameters. Furthermore, biogeochemical cycling in Antarctic ice sheet is more significant during the summer season due to higher temperature conditions, photochemical activity and melting. Thus, experiments, aiming to quantitatively determine the change in DOM composition before it is exported to the aquatic system downstream, needs to be conducted in different regions of the continent.

This would help to better understand the impact of glacial melting on downstream ecological functioning. Additionally, environmental processes involving DOM also results in production of gaseous species which may impact the chemical characteristics of the overlying atmosphere. Therefore, experiments need to be carried out to characterise and quantify the production of gaseous species during DOM cycling.

References

Al-Hosney, H. A., Carlos-Cuellar, S., Baltrusaitis, J., Grassian, V. H., 2005. Heterogeneous uptake and reactivity of formic acid on calcium carbonate particles: a Knudsen cell reactor, FTIR and SEM study. Phys. Chem. Chem. Phys. 7, 3587-3595.

Amato, P., Hennebelle, R., Magand, O., Sancelme, M., Delort, A. M., Barbante, C., Bourtron, C., Ferrari, C., 2007. Bacterial characterization of the snow cover at Spitzberg, Svalbard. FEMS Microbiol. Ecol. 59, 255–264.

Anastasio, C., Galbavy, E. S., Hutterli, M. A., Burkhart, J. F., Friel, D. K., 2007. Photoformation of hydroxyl radical on snow grains at Summit, Greenland. Atmos. Environ. 41, 5110-5121.

Anesio, A. M., Cook, J. M., Hodson, A. J., Anesio, A. M., Hanna, E., Yallop, M., Stibal, M., Telling, J., Huybrechts, P., 2012. An improved estimate of microbially mediated carbon fluxes from the Greenland ice sheet. J. Glaciol. 58, 1098-1108.

Anesio, A. M., Sattler, B., Foreman, C., Telling, J., Hodson, A., Tranter, M., Psenner. R., 2010. Carbon fluxes through bacterial communities on glacier surfaces. Ann. Glaciol. 51, 32-40.

Anesio, A. M., Hodson, A. J., Fritz, A., Psenner, R., Sattler, B., 2009. High microbial activity on glaciers: importance to the global carbon cycle. Glob Chang Biol. 15(4), 955-960.

Anesio, A. M., Mindl, B., Laybourn-Parry, J., Hodson, A. J., Sattler, B., 2007. Viral dynamics in cryoconite holes on a high Arctic glacier (Svalbard). J. Geophys. Res. 112, G04S31.

Antony, R., Willoughby, A. S., Grannas, A. M., Catanzano, V., Sleighter, R. L., Thamban, M., Hatcher, P. G., Nair, S., 2017. Molecular insights on dissolved organic matter transformation by supraglacial microbial communities. Environ. Sci. Technol. 51, 4321-4337.

Antony, R., Sanyal, A., Kapse, N., Dhakephalkar, P. K., Thamban, M., Nair, S., 2016. Microbial communities associated with Antarctic snowpack and their biogeochemical implications. Microbiol. Res. 192, 192–202.

Antony, R., Grannas, A. M., Willoughby, A. S., Sleighter, R. L., Thamban, M., Hatcher, P. G., 2014. Origin and sources of dissolved organic matter in snow on the East Antarctic ice sheet. Environ. Sci. Technol. 48, 6151–6159.

Antony, R., Mahalinganathan, K., Thamban, M., Nair, S., 2011. Organic carbon in Antarctic snow: spatial trends and possible sources. Environ. Sci. Technol., 45, 9944–9950.

Atkinson, R., 2007. Gas-phase tropospheric chemistry of organic compounds: a review. Atmos. Environ. 41, 200-240.

Autenboer, T. van, 1962. Ice mounds and melt phenomena in the Sor-Rondane Antarctica. J. Glaciol. 4(33), 349-354.

Backlund, P., 1996. Degradation of aquatic humic material by ultraviolet light. Chemosphere 12, 1869-1878.

Bagshaw, E. A., Wadham, J. L., Tranter, M., Perkins, R., Morgan, A., Williamson, C. J., Fountain, A. G., Fitzsimons, S., Dubnick, A., 2016. Response of Antarctic cryoconite microbial communities to light. FEMS Microbiol. Ecol. 92, 1-11.

Bagshaw, E.A., Tranter, M., Wadham, J.L., Fountain, A.G., Dubnick, A., Fitzsimons, S., 2016. Processes controlling carbon cycling in Antarctic glacier surface ecosystems. Geochem. Perspect. Lett. 2, 44–54.

Bagshaw, E.A., Tranter, M., Fountain, A.G., Welch, K., Basagic, H.J., Lyons, W.B., 2013. Do cryoconite holes have the potential to be significant sources of C, N, and P to downstream depauperate ecosystems of Taylor Valley, Antarctica? Arct. Antarct. Alp. Res. 45, 440–454.

Bagshaw, E.A., Tranter, M., Fountain, A.G., Welch, K.A., Basagic, H., Lyons, W.B., 2007. Biogeochemical evolution of cryoconite holes on Canada Glacier, Taylor Valley, Antarctica. J. Geophys. Res.112, GO4S35.

Bauer, W., Fitzner, B., 2003. Salt crusts on bedrock exposures in Dronning Maud Land, East Antarctica. Polarforchung 73(1), 1-4.

Bell, R.E., Chu, W., Kingslake, J., Das, I., Tedesco, M., Tinto, K.J., Zappa, C.J., Frezzotti, M., Boghosian, Al., Lee, W.S., 2017. Antarctic ice shelf

potentially stabilized by export of meltwater in surface river. Nature 544, 344-348.

Bellas, C. M., Anesio, A. M., Telling, J., Stibal, M., Tranter, M., Davis, S., 2013. Viral impacts on bacterial communities in Arctic cryoconite. Env. Res. Lett. 8, 045021.

Benassai, S., Becagli, S., Gragnani, R., Magand, O., Proposito, M., Fattori, I., Traversi, R., Udisti, R., 2005. Sea-spray deposition in Antarctic coastal and plateau areas from ITASE traverses. Ann. Glaciol. 41, 32-40.

Bertilsson, S., Tranvik. L. J., 1998. Photochemically produced carboxylic acids as substrates for freshwater bacterioplankton. Limnol. Oceanogr. 43, 885–895.

Bertler, N., Mayewski, P. A., Aristarain, A., Barrett, P., Becagli, S., Bernardo, R., Bo, S., Xiao, C., Curran, M., Qin, D., Dixon, D. A., Ferron, F., Fischer, H., Frey, M., Frezzotti, M., Fundel, F., Genthon, C., Gragnani, R., Hamilton, G. S., Handley, M., Hong, S., Isaksson, E., Kang, J., Ren, J., Kamiyama, K., Kanamori, S., Kärkäs, E., Karlöf, L., Kaspari, S., Kreutz, K., Kurbatov, A., Meyerson, E., Ming, Y., Zhang, M., Motoyama, H., Mulvaney, R., Oerter, H., Osterberg, E., Proposito, M., Pyne, A., Ruth, U., Simões, J., Smith, B., Sneed, S., Teinilä, K., Traufetter, F., Udisti, R., Virkkula, A., Watanabe, O., Williamson, B., Winther, J-G., Li, Y., Wolff, E., Li, Z., Zielinski, A., 2005. Snow chemistry across Antarctica. Ann. Glaciol. 41, 167–179.

Bhatia, M. P., Das, S. B., Longnecker, K., Charette, M. A., Kujawinski, E. B., 2010. Molecular characterization of dissolved organic matter associated with the Greenland ice sheet. Geochim. Cosmochim. Ac. 74, 3768-3784.

Bintanja, R., 1999. On the glaciological, meteorological, and significance of Antarctic blue ice areas. Rev. Geophys. 37, 337-359.

Bintanja, R., Jonsson, S., Knap, W. H., 1997. The annual cycle of the surface energy balance of Antarctic blue ice. J. Geophys. Res. 102, 1867-1881.

Bintanja, R., Van den Broeke, M.R., Portanger, M.J., 1993. A meteorological and glaciological experiment on a blue ice area in the Heimefront Range, Queen Maud Land, Antarctica. Svea Field Report (pp. 29), Institute for Marine and Atmospheric Research Utrecht, Utrecht University, Netherlands.

Bock, J., Jacobi, H-W., 2010. Development of a mechanism for nitrate photochemistry in snow. J. Phys. Chem. A 114, 1790-1796.

Boggild, C. E., Winther, J. G., Sand, K., Elvehoy, H., 1995. Sub-surface melting in blue-ice fields in Dronning Maud Land , Antarctica : observations and modelling. Ann. Glaciol. 21, 162-168.

Bottenheim, J. W., Boudries, H., Brickell, P. C., Atlas, E., 2002. Alkenes in the Arctic boundary layer at Alert, Nunavut, Canada. Atmos. Environ. 36, 2585-2594.

Boxe, C. S., Saiz-Lopez, A., 2008. Multiphase modelling of nitrate photochemistry in the quasi-liquid layer (QLL): implications for NOx release from the Arctic and coastal Antarctic snowpack. Atmos. Chem. Phys. 8, 4855-4864.

Brinkmann, T., Horsch, P., Saritorius, D., Frimmel, F., 2003. Photoformation of low-molecular-weight organic acids from brown water dissolved organic matter. Environ. Sci. Technol. 37, 4190-4198.

Bushaw-Newton, K. L., Moran, M. A., 1999. Photochemical formation of biologically available nitrogen from dissolved humic substances in coastal marine systems. Aquat. Microb. Ecol. 18, 285-292.

Carpenter, E. J., Dunhem, S., 1985. Nitrogenous nutrient uptake, primary production and species composition of phytoplankton in the Carmans River estuary, Long Island, New York. Limnol. Oceanogr. 30, 513-526.

Carpenter, E. J., Lin, S., Capone, D. G., 2000. Bacterial Activity in South Pole Snow. App. Environ. Microbiol. 66, 4514-4517.

Chebbi, A., Carlier, P., 1996. Carboxylic acids in the troposphere, occurrence, sources and sinks: A review. Atmos. Environ. 30(24), 4233-4249.

Chester, R., 2003. Marine geochemistry. Blackwell Science, Oxford, pp. 506.

Cochlan, W. P., 1989. Nitrogen uptake by marine phytoplankton: The effects of irradiance, nitrogen supply and diel periodicity. PhD dissertation. University of British Columbia, Vancouver, BC, Canada.

Cook, J., 2016. Supraglacial biogeochemistry. Geomorphological Techniques. Chap. 3, Sec. 4.11.

Cory, R. M., Kling, G. W., 2018. Interactions between sunlight and microorganisms influence dissolved organic matter degradation along the aquatic continuum Limnol. Oceanogr. Lett. 3, 102–116.

Cory, R. M., Crump, B. C., Dobkowskic, J. A., Kling, G. W., 2013. Surface exposure to sunlight stimulates CO_2 release from permafrost soil carbon in the Arctic. Proc. Natl. Acad. Sci. USA 110, 3429–3434.

Cory, R. M., Mcneill, K., Cotner, J. P., Amado, A., Purcell, J. M., Marshall. A. G., 2010. Singlet oxygen in the coupled photochemical and biochemical oxidation of dissolved organic matter. Environ. Sci. Technol. 44, 3683–3689.

Cory, R. M., Mcknight, D. M., Chin, Y. P., Miller, P., Jaros, C. L., 2007. Chemical characteristics of fulvic acids from Arctic surface waters: Microbial contributions and photochemical transformations. J. Geophys. Res. Biogeosci. 112, G04S51.

Couch, T. L., Sumner, A. L., Dassau, T. M., Shepson, P. B., Honrath, R. E., 2000. An investigation of the interaction of carbonyl compounds with the snowpack. Geophys. Res. Lett. 27, 2241–2244.

Cragin, J. H., McGilvary, R., 1995. Can inorganic species volatilize from snow?. In: Tonnesson, K. A., Williams, M. W., Tranter, M. (Eds.), Biogeochemistry of Seasonally Snow-Covered Catchments, Vol. 228 (pp. 11 – 16).

Dana, G. L., Wharton, R. A., Dubayah, R., 1998. Ecosystem Dynamics in a Polar Desert: the Mcmurdo Dry Valleys, Antarctica. Priscu, J. (Eds.) American Geophysical Union.

Davies, T. D., 1994. Snow cover-atmosphere interactions. In: Snow and Ice Covers: Interactions with the Atmosphere and Ecosystem.

Davies, T. D., Tranter, M., Jickells, T. D., Abrahams, P. W., Landsberger, S., Jarvis, K., Pierce, C. E., 1992. Heavily-contaminated snowfalls in the remote Scottish Highlands: A consequence of regional-scale mixing and transport. Atmos. Environ. 26, 95-112.

De Angelis, M., Legrand, M., 1995. Preliminary investigations of post-depositional effects of HCl, HNO_3 and organic acids in polar firn layers. In:

Delmas, R.J. (Ed.), Ice Core Studies of Global Biogeochemical Cycles, Vol. 30 (pp. 361–381). NATO ASI Ser. Springer, Berlin, Heidelberg.

De Angelis, M., Traversi, R., Udisti, R., 2012. Long-term trends of mono-carboxylic acids in Antarctica: comparison of changes in sources and transport processes at the two EPICA deep drilling sites. Tellus B 64, 17331.

Delmas R. J., Gravenhorst G., 1982. Background precipitation acidity. In Proc. C.E.C. Workshop "Acid Deposition', Berlin.

Dibb, J. E., Arsenault, M., 2002. Shouldn't snowpacks be sources of monocarboxylic acids? Atmos. Environ. 36, 2513–2522.

Dibb, J. E., Jaffrezo, J. L., 1997. Air-snow exchange investigations at Summit, Greenland: an overview. J. Geophys. Res. 102, 26795–26807.

Dibb, J. E., Arsenault, M., Peterson, M. C., Honrath, R. E., 2002. Fast nitrogen oxide photochemistry in Summit, Greenland snow. Atmos. Environ. 36, 2501–2511.

Doherty, S. J., Warren, S. G., Grenfell, T. C., Clarke, A. D., Brandt, R. E., 2010. Light-absorbing impurities in Arctic snow. Atmos. Chem. Phys. 10, 11647-11680.

Dutton, M. V., Evans, C. S., 1996. Oxalate production by fungi: its role in pathogenicity and ecology in the soil environment. Can. J. Microbiol. 42, 881–895.

Edwards, A., Anesio, A. M., Rassner, S. M., Sattler, B., Hubbard, B., Perkins, W. T., Young, M., Griffith, G. W., 2011. Possible intercations between bacterial diversity, microbial activity and supraglacial hydrology of cryoconite holes in Svalbard. ISME J. 5(1), 150-160.

Erbland. J., Savarino, J., Morin, S., France, J. L., Frey, M. M., King, M. D., 2015. Air–snow transfer of nitrate on the East Antarctic Plateau – Part 2: An isotopic model for the interpretation of deep ice-core records. Atmos. Chem. Phys. 15, 12079–12113.

Erbland, J., Vicars, W. C., Savarino, J., Morin, S., Frey, M. M., Frosini, D., Vince, E., Martins, J. M. F., 2013. Air–snow transfer of nitrate on the East Antarctic Plateau – Part 1: Isotopic evidence for a photolytically driven dynamic equilibrium in summer. Atmos. Chem. Phys. 13, 6403–6419.

Fuhrman, J. A., Azam, E., 1982. Thymidine incorporation as a measure of heterotrophic bacterioplankton production in marine surface waters: evaluation and field results. Mar. Biol. 66, 109-120.

Fuhrman, J. A., Suttle, C. A., 1993. Viruses in marine planktonic systems. Oceanography 6, 51-63.

Foreman, C. M., Sattler, B., Mikucki, J. A., Porazinska, D. L., Priscu, J. C., 2007. Metabolic activity and diversity of cryoconites in the Taylor valley, Antarctica. J. Geophys. Res. 112, G04S32.

Foreman, C. M., Wolf, C. F., Priscu, J. C., 2004. Impact of episodic warming events on the physical, chemical and biological relationships of lakes in the McMurdo Dry Valleys, Antarctica. Aquatic Geochem. 10, 239-268.

Fountain, A. G., Tranter, M., 2008. Introduction to special section on microcosms in Ice: The biogeochemistry of cryoconite holes. J. Geophys. Res. 113, G02S91.

Fountain, A. G., Tranter, M., Nylen, T. H., Lewis, K. J., Mueller, D. R., 2004. Evolution of cryoconite holes and their contribution to meltwater runoff from glaciers in the McMurdo DryValleys, Antarctica. J. Glaciol. 50, 35–45.

Fretwell, P., Pritchard, H. D., Vaughan, D. G., Bamber, J. L., Barrand, N. E., Bell, R., Bianchi, C., Bingham, R. G.,, Blankenship, D. D., Casassa, G., Catania, G., Callens, D., Conway, H., Cook, A. J., Corr, H. F.J., Damaske, D., Damm, V., Ferraccioli, F., Forsberg, R., Fujita, S., Gim, Y., Gogineni, P., Griggs, J. A., Hindmarsh, R. C. A., Holmlund, P., Holt, J. W., Jacobel, R. W., Jenkins, A., Jokat, W., Jordan, T., King, E. C., Kohler, J., Krabill, W., Riger-Kusk, M., Langley, K. A., Leitchenkov, G., Leuschen, C., Luyendyk, B. P., Matsuoka, K., Mouginot, J., Nitsche, F. O., Nogi, Y., Nost, O. A., Popov, S. V., Rignot, E., Rippin, D. M., Rivera, A., Roberts, J., Ross, N., Siegert, M. J., Smith, A. M., Steinhage, D., Studinger, M., Sun, B., Tinto, B. K., Welch, B. C., Wilson, D., Young, D. A., Xiangbin, C., Zirizzotti, A., 2013. Bedmap2: Improved ice bed, surface and thickness datasets for Antarctica. Cryosphere 7, 375-393.

Frey, B., Rieder, S. R., Brunner, I., Plotze, M., Koetsch, S., Lapanje, A., Brandt, H., Furrer, G., 2010. Weathering-associated bacteria from the damma glacier forefield: physiological capabilities and impact on granite dissolution. Appl. Environ. Microbiol. 76, 4788–4796.

Frick, T. D., Crawford, R. L., 1983. Mechanisms of microbial demethylation of lignin model polymers. In: Higuchi, T., Chang, M., Tirk, T.K. (Eds.), Recent Advances in Lignin Biodegradation Research (pp. 143–152). Uni Publishers Co. Ltd., Tokyo.

Fuhrman, J. A., Suttle, C. A., 1993. Viruses in marine planktonic systems. Oceanography 6, 51-63.

Galloway, J. N., Likens, G. E., Keene, W. C., Miller, J. M., 1982. The composition of precipitation in remote areas of the world. J. Geophys. Res. 87, 8771-8786.

Gerdel, R. W., Drouet, F., 1960. The cryoconite of the Thule area, Greenland. (Vol. 79) Transactions of the American Microbiology Society, Washington, DC 20036.

Gharieb, M. M., 2000. Nutritional effects on oxalic acid production and solubilization of gypsum by Aspergillus niger. Mycol. Res. 104, 550–556.

Gibson, E. R., Hudson, P. K., Grassian, V. H., 2006. Physicochemical properties of nitrate aerosols: implications for the atmosphere. J. Phys. Chem. A 110, 11785-11799.

Gold, M.H., Kutuski, H., Morgan, M.A., 1983. Oxidative degradation of lignin by photochemical and chemical radical generating systems. Photochem. Photobiol. 38, 647–651.

Gooseff, M.N., McKnight, D.M., Runkel, R.L., 2004. Reach-scale cation exchange controls on major ion chemistry of an Antarctic glacial meltwater stream. Aquat. Geochem. 10, 221–238.

Graneli, W., Carlsson, P., Bertilssonc, S., 2004. Bacterial abundance, production and organic carbon limitation in the Southern Ocean (39–621S,4–141E) during the austral summer 1997/1998. Deep-Sea Res. II 51, 2569–2582.

Grannas, A. M, Jones, A. E., Dibb, J., Ammann, M., Anastasio, C., Beine, H., Bergin, M., Bottenheim, J., Boxe, C. S., Carver, G., Crawford, J. H., Domine, F., Frey, M. M., Guzman, M. I., Heard, D., Helmig, D., Hoffmann, M. R., Honrath, R. E., Huey, L. G., Jacobi, H. -W., Klan, P., McConnell, J., Sander, R., Savarino, J., Shepson, P. B., Simpson, W. R., Sodeau, J., von Glasgow, R., Weller, R., Wolff, E., Zhu, T., 2007. An overview of snow

photochemistry: evidence, mechanisms and impacts. Atmos. Chem. Phys. 7, 4329–4373.

Grannas, A. M., Shepson, P. B., Filley, T. R., 2004. Photochemistry and nature of organic matter in Arctic and Antarctic snow. Glob. Biogeochem. Cy. 18, GB1006.

Hansen, J., Nazarenko, L., 2004. Soot climate forcing via snow and ice albedos. P. Natl. Acad. Sci. USA 101, 423-428.

Hasnain, S. I., Thayyen, R. J., 1999. Controls on the major-ion chemistry of the Dokriani glacier melterwaters, Ganga basin, Garhwal Himalaya, India. J. Glaciol. 45, 87–92.

Hodson, A. J., Patterson, H., Westwood, K., Cameron, K., Laybourn-Parry, J., 2013. A blue-ice ecosystem on the margins of the East Antarctic ice sheet. J. Glaciol. 59(214), 255-268.

Hodson, A., Bøggild, C., Hanna, E., Huybrechts, P., Langford, H., Cameron, K., Houldsworth, A., 2010. The cryoconite ecosystem on the Greenland ice sheet. Ann. Glaciol. 51, 123-129.

Hodson, A., Anesio, A. M., Tranter, M., Fountain, A., Osborn, M., Priscu, J., Laybourn-Parry, J., Sattler, B., 2008. Glacial ecosystems. Ecol, Monogr. 78, 41–67.

Hodson, A. J., Mumford, P. N., Kohler, J., Wynn, P. M., 2005. The High Arctic glacial ecosystem: new insights from nutrient budgets. Biogeochemistry 72, 233–256.

Hoinkes, H. C., 1960. Studies of solar radiation and albedo in the antarctic. Arch. Meteor. Geophy. B10, 175–181.

Honrath, R. E., Guo, S., Peterson, M. C., Dziobak, M. P., Dibb, J. E., Arsenault, M. A., 2000, Photochemical production of gas phase NOx from ice crystal NO_3^-. J. Geophys. Res. 105(D19), 24183–24190.

Hood, E., Battin, T. J., Fellman, J., O'Neel, S., Spencer, R. G. M., 2015. Storage and release of organic carbon from glaciers and ice sheets. Nat. Geosci. 8, 91-96.

Hood, E., Fellman, J., Spencer, R. G. M., Hernes, P. J., Edwards, R., D'Amore, D., Scott, D., 2009. Glaciers as a source of ancient and labile organic matter to the marine environment. Nature 462, 1044-1047.

Hu, Q-H., Xie, Z-Q., Wang, X-M., Kang, H., Zhang, P., 2013. Levoglucosan indicates high levels of biomass burning aerosols over oceans from the Arctic to Antarctic. Sci. Rep. 3, 3119.

Hutterli, M. A., McConnell, J. R., Chen, G., Bales, R. C., Davis, D. D., Lenschow, D. H., 2004. Formaldehyde and hydrogen peroxide in air, snow and interstitial air at South Pole. Atmos. Environ. 38, 5439–5450.

Jacob, D.J., 1986. Chemistry of OH in remote clouds and its role in the production of formic acid and peroxymonosulfate. J. Geophys. Res. 91, 9807-9826.

Jacob, D. J., Wofsy, S. C., 1988. Photochemistry of biogenic emissions over the Amazon forest. J. Geophys. Res. 93, 1477–1486.

Jacobi, H-W., Annor, T., Quansah, E., 2006. Investigation of the photochemical decomposition of nitrate, hydrogen peroxide, and formaldehyde in artificial snow. J. Photochem. Photobiol. A 179, 330-338.

Joshi, A., Pant, N. C., 1995. Petrology, geochemistry and evolution of the charnockite suite of the Petermann Ranges of East Antarctica. In: India and Antarctica during Precambrian. Yoshida, M., Santosh, M. (Eds.) Vol. 34 (pp. 241-258) Mem. Geol. Soc. India.

Kahler, P., Bronsen, P. K., Lochte, K., Antia, A., 1997. Dissolved organic matter and its utilization by bacteria during spring in the Southern Ocean. Deep-Sea Res. II, 341-353.

Keene, W. C., Galloway, J. N., 1988. The biogeochemical cycling of formic and acetic acids through the troposphere: an overview of current understanding. Tellus 40B, 322-334.

Kieber, R. J., Li, A., Seaton, P. J., 1999. Production of nitrite from the photo-degradation of dissolved organic matter in natural waters. Environ. Sci. Technol. 33, 993–998.

King, M. D., France, J. L., Fisher, F. N., Beine, H. J., 2005. Measurement and modelling of UV radiation penetration and photolysis rates of nitrate and hydrogen peroxide in Antarctic sea ice: An estimate of the production rate

of hydroxyl radicals in first-year sea ice. J. Photochem. Photobiol. A. Chem. 176, 39–49.

Kingslake, J., Ely, J. C., Das, I., Bell, R. E., 2017. Widespread movement of meltwater onto and across Antarctic ice shelves. Nature 544, 349-352.

Knap, A., Michaels, A., Close, A., Ducklow, H., Dickson A., 1996. Protocols for the Joint Global Ocean Flux Study (JGOFS) Core Measurements.

Käkölä, J. M., Alén, R. J., Isoaho, J. P., Matilainen, R. B., 2008. Determination of low-molecular-mass aliphatic carboxylic acids and inorganic anions from Kraft black liquors by ion chromatography. J. Chromatogr. A 1190, 150–156.

Larose, C., Dommergue, A., Vogel, T. M., 2013. Microbial nitrogen cycling in Arctic snowpacks. Environ. Res. Lett. 8, 035004.

Larsen, K. S., Ibrom, A., Jonasson, S., Michelsen, A., Beier, C., 2007. Significance of cold-season respiration and photosynthesis in a subarctic heath ecosystem in Northern Sweden. Glob. Chang. Biol. 13, 1498–1508.

Lee, X., Qin, D., Jiang, G., Duan, K., Zhou, H., 2003. Atmospheric pollution of a remote area of Tianshan Mountain: Ice core record. J. Geophys. Res. 108, 4406.

Legrand, M., 1987. Chemistry of Antarctic snow and ice. J. Phys. Colloques 48 (C1), 77-86.

Legrand, M., De Angelis, M., 1996. Light carboxylic acids in Greenland ice: a record of past forest fires and vegetation emissions from the boreal zone. J. Geophys. Res. 101, 4129-4145.

Legrand, M., De Angelis, M., 1995. Origins and variations of light carboxylic acids in polar precipitation. J. Geophys. Res. 100, 1445–1462.

Legrand, M., Delmas, R. J., 1988. Formation of HCl in the Antarctic atmosphere. J. Geophys. Res. 93, 7153-7168.

Legrand, M., Delmas, R. J., 1986. Relative contributions of tropospheric and stratospheric sources to nitrate in Antarctic snow. Tellus 38B, 236-249.

Legrand, M., Mayewski, 1997. Glaciochemistry of polar ice cores: A review. Rev. Geophys. 35, 219-243.

Legrand, M., Pasteur, E. C., 1998. Methane sulfonic acid to non-sea-salt sulfate ratio in coastal Antarctic aerosol and surface snow. J. Geophys. Res. 103, 10991-11006.

Legrand, M., Saigne, C., 1988. Formate, Acetate and Methanesulfonate measurements in Antarctic ice: some geochemical implications. Atmos. Environ. 22, 1011-1017.

Legrand, M., Preunkert, S., Jourdain, B., Guilhermet, J., Faïn, X., Alekhina, I., Petit, J. R., 2013. Water-soluble organic carbon in snow and ice deposited at Alpine, Greenland, and Antarctic sites: a critical review of available data and their atmospheric relevance. Clim. Past 9, 2195-2211.

Legrand, M., Gros, V., Preunkert, S., Sarda-Estève, R., Thierry, A. -M., Pépy, G., Jourdain, B., 2012. A reassessment of the budget of formic and acetic acids in the boundary layers at Dumont d'Urville (coastal Antarctica): the role of penguin emissions on the budget of several oxygenated volatile organic compounds. J. Geophys. Res. 117, D06308.

Legrand, M., Preunkert, S., Jourdain, B., Aumont, B., 2004. Year-round records of gas and particulate formic and acetic acids in the boundary layer at Dumont d'Urville, coastal Antarctica. J. Geophys. Res. 109, D06313.

Lenaerts, J. T. M., Lhermitte, S., Drews, R., Ligtenberg, S. R. M., Berger, S., Helm, V., Smeets, C. J. P. P., van den Broeke, M. R., van De Berg, W. J., van Meijgaard, E., Eijkelboom, M., Eisen, O., Pattyn, F., 2017. Meltwater produced by wind-albedo interaction stored in an East Antarctic ice shelf. Nat. Clim. Chang. 7, 58-62.

Li, C., Xiao, C., Shi, G., Ding, M., Kang, S., Zhang, L., Hou, S., Sun, B., Qin, D., Ren, J. 2015. Spatiotemporal variations of monocarboxylic acids in snow layers along a transect from Zhongshan Station to Dome A, eastern Antarctica. Atmos. Res. 158-159, 79-87.

Liston, G. E., Winther, J. G., 2005. Antarctic surface and subsurface snow and ice melt fluxes. J. Climate 18, 1469-1481.

Liston, G. E., Winther, J. G., Bruland, O., Elvehøy, H., Sand, K., 1999. Below surface ice melt on the coastal Antarctic ice sheet. J. Glaciol. 45(150), 273-285.

Lopatina, A., Krylenkov, V., Severinov, K., 2013. Activity and bacterial diversity of snow around Russian Antarctic stations. Res. Microbiol. 164, 949–958.

Lyons, W. B., Welch, K. A., Doggett, J. K., 2007. Organic carbon in Antarctic snow. Geophys. Res. Lett. 34, L02501.

Lyons, W. B., Welch, K. A.,Fountain, A. G., Dana, G. L., Vaughn, B. H., Mcknight, D. M., 2003. Surface glaciochemistry of taylor valley, southern victoria Land, Antarctica and its relationship to stream chemistry. Hydrol. Process. 17, 115–130.

Lyons, W. B., Fountain, A., Doran, P. T., Priscu, J. C., Neumann, K., Welch, K. A., 2000. Importance of landscape position and legacy: the evolution of the lakes in Taylor Valley, Antarctica. Freshwater Biol. 43, 355–367.

Lythe, M. B., Vaughan, D. G., The BEDMAP Consortium, 2001. BEDMAP: A new ice thickness and subglacial topographic model of Antarctica. J. Geophys. Res. 106, 11335-11351.

MacDonnell, S. A., Fitzsimons, S. J., 2012. Observations of cryoconite hole system processes on an Antarctic glacier. Rev. Chil. Hist. Nat. 85, 393–407.

Mahalinganathan, K., Thamban, M., 2016. Potential genesis and implications of calcium nitrate in Antarctic snow. Cryosphere 10, 825-836.

Mahalinganathan, K., Thamban, M., Laluraj, C. M., Redkar, B. L., 2012. Relation between surface topography and sea-salt snow chemistry from Princess Elizabeth Land, East Antarctica. Cryosphere 6, 505–515.

Malton, W. I., Grew, E. S., Hofmann, J., Sheraton, J. W., 1992. Granite rocks of the Jetty Peninsula, Amery Ice Shelf area, East Antarctica. In: Yoshida Y., Kaminuma K. and Shiraishi K. (Eds.) (pp. 179-189) Recent Progress in Antarctic Earth Sciences, Saitama, Japan.

Maupetit, F., Delmas, R. J., 1994. Carboxylic acids in high-elevation Alpine glacier snow. J. Geophys. Res. 99, 16491–16500.

McConnell, J. R, Edwards, R., Kok, G. L., Flanner, M. G., Zender, C. S., Saltzman, E. S., Banta, J. R., Pasteris, D. R., Carter, M. M., Kahl, J. D. W., 2007. 20th-Century Industrial Black Carbon Emissions Altered Arctic Climate Forcing. Science 317, 1381-1384.

McIntyre, N. F., 1984. Cryoconite hole thermodynamics. Can. J. Earth Sci. 21(2), 152–156.

Menzies, J., Shilts, W.W., 2002. Subglacial environments. In: John Menzies (Eds.). Modern and Past Glacial Environments. Butterworth- Heinemann, Oxford.

Michaud, L., Lo Giudice, A., Mysara, M., Monsieurs, P., Raffa, C., Leys, N., Amalfitano, S., Van Houdt, R., 2014. Snow Surface Microbiome on the High Antarctic Plateau (DOME C). PloS ONE 9, e104505.

Mikhalsky, E.V., Sheraton, J.W., Laiba, A.A., Tingey, R.J., Thost, D.E., Kamenev, E.N., Fedorov, L.V., 2001. Geology of the Prince Charles Mountains, Antarctica. Bulletin 247, AGSO – Geoscience Australia, Canberra.

Mikucki, J. A., Priscu, J. C., 2007. Bacterial diversity associated with Blood Falls, a subglacial outflow from the Taylor glacier, Antarctica. Appl. Environ. Microbiol. 73, 4029–4039.

Miller, R. V., Whyte, L., 2011. Polar Microbiology: Life in a Deep Freeze. American Society of Microbiology, Washington DC.

Moran, M. A., Zepp. R. G., 1997. Role of photoreactions in the formation of biologically labile compounds from dissolved organic matter. Limnol. Oceanogr. 42, 1307–1316.

Müller-Tautges, C., Eichler, A., Schwikowski, M., Pezzatti, G. B., Conedera, M., Hoffmann, T., 2016. Historic records of organic compounds from a high Alpine glacier: influences of biomass burning, anthropogenic emissions, and dust transport. Atmos. Chem. Phys. 16, 1029–1043.

Munir, E., Yoon, J. J., Tokimatsu, T., Hattori, T., Shimada, M., 2001. A physiological role for oxalic acid biosynthesis in the wood-rotting basidiomycete Fomitopsis palustris. Proc. Natl. Acad. Sci. USA 98, 11126–11130.

Musta, B., Tahir, E. H., 2012. Geochemical Study of Weathered Gneiss Rock from Schirmarcher Oasis, Antarctica. Vol. 22 (pp. 187-197) Twenty fourth Indian Antarctic Expedition 2003-2005.

Nataka, P. A., He, C., 2010. Oxalic acid biosynthesis is encoded by anoperon in Burkholderia glumae. FEMS. Microbiol. Lett. 304, 177–182.

Obernosterer, I., Benner, R., 2004. Competition between biological and photochemical processes in the mineralization of dissolved organic carbon. Limnol. Oceanogr. 49, 117-124.

Opsahl, S., Benner, R., 1998. Photochemical reactivity of dissolved lignin in river and ocean waters. Limnol. Oceanogr. 43, 1297–1304.

Orheim, O., Lucchitta, B. K. 1988: Numerical analysis of Landsat thematic mapper images of Antarctica: surface temperatures and physical properties. Ann. Glaciol. 11, 109–120.

Paulot, F., Wunch, D., Crounse, J. D., Toon, G. C., Millet, D. B., DeCarlo, P. F., Vigouroux, C., Deutscher, N. M., González Abad, G., Notholt, J., Warneke, T., Hannigan, J. W., Warneke, C., de Gouw, J. A., Dunlea, E. J., De Mazière, M., Griffith, D. W. T., Bernath, P., Jimenez, J. L., Wennberg, P. O., 2011. Importance of secondary sources in the atmospheric budgets of formic and acetic acids. Atmos. Chem. Phys. 11, 1989–2013.

Peel, D., 1992. Merely the tip of the ice core. Nature 359, 274-275.

Podgrony, I. A., Grenfell, T. C., 1996. Absorption of solar energy in a cryoconite hole. Geophys. Res. Lett. 23(18), 2465–2468.

Porazinska, D. L., Fountain, A. G., Nylen, T. H., Tranter, M., Virginia, R. A., Wall, D. H., 2004. The biodiversity and biogeochemistry of cryoconite holes from McMurdo Dry Valley glaciers, Antarctica. Arc. Antarc. Alp. Res. 36, 84–91.

Prince, A. P., Kleiber, P. D., Grassian, V. H., Young, M. A., 2008. Reactive uptake of acetic acid on calcite and nitric acid reacted calcite aerosol in an environmental reaction chamber. Phys. Chem. Chem. Phys. 10, 142–152.

Rankin, A. M., Auld, V., Wolff, E. W., 2000. Frost flowers as a source of fractionated sea salt aerosol in the polar regions. Geophys. Res. Lett. 27, 3469-3472.

Ravich, M. G., Kamanev, E. V., 1975. Crystalline basement of Antarctic platform. Wiley, New York.

Remy, F., Legresy, B., 2004. Subglacial hydrological networks in Antarctica and their impact on ice flow. Ann. Glaciol. 39, 67-72.

Röthlisberger, R., Mulvaney, R., Wolff, E. W., Hutterli, M. A., Bigler, M., Sommer, S., Jouzel, J., 2002. Dust and sea salt variability in central East Antarctica (Dome C) over the last 45 kyrs and its implications for southern high-latitude climate. Geophys. Res. Lett. 29.

Röthlisberger, R., Hutterli, M. A., Sommer, S., Wolff, E. W., Mulvaney, R., 2000. Factors controlling nitrate in ice cores: Evidence from the Dome C deep ice core. J. Geophys. Res. 105, 20565–20572.

Ruth, U., Barbante, C., Bigler, M., Delmonte, B., Fischer, H., Gabrielli, P., Gaspari, V., Kaufmann, P., Lambert, F., Maggi, V., Marino, F., Petit, J-R., Udisti, R., Wagenbach, D., Wegner, A., Wolff, E. W., 2008. Proxies and measurement techniques for mineral dust in Antarctic ice cores. Environ. Sci. Technol. 42, 5675–5681.

Samui, G., Antony, R., Mahalinganathan, K., Thamban, M., 2017. Spatial variability and possible sources of acetate and formate in the surface snow of East Antarctica. J. Environ. Sci. 57, 258–269.

Sanhueza, E., Figueroa, L., Santana, M., 1996. Atmospheric formic and acetic acids in Venezuela. Atmos. Environ. 30, 1861-1873.

Sanyal, A., Antony, R., Samui, G., Thamban, M., 2018. Microbial communities and potential for degradation of dissolved organic carbon in cryoconite hole environments of Himalaya and Antarctica. Microbial. Res. 208, 32-42.

Säwström, C., Granéli, W., Laybourn-Parry, J., Anesio, A. M., 2007. High viral infection rates in Antarctic and Arctic bacterioplankton. Environ. Microbiol. 9, 250–255.

Säwström, C., Mumford, P., Marshall, W., Hodson, A., Laybourn-Parry, J., 2002. The microbial communities and primary productivity of cryoconite holes in an Arctic glacier (Svalbard 79° N). Polar Biol. 25, 591–596.

Scambos, T. A., Campbell, G. G., Pope, A., Haran, T., Muto, A., Lazzara, M., Reijmer, C. H., van den Broeke, M. R., 2018. Ultra-low surface temperatures in east Antarctica from satellite thermal infrared mapping: the coldest places on earth. Geophys. Res. Lett. 45, 6124-6133.

Schoeberl, M. R., Hartmann, D. L., 1991. The dynamics of the stratospheric polar vortex and its relation to springtime ozone depletions. Science 251, 46-52.

Sengupta, S., 1986. Geology of Schirmacher Range (Dakshin Gangotri), East

Antarctica-Vol. 3 (pp. 187-217), Third Indian Antarctic Expedition.

Sharp, M., Parkes, J., Cragg, B., Fairchild, I. J., Lamb, H., Tranter, M., 1999. Widespread bacterial populations at glacier beds and their relationship to rock weathering and carbon cycling. Geology 27, 107–110.

Shimada, M., Ma, D-B., Akamatsu, Y., Hattori, T., 1994. A proposed role of oxalic acid in wood decay systems of wood-rotting basidiomycetes. FEMS Microbiol. Rev. 13, 285–296.

Singer, G. A., Fasching, C., Wilhelm, L., Niggemann, J., Steier, P., Dittmar, T., Battin, T. J., 2012. Biogeochemically diverse organic matter in Alpine glaciers and its downstream fate. Nat. Geosci. 5, 710-714.

Skidmore, M. L., Foght, J. M., Sharp, M. J., 2000. Microbial life beneath a high Arctic glacier. Appl. Environ. Microb. 66, 3214–3220.

Souza, S. R., Carvalho, L. R. F., 2001. Seasonality influence in the distribution of formic and acetic acids in the urban atmosphere of São Paulo City Brazil. J. Braz. Chem. Soc. 12, 755–762.

Stanish, L. F., Bagshaw, E. A., McKnight, D. M, Fountain, A. G., Tranter, M., 2013. Environmental factors influencing diatom communities in Antarctic cryoconite holes. Environ. Res. Lett. 8, 045006.

Steinbock, O., 1936. Cryoconite holes and their biological significance. Z. Gletscherkunde 24, 1–21.

Stibal, M., Bradley, J. M., Box, J. E., 2017. Ecological modeling of the supraglacial ecosystem: a process-based perspective. Front. Earth Sci. 5, 52.

Stibal, M., Wadham, J. L., Lis, G. P., Telling, J., Pancost, R. D., Dubnick, A., Sharp, M. J., Lawson, E. C, Butler, C. E. H., Hasan, F., Tranter, M., Anesio, A. M., 2012. Methanogenic potential of Arctic and Antarctic subglacial environments with contrasting organic carbon sources. Glob. Chang. Biol. 18, 3332-3345.

Stibal, M., Tranter, M., Benning, L. G., Rehak, J., 2008. Microbial primary production on an Arctic glacier is insignificant in comparison with allochthonous organic carbon input. Environ. Microbiol. 10, 2172-2178.

Stibal, M., Tranter, M., 2007. Laboratory investigation of inorganic carbon uptake by cryoconite debris from Werenskioldbreen, Svalbard. J. Geophys. Res. 112, GO4S33.

Stubbins, A., Spencer, R. G. M., Chen, H., Hatcher, P. G., Mopper, K., Hernes, P. J., Mwamba, V. L., Mangangu, A. M.,Wabakang- hanzi, J. N., Six, J., 2010. Illuminated darkness: Molecular signatures of Congo River dissolved organic matter and its photochemical alteration as revealed by ultrahigh precision mass spectrometry. Limnol. Oceanogr. 55, 1467–1477.

Sugimae, A., 1984. Elemental constituents of atmospheric particulates and particle density. Nature 307, 145–147.

Sumner, A. L., Shepson, P. B., 1999. Snowpack production of formaldehyde and its effect on the Arctic troposphere. Nature 398, 230-233.

Svensson, T., Lovett, G. M., Likens, G. E., 2012. Is chloride a conservative proxy in forest ecosystems?. Biogeochemistry 107(1-3), 125-134.

Swanson, A. L., Blake, N. J., Dibb, J. E., Albert, M. R., Blake, D. R., Rowland, F. S., 2002. Photochemically induced production of CH_3Br, CH_3I, C_2H_5I, ethene and propene within surface snow at Summit, Greenland. Atmos. Environ. 36, 2671–2682.

Takacs, C. D., Priscu, J. C., 1998. Bacterioplankton dynamics in the McMurdo Dry Valley lakes, Antarctica: production and biomass loss over four seasons. Microb. Ecol. 36, 239-250.

Takacs, C. D., Priscu, J. C., McKnight, D. M., 2001. Bacterial dissolved organic carbon demand in McMurdo Dry Valley lakes, Antarctica. Limnol. Oceanogr. 46(5), 1189–1194.

Takeuchi, N., 2002. Optical characteristics of cryoconite (surface dust) on glaciers: the relationship between light absorbancy and the property of organic matter contained within the cryoconite. Ann. Glaciol. 34, 409–414.

Takeuchi, N., Kohshima, S., Yoshimura, Y., Seko, K., Fujita, K., 2000. Characteristics of cryoconite holes on a Himalayan glacier: Yala Glacier, Central Nepal. B. Glaciolo. Res. 17, 51–59.

Talbot, R. W., Beecher, K. M., Harriss, R. C., Cofer III, W. R., 1988. Atmospheric geochemistry of formic and acetic acids at a mid-latitude temperate site. J. Geophys. Res. 93, 1638–1652.

Telling, J., Anesio, A. M., Tranter, M., Fountain, A. G., Nylen, T., Hawkings, J., Singh, V. B., Kaur, P., Musilova, M., Wadham, J. L., 2014. Spring thaw ionic pulses boost nutrient availability and microbial growth in entombed Antarctic dry valley cryoconite holes. Front. Microbiol. 5, 694.

Thamban, M., Laluraj, C. M., Mahalinganathan, K., Redkar, B. L., Naik, S. S., Shrivastava, P. K., 2010. Glaciochemistry of surface snow from the Ingrid Christensen Coast, East Antarctica, and its environmental implications. Antarct. Sci. 22, 435-441.

Toom-Sauntrya, D., Leonard, A. Barrie, L. A., 2002. Chemical composition of snowfall in the high Arctic: 1990–1994. Atmos. Environ. 36, 2683–2693.

Tranter, M., Fountain, A. G., Lyons, W. B., Nylen, T. H., Welch, K. A., 2005. The chemical composition of runoff from Canada Glacier, Antarctica : implications for glacier hydrology during a cool summer. Ann. Glaciol. 40, 15–19.

Tranter, M., Fountain, A. G., Fritsen, C. H., Lyons, W. B., Priscu, J. C., Statham, P. J., Welch, K. A., 2004. Extreme hydrochemical conditions in natural microcosms entombed within Antarctic ice. Hydrol. Process. 18, 379–387.

Tranvik, L. J., Bertilsson, S., 2001. Contrasting effects of solar UV radiation on dissolved organic sources for bacterial growth. Ecol. Lett. 4, 458–463.

Traversi, R., Becagli, S., Castellano, E., Largiuni, O., Migliori, A., Severi, M., Frezzotti,M., Udisti, R., 2004. Spatial and temporal distribution of environmental markers from coastal to plateau areas in Antarctica by firn core chemical analysis. Int. J. Environ. Anal. Chem. 84, 457–470.

Trenberth, K. E., Caron, J. M., 2001. Estimates of meridional atmosphere and ocean heat transports. J.Climat. 13, 4358-4365.

Tschumi, J., Stauffer, B., 2000. Reconstructing past atmospheric CO_2 concentrations based on ice core analyses: Open questions due to in situ production of CO_2 in the ice. J. Glaciol. 46, 45–53.

Turner, J., Anderson, P., Lachlan-Cope, T., Colwell, S., Phillips, T., Kirchgaessner, A., Marshall, G. J., King, J. C., Bracegirdle, T., Vaughan, D. G., Lagun, V., Orr, A., 2009a. Record low surface air temperature at Vostok station, Antarctica. J. Geophys. Res. 114, D24102.

Turner, J., Chenoli, S. N., abu Samah, A., Marshall, G., Phillips, T., Orr, A., 2009b. Strong wind events in the Antarctic. J. Geophys. Res. 114, D18103.

Udisti, R., Becagli, S., Castellano, E., Traversi, R., Vermigli, S., Piccardi, G., 1999. Sea-Spray and marine biogenic seasonal contribution to snow composition at Terra Nova Bay, Antarctica. Ann. Glaciol. 29, 77-83.

Udisti, R., Becagli, S., Traversi, R., Vermigli, S., Piccardi, G., 1998. Preliminary evidence of a biomass-burning event from a 60 year-old firn core from Antarctica by ion chromatographic determination of carboxylic acids. Ann. Glaciol. 27, 391–397.

Udisti, R., Barbolani, S., Piccardi, G., 1991. Determination of some organic and inorganic substances at ppb levels in Antarctic snow and ice by Ion Chromatography. Ann. Chim. (Rome) 81, 325-341.

Usher, C. R., Michel, A. E., Grassian, V. H., 2003. Reactions on mineral dust. Chem. Rev. 103, 4883–4940.

Vaïtilingom, M., Charbouillot, T., Deguillaume, L., Maisonobe, R., Parazols, M., Amato, P., Sancelme, M., Delort, A. M., 2011. Atmospheric chemistry of carboxylic acids: microbial implication versus photochemistry. Atmos. Chem. Phys. 11, 8721-8733.

Ward, C., Cory, R., 2016. Complete and partial photo-oxidation of dissolved organic matter draining permafrost soils. Environ. Sci. Technol. 50, 3545–3553.

Ward, C. P., Nalven, S. G., Crump, B. C., Kling, G. W., Cory, R. M., 2016. Photochemical alteration of organic carbon draining permafrost soils shifts microbial metabolic pathways and stimulates respiration. Nat. Commun. 8, 772.

Wetzel, R. G., Hatcher, P. G., Bianchi, T. S., 1995. Natural photolysis by ultraviolet irradiance of recalcitrant dissolved organic matter to simple substrates for rapid bacterial metabolism. Limnol. Oceanogr. 40, 1369-380.

Wilhelm, S. W., Suttle, C. A., 1998. Viruses and nutrient cycles in the sea. Bioscience 49, 781-789.

Williams, C. M., Dupont, A. M., Loevenich, J., Post, A. F., Dinasquet, J., Yager, P. L., 2016. Pelagic microbial heterotrophy in response to a highly

productive bloom of Phaeocystis Antarctica in the Amundsen Sea Polynya, Antarctica. Elem. Sci. Anth. 4, 000102.

Winther, J. G., Jespersen, M. N., Liston, G. E., 2001. Blue ice areas in Antarctica derived from NOAA AVHRR satellite data. J. Glaciol. 47(157), 325–34.

Wynn, P. M., Hodson, A. J., Heaton, T. H. E., Chenery, S. R., 2007. Nitrate production beneath a high Arctic glacier, Svalbard. Chem. Geol. 244, 88–102.

Yallop L. M., Anesio, A. M., 2010. Benthic diatom flora in supraglacial habitats: a generic-level comparison. Ann. Glaciol. 51, 15-22.

Yallop, M. L., Anesio, A. M., Perkins, R. G., Cook, J., Telling, J., Fagan, D., MacFarlane, J., Stibal, M., Barker, G., Bellas, C., Hodson, A., 2012. Photophysiology and albedo-changing potential of the ice algal community on the surface of the Greenland ice sheet. ISME J. 6(12), 2302.

Yan, P., Hou, S., Chen, T., Ma, X., Zhang, S., 2012. Culturable bacteria isolated from snow cores along the 1300 km traverse from Zhongshan Station to Dome A, East Antarctica. Extremophiles 16, 345–354.

Zellweger, G. W., 1994. Testing and comparison of four ionic tracers to measure stream flow loss by multiple tracer injection. Hydrol. Process. 8(2), 155-165.

ZoBell, C. E., 1933. Photochemical nitrification in sea water. Science 77, 27–28.

List of publications from thesis

1. **Gautami Samui**, Runa Antony, Kanthanathan Mahalinganathan, Meloth Thamban (2017). Spatial variability and possible sources of acetate and formate in the surface snow of East Antarctica. *Journal of Environmental Sciences*, 57, 258-269. (**Impact Factor: 3.12**)
2. Aritri Sanyal, Runa Antony, **Gautami Samui,** Meloth Thamban (2018). Microbial communities and their potential for degradation of dissolved organic carbon in cryoconite hole environments of Himalaya and Antarctica. *Microbiological Research*, 208, 32-42. **(Impact Factor: 2.56)**
3. **Gautami Samui**, Runa Antony, Meloth Thamban (2018). Chemical characteristics of hydrologically distinct Cryoconite holes in coastal Antarctica. *Annals of Glaciology*, 59, 69-76. (**Impact Factor: 2.76**)

Papers presented at national/international conferences

1. **Gautami Samui**, Runa Antony, Meloth Thamban. Nutrient cycling in supraglacial ecosystems in coastal Antarctica. Presented at Polar 2018, **XXXV SCAR Open Science Conference**, Davos, Switzerland, 19-23 June, 2018. ***(Awarded Best Poster prize, Asia Region)***
2. **Gautami Samui**, Runa Antony, Meloth Thamban. Biogeochemical characteristics of hydrologically connected and isolated cryoconite holes in coastal Antarctica. Presented at **National Conference on Polar Sciences**, Goa, India, 13-14 May, 2017. ***(Awarded Best Poster prize)***
3. **Gautami Samui**, Runa Antony, Kanthanathan Mahalinganathan, Meloth Thamban. Spatial variability and possible sources of carboxylate ions in the surface snow samples in Princess Elizabeth Land, East Antarctica. Presented at **XII International symposium on Antarctic Earth Sciences**, Goa, 13-17 July, India, 2015.